

Circumstellar disks and planets

Science cases for next-generation optical/infrared long-baseline interferometers

**S. Wolf¹, F. Malbet², R. Alexander³, J.-Ph. Berger⁴,
 M. Creech-Eakman⁵, G. Duchêne^{6,2}, A. Dutrey⁷, C.
 Mordasini⁸, E. Pantin⁹, F. Pont¹⁰, J.-U. Pott⁸, E.
 Tatulli², L. Testi¹¹**

Received: October 2011 / Accepted: February 2012

Abstract We present a review of the interplay between the evolution of circumstellar disks and the formation of planets, both from the perspective of theoretical models and dedicated observations. Based on this, we identify and discuss fundamental questions concerning the formation and evolution of circumstellar disks and planets which can be addressed in the near future with optical and infrared long-baseline interferometers. Furthermore, the importance of complementary observations with long-baseline (sub)millimeter interferometers and high-sensitivity infrared observatories is outlined.

Keywords Interferometric instruments · Protoplanetary disks · Planet formation · Debris disks · Extrasolar planets

PACS 95.55.Br · 97.82.Jw · 97.82.-j · 96.15.Bc · 97.21.+a · 97.82.Fs

1 Introduction

To understand the formation of planets, one can either attempt to observe them in regions where they are still in their infancy or increase the number of discoveries of mature planetary systems, i.e., of the resulting product of the formation process. Both extrasolar planets as well as their potential birth regions in circumstellar disks are usually located between 0.1 AU to 100 AU from their parent star. For nearby star-forming regions, the angular resolution required to investigate the innermost regions is therefore of the order of (sub)milliarcseconds.

1: University of Kiel, Institute for Theoretical Physics and Astrophysics, Leibnizstr. 15, 24118 Kiel, Germany · **2:** UJF-Grenoble 1 / CNRS-INSU, Institut de Planétologie et d’Astrophysique de Grenoble (IPAG) UMR 5274, Grenoble, F-38041, France · **3:** Department of Physics & Astronomy, University of Leicester, University Road, Leicester LE1 7RH, UK · **4:** European Organisation for Astronomical Research in the Southern Hemisphere (ESO), Casilla 19001, Santiago 19, Chile · **5:** New Mexico Institute of Mining and Technology, Department of Physics, 801 Leroy Place, Socorro, NM 87801, USA · **6:** Astronomy Department, B-20 Hearst Field Annex #3411, UC Berkeley, Berkeley CA 94720-3411, USA · **7:** University of Bordeaux, Observatoire Aquitain des Sciences de l’Univers, CNRS, UMR5804, Laboratoire d’Astrophysique de Bordeaux, 2 rue de l’Observatoire, BP89, F-33271 Floirac Cedex, France · **8:** Max Planck Institute for Astronomy, Königstuhl 17, 69117 Heidelberg, Germany · **9:** CEA/DSM/IRFU/Service d’Astrophysique, CE Saclay, 91191, Gif-sur-Yvette, France · **10:** Astrophysics group, School of Physics, University of Exeter, Stocker Road, Exeter EX4 4QL, UK · **11:** European Organisation for Astronomical Research in the Southern Hemisphere, Karl-Schwarzschild-Str. 2, 85748 Garching bei München, Germany

Furthermore, the temperatures of the emitting inner disk material or close-in planets are in the range of hundreds to thousands of degrees Kelvin. Given these constraints, currently operating optical to infrared (IR) long-baseline interferometers are well suited to investigate the planet-formation process: They provide information at the milliarcsecond (mas) scale in the wavelength range where the emission of these objects has its maximum. In this article, we review the field of protoplanetary disks and exoplanets in the context of high angular resolution techniques, emphasizing the role of optical/IR interferometry. Furthermore, we illustrate the potential of the second generation VLTI¹ instrumentation in this field, taking into account synergies from observations obtained at complementary wavelengths and lower angular resolution.

We first provide a brief review about currently existing theoretical models and observations of protoplanetary disks and exoplanets (resp., Sect. 2 and 3). Based on this knowledge, the scientific potential of optical to mid-IR interferometers and the role of selected complementary observatories are discussed (resp., Sect. 4 and 5).

2 Theory of disk evolution and planet formation

In this section, we give an introductory overview about the theory of disk evolution and planet formation. As a short introduction, it can necessarily only provide a simplified description of the most important lines of reasoning of these theories and many important aspects have to remain unaddressed. Instead, relevant comprehensive reviews are referred to if necessary. The objective is to have an overall understanding of planet formation from the disk stage to mature planets.

2.1 Evolution of protoplanetary disks

The most common means of observing disks around young stars is the detection of continuum emission from warm dust in the disk. This emission is brighter than the stellar photosphere at IR and even more at longer wavelengths, and such “excess” emission is usually associated with the presence of a dust disk at \sim AU radii (Kenyon and Hartmann, 1995; Haisch et al, 2001).

Observing gas in disks is much more difficult, as the trace dust component dominates the disk opacity. We can detect line emission from atoms and molecules of heavy elements, or from the warm surface layers of the disk, but the most common means of observing gas in disks is through signatures of accretion onto the stellar surface. Typically we detect either the accretion luminosity, observed as UV continuum emission or veiling of photospheric lines, or broad emission lines (such as H α) that originate in the hot accretion flow (Hartigan et al, 1995; Gullbring et al, 1998; Muzerolle et al, 2000). There is a near one-to-one correspondence between solar-mass objects showing accretion signatures (usually referred to as classical T Tauri stars, henceforth CTTs) and those showing the IR excess characteristic of inner dust disks (IR Class II). In addition, recent non-detection of warm H₂ emission sets very strict upper limits to the gas mass around non-accreting, also called weak-lined T Tauri stars (WTTS; Ingleby et al, 2009), suggesting that the mechanism for clearing inner disks is very efficient indeed.

The vast majority of young stars fall into the categories of disk-bearing CTTs or disk-less WTTS, but some show properties intermediate between these two states. These latter

¹ Very Large Telescope Interferometer

objects were named “transitional” disks by Strom et al (1989), and typically show evidence of inner disk clearing. These objects are rare, accounting for $\lesssim 10\%$ of the TT population, and this relative lack of objects between the CTT & WTT states has long been interpreted as evidence that the transition from disk-bearing to disk-less is rapid, occurring on a time scale 1–2 orders of magnitude shorter than the Myr disk lifetime (Skrutskie et al, 1990; Kenyon and Hartmann, 1995; Simon and Prato, 1995; Wolk and Walter, 1996). In recent years, it has become clear that the transitional disks are not a homologous class of objects (Salyk et al, 2009), and a number of different mechanisms have been proposed for their origin (Najita et al, 2007; Chiang and Murray-Clay, 2007; Ireland and Kraus, 2008; Alexander, 2008a; Cieza et al, 2008; Alexander and Armitage, 2009). It is clear, however, that transitional disks have undergone significant evolution, and further investigation of them may be crucial to our understanding of disk evolution and clearing.

Protoplanetary disks typically live for a few Myr, with a spread of lifetimes of at least an order of magnitude. Disks have been found to cover a mass range of $\sim 0.1 - 0.001 M_{\odot}$ (Andrews and Williams, 2005), and to possess accretion rates of $\sim 10^{-7} - 10^{-10} M_{\odot} \text{ yr}^{-1}$ (Hartigan et al, 1995; Gullbring et al, 1998; Muzerolle et al, 2000). The relative lack of objects seen between the disk-bearing Class II and disk-less Class III states implies that the dust clearing time scale is short ($\sim 10^5 \text{ yr}$), and recent observations suggest that this two-time-scale constraint applies to the gaseous component of the disk also (Ingleby et al, 2009). Models of disk evolution must satisfy all of these constraints. Moreover, the mass budget demands that all gas giant planets must form before their parent disks are dispersed, and thus understanding protoplanetary disk evolution is crucial to understanding how planetary systems are formed.

2.1.1 Role of accretion in the standard disk theory

Angular momentum conservation is fundamental to the evolution of protoplanetary disks. Disks form because angular momentum is conserved during protostellar collapse, and estimates of the rotational velocities of molecular cores (Goodman et al, 1993) imply that young stars should be surrounded by centrifugally supported disks of tens to hundreds of AU in size (as observed). Material in such a disk must lose angular momentum if it is to accrete, so further evolution requires the transport of angular momentum through the disk. Understanding how angular momentum is transported is therefore crucial to understanding how protoplanetary disks evolve. The theory of protoplanetary disk evolution has been discussed in depth in a number of review articles in recent years (Dullemond et al, 2007; Alexander, 2008a; Lodato, 2008; Armitage, 2007, 2010); here we present only a brief summary of the salient points.

Classical accretion disk theory invokes a fluid viscosity as the source of angular momentum transport (Shakura and Sunyaev, 1973; Lynden-Bell and Pringle, 1974), but from an early stage it was clear that ordinary molecular viscosity is many orders of magnitude too inefficient to be responsible for the accretion we see in real astrophysical disks. Early models side-stepped this problem by appealing to turbulence in the disk as a source of angular momentum transport, but the physical origin of such turbulence remained elusive. The seminal work of Shakura and Sunyaev (1973) introduced the famous alpha-prescription, where the efficiency of angular momentum transport is given by the expression $\nu = \alpha c_s H$ where ν is the kinematic viscosity, c_s is the local sound speed, and H is the scale height of the disk. The quantity $\alpha \leq 1$ is a dimensionless parameter which characterizes the strength of the turbulence (formally the ratio of the turbulent stress to the local pressure), and essentially encapsulates all that one does not understand about how angular momentum is transported

in accretion disks. However, simple models of this type provide considerable insight into how disks around young stars evolve, and the basic paradigm of viscous disk accretion is broadly consistent with the observed data. Angular momentum is transported outward which allows mass to be accreted. In the absence of infall onto the disk the disk mass and accretion rate decline with time, while the disk spreads radially to conserve angular momentum (Lynden-Bell and Pringle, 1974; Pringle, 1981; Hartmann et al, 1998).

We now know of a number of potential mechanisms for angular momentum transport in disks, the most relevant of which are magneto-hydrodynamic (MHD) turbulence (driven by the magneto-rotational instability, MRI; Balbus and Hawley, 1991; Balbus, 2009), and gravitational instabilities (GIs; Toomre, 1964; Lodato and Rice, 2004, 2005). Disks become unstable to GIs if they are sufficiently massive and/or cold. Detailed calculations suggest that protoplanetary disks are only likely to be gravitationally unstable if they have masses $\gtrsim 0.1 M_{\odot}$ (Rafikov, 2009; Clarke, 2009), and even then GIs can only occur in the cold, outer regions of the disk. Disk masses decline with time as the disk accretes onto the star, and consequently GIs dominate only at very early times. Angular momentum transport by GIs may well be responsible for the accretion of much of the stellar mass through the disk at early times, but they cannot be significant for the majority of the disk lifetime.

By contrast, the MRI is expected to operate in any weakly magnetized shear flow, provided that the gas is sufficiently ionized to couple to the magnetic field. However, in protoplanetary disks it is not clear that this ionization threshold is always met. The disk is thermally ionized very close to the star, and cosmic rays and stellar X-rays ionize a moderately thick surface layer, but MRI-“dead” zones can exist at the midplane at \sim AU radii (Gammie, 1996; Armitage et al, 2001; Zhu et al, 2009). The rate of angular momentum transport due to the MRI remains the subject of current research, but numerical simulations of MHD turbulence suggest that it can transport angular momentum with an efficiency of $\alpha \sim 0.001 - 0.1$ (Stone et al, 1996).

Observations provide us with only limited insight into how angular momentum is transported in protoplanetary disks. Accretion histories of CTTs are generally consistent with simple, constant- α viscous accretion disk models, but the data do not give strong constraints on the model parameters. Hartmann et al (1998) showed that the viscous accretion models of Lynden-Bell and Pringle (1974) can reproduce the observed decline in CTT accretion rates with time, and estimated a typical $\alpha \sim 0.01$. The basic paradigm of viscous accretion in protoplanetary disks remains broadly consistent with the observed accretion histories of T Tauri stars (Sicilia-Aguilar et al, 2010).

Where pure accretion disk models fail, however, is in the final clearing stage. Viscous accretion disk models predict that the various observable quantities (mass, accretion rate, surface density) should decline as power laws in time, and thus the time required for a viscous disk to evolve from one state into another is always of order the disk age. This is dramatically inconsistent with the rapid disk clearing observed in T Tauris, and strongly suggests that some other mechanism plays a dominant role in the latter stages of protoplanetary disk evolution. At present, the favored process is that of disk photoevaporation.

2.1.2 *Importance of photoevaporation in disk evolution*

The basic principle of photoevaporation is simple: high-energy (UV or X-ray) photons heat the disk surface, and beyond some radius the hot surface layer contains sufficient thermal energy to escape the stellar gravitational potential and flow as a wind. The critical length-scale for photoevaporation (the “gravitational radius” R_g) can be estimated by equating the thermal energy (per particle) of the heated layer with the gravitational binding energy, so

$R_g = GM_*/c_{\text{hot}}^2$ where M_* is the stellar mass, and c_{hot} is the sound speed in the hot surface layer. Careful consideration of the pressure forces tells us that the bulk of the mass loss in fact comes from a factor of a few inside R_g (Liffman, 2003; Font et al, 2004), and the resulting winds are analogous to, for example, Compton-heated winds from the disks around AGNs (Begelman et al, 1983).

The temperature of the heated layer, and thus the value of c_{hot} , depends on the nature of the irradiation. In the case of protoplanetary disks, there are three important cases to consider: extreme ultraviolet (EUV) ionizing photons; far-ultraviolet (FUV); and X-rays. EUV irradiation creates an ionized layer on the disk surface, akin to an HII region, with $T \simeq 10^4$ K and $c_{\text{hot}} \simeq 10$ km/s, so the critical length-scale for EUV photoevaporation is typically $\simeq 1 - 2$ AU. Heating by FUV or X-rays is more complex, leading to a range of temperatures in the disk atmosphere, but in general the critical radii range from a few AU to a few tens of AU, depending on the flux and spectrum of the incident radiation field. The irradiation can arise from the star irradiating its own disk, or come from external sources such as nearby O-stars. External irradiation is observed to drive disk photoevaporation in some cases, such as the “proplyds” in the Orion Nebula (Johnstone et al, 1998), but for most T Tauri disks irradiation from the central star dominates.

In general, computing the structure of photoevaporative winds is a complicated problem in both radiative transfer and hydrodynamics. In the EV case the wind structure has been computed by Hollenbach et al (1994) and Font et al (2004). It gives rise to a wind rate which is given by $\dot{M}_w \simeq 10^{-10} \Phi_{41}^{1/2} (M_*/M_\odot)^{1/2} M_\odot \text{ yr}^{-1}$ (where Φ_{41} is the stellar ionizing flux in units of 10^{41} ionizing photons per second). The ionizing luminosities of T Tauri stars are in general not well known, but typical estimates suggest values in the range $10^{40} - 10^{42}$ photons/s (Alexander et al, 2005; Herczeg, 2007). The bulk of the ionizing emission from T Tauri stars arises in the stellar chromosphere (Alexander et al, 2004, 2005) and is thus largely independent of the evolutionary state of the disk, so the wind rate is approximately constant over the Myr disk lifetime.

When combined with viscous evolution of the disk, EUV photoevaporation gives rise to some rather surprising behavior. At early times, the accretion rate through the disk exceeds the wind rate by several orders of magnitude, so the wind is negligible. However, the accretion rate declines with time, and eventually (typically after a few Myr) reaches the same level as the (constant) wind rate. The mass loss due to the wind is concentrated at radii of a few AU, so at this point the wind cuts off the inner disk from re-supply. The inner disk then drains on its (short) viscous time scale, leaving an \sim AU-sized “hole” in the disk (Clarke et al, 2001). As it drains, the inner disk becomes optically thin to EUV photons, which increases the wind rate by a factor of ~ 10 , and the wind then clears the disk from the inside-out in $\sim 10^5$ yr (Alexander et al, 2006a,b). This rapid clearing after a long lifetime appears to be consistent with observations of disk evolution (Alexander et al, 2006b; Alexander and Armitage, 2009), and due to the role of the wind in precipitating disk clearing, this class of models are often referred to as “UV-switch” models (Clarke et al, 2001).

Photoevaporation by FUV radiation and/or X-rays is a much more complex problem (both in terms of radiative transfer and hydrodynamics), and consequently models of X-ray and FUV photoevaporation are not yet as advanced as for EUV photoevaporation. However, significant progress has been made in this area recently, using sophisticated radiative transfer codes and numerical hydrodynamics (Ercolano et al, 2009; Gorti and Hollenbach, 2009; Gorti et al, 2009; Owen et al, 2010, 2011). Models of both X-ray- and FUV-driven winds suggest maximum wind rates as high as $\sim 10^{-8} M_\odot \text{ yr}^{-1}$, and when coupled with viscous evolution these models predict a similar “switch” behavior to the EUV case albeit at a much

higher accretion rate (Gorti et al, 2009; Owen et al, 2010). Such high wind rates are unlikely to occur in all objects, however, and it remains to be seen how these results scale with various model parameters. These results all suggest that photoevaporation plays a dominant role in disk evolution at late times. This theoretical view is supported by recent observations of blue-shifted forbidden emission lines from some T Tauri stars (Pascucci and Sterzik, 2009; Pascucci et al, 2011). These observations unambiguously detect a slow (~ 10 km/s), ionized wind, and are broadly consistent with the predictions of photoevaporation models (Alexander, 2008b; Ercolano and Owen, 2010); further such data will provide important new insight into the processes driving disk clearing.

2.2 Formation of planets

While the structure and evolution of protoplanetary disks has been discussed in the previous section, these objects are now considered as the environment for the formation of planets therein. For more comprehensive reviews, we refer the reader to Lissauer (1993), Papaloizou and Terquem (2006), Armitage (2007), and the book of Klahr and Brandner (2006).

2.2.1 *Observational constraints*

The guidelines to understand the physics involved in the different stages of planet formation come from observational constraints derived from three different classes of astrophysical objects. The first one is our own planetary system, i.e. the Solar System. Studies of the solar system include remote observations of the Sun, the planets and the minor bodies, laboratory analysis of meteorites, in-situ measurements by space probes, possibly including sample returns, as well as theoretical work and numerical modeling.

The second class of astrophysical objects leading to important constraints on planetary formation are protoplanetary disks. As planets are believed to form in protoplanetary disks, the conditions in them are the initial and boundary conditions for the formation process. As already discussed in Sect. 2.1, the fraction of disk-bearing stars is a roughly linearly decreasing function of cluster age, disappearing after about 4-6 Myr. Giant planets must have formed at this moment. This represents a non-trivial constraint on classical giant planet-formation models.

The third class are finally the extrasolar planets, which can all be regarded as different examples of the final outcome of the formation process (see Sect. 3.2). Especially the fact that many extrasolar planets were found exactly where one did not expect to find them pointed towards a serious gap in the understanding of planet formation derived from the Solar System alone, so that the mentioned orbital migration which we will address in Sect. 2.2.6 is nowadays regarded as an integral component of modern planet-formation theory.

The already large number of extrasolar planets also gives us the possibility to look in a new way at all these discoveries: to see them no more just as single objects, but as a population with distributions of extrasolar planet masses, semimajor axes, host star metallicities and so on, as well as all kinds of correlations between them. A theoretical study of these statistical properties of the exoplanet population is done best by the method of planetary population synthesis (Ida and Lin, 2004a,b; Mordasini et al, 2009a,b).

2.2.2 From dust to planetesimals

The first stage of planetary growth starts with roughly micro-meter sized dust grains, similar to those found in the interstellar medium. These tiny objects are well coupled to the motion of the gas in the protoplanetary disk via gas drag. With increasing mass, gravity becomes important also, and the particles decouple from the pure gas motion. This stage involves the growth of the dust grains via coagulation (sticking), their sedimentation towards the disk midplane, and their radial drift towards the star. In this context, the gas and the solid particles move around the star at a slightly different orbital speed. The reason for this is that the gas is partially pressure supported (both the centrifugal force and the gas pressure counteract the gravity), and therefore moves slightly slower (sub-Keplerian) around the star. The resulting gas drag in turn causes the drift of the solid particles towards the star.

In the picture of classical coagulation, bodies grow all the way to kilometer size by two-body collisions. While growth from dust grains to roughly meter sized bodies can be reasonably well modeled with classical coagulation simulations as for example in Brauer et al (2008a), two significant problems arise at the so-called “meter barrier”:

- For typical disk properties, objects which are roughly meter sized drift extremely quickly towards the central star where they are destroyed by the high temperatures. The drift time scale at this size becomes in particular shorter than the time scale for further growth (Klahr and Bodenheimer, 2006), so that growth effectively stops.
- The second problem arises from the fact that meter sized boulders do not stick well together, but rather shatter at the typical collision speeds which arise from the turbulent motion of the disk gas, and the differential radial drift motion.

First ideas on how to bypass the critical meter size were put forward already a long time ago, and invoke the instability of the dust layer to its own gravity, which can produce full blown planetesimals from small sub-meter objects. In the classical model of Goldreich and Ward (1973), dust settles into a thin layer in the disk midplane. If the concentration of the dust becomes sufficiently high, the dust becomes unstable to its own gravity and collapses to form planetesimals directly. The turbulent speed of the grains, however, must be very low to reach the necessary concentration. This condition is difficult to meet, as the vertical velocity shear between the dust disk rotation at the Keplerian frequency and the dust poor gas above and below the midplane rotating slightly sub-Keplerian causes the development of Kelvin-Helmholtz instabilities. The resulting turbulence is sufficiently strong to decrease the particle concentration below the threshold necessary for the gravitational collapse. This is why self-gravity of the dust, and gas turbulence, either due to the Kelvin-Helmholtz mechanism, or due to the magneto-rotational instability (Balbus and Hawley, 1998), were for a long time thought to be mutually exclusive.

In the recent years, however, significant progress has been made in the direction of planetesimal formation by self-gravity (Johansen et al, 2006; Cuzzi et al, 2008). In particular, it was understood that turbulence can actually aid the formation of planetesimals, rather than hindering it. The reason is that turbulence can locally lead to severe over-densities of the solid particle concentration by a factor as high as 80 compared to the normal dust to gas ratio on large scales of the turbulence (Johansen et al, 2006) or by $\sim 10^3$ on small scales (Cuzzi et al, 2008). Further concentration can occur thanks to the streaming instability (Youdin and Goodman, 2005), which all together can lead to the formation of gravitationally bound clusters with already impressive masses, comparable to dwarf planets (Johansen et al, 2007), on a time-scale much shorter than the drift timescale. This so-called gravoturbulent planetesimal formation should leave imprints visible in the solar system distinguishing it

from the classical pure coagulation mechanism. The recent work of Morbidelli et al (2009) finds that the observed size frequency distribution in the asteroid belt cannot be reproduced with planetesimals that grow (and fragment) starting at a small size. It rather seems that planetesimals need to get born big in order to satisfy this observational constraint, with initial sizes between already 100 and 1000 km. On the other hand, too large initial sizes for the majority of the planetesimals might not be desirable either, as this could slow down the formation of giant planet cores, at least if the planetesimal accretion occurs through a mechanism similar as described in Pollack et al (1996). This is due to the higher random velocities of massive planetesimals, and the less effective capture of larger bodies by the protoplanetary gaseous envelope.

2.2.3 From planetesimals to protoplanets

At the size of planetesimals (\sim kilometers), gravity is clearly the dominant force, even though the gas drag still plays a role. However, the growth stage from planetesimals to protoplanets (with radii of order a thousand kilometers) remains challenging to study because of the following reasons:

- The initial conditions are poorly known since the formation mechanism and thus the size distribution of the first planetesimals, is not yet clearly understood (see previous section).
- The very large number of planetesimals to follow prevents any direct N-body integrations with current computational capabilities. For example, a planet with a mass of about ten Earth masses consists of more than 10^8 planetesimals with a radius of 30 km.
- The time sequence to be simulated (typically several million years) is very long, equivalent to the same number of dynamical time-scales (at 1 AU).
- The growth process is highly non-linear and involves complex feedback mechanisms since the growing bodies play an increasing role in the dynamics of the system.
- The physics describing the collisions which are ultimately needed for growth is non-trivial and includes for example shock waves, multi-phase fluids and fracturing.

The planetesimals-to-protoplanets growth stage has therefore been modelled with different methods, each having different abilities to address the listed issues. Here, we only address the most basic approach. Other, more complex methods which yield a more realistic description of this stage are statistical methods (Inaba et al, 2001) or Monte Carlo methods (Ormel et al, 2010).

In the *rate equations* approach, the growth of a body is described in the form of a rate equation which directly gives the mass growth rate dM/dt of a body as a function of several quantities. Usually it is assumed that one large body (the protoplanet) collisionally grows from the accretion of much smaller background planetesimal (see e.g. Goldreich et al, 2004). These background planetesimals are characterized by a size (or a size distribution), a surface density and a dynamical state (eccentricity and inclination). The growth rate is then described with a Safronov (1969) type equation,

$$\frac{dM}{dt} = \pi R^2 \Omega \Sigma_p F_G \quad (1)$$

where Ω is the Keplerian frequency of the large body at an orbital distance a around the star of mass M_* , and Σ_p is the surface density of the field planetesimals, R is the radius of the large body, and F_G is the gravitational focusing factor. It reflects the fact that due to gravity, the effective collisional cross section of the body is larger than the purely geometrical one,

πR^2 , since the trajectories get bent towards the large body. The focusing factor is the key parameter in this equation, as it gives raise to different growth regimes: *runaway*, *oligarchic* or *orderly growth*, which come with very different growth rates (Rafikov, 2003). Its value depends on the random velocity of the small bodies v_{ran} relative to the local circular motion. It scales with their eccentricity and inclination. The small bodies are mutually affected by the encounters between them, and with the large body (which increases the random velocity) and the damping influence by the gas (which decreases it).

In the simplest approximation, where one neglects the influence of the star, F_G is given as $1 + v_{\text{esc}}^2/v_{\text{ran}}^2$, where v_{esc} is the escape velocity from the big body. One notes that if the planetesimals have small random velocities in comparison with v_{esc} , then F_G is large and fast accretion occurs. The mass accretion rate is then proportional to R^4 , i.e. strongly non-linear. This is the case in the so-called runaway growth regime, where massive bodies grow quicker than small ones, so that these runaway bodies detach from the remaining population of small planetesimals (Weidenschilling et al, 1997). However, with increasing mass, these big bodies start to increase the random velocities of the small ones, so that the growth becomes slower, and the mode changes to the so-called oligarchic mode, where the big bodies grow in lockstep (Ida and Makino, 1993).

As the planet grows in mass, the surface density of planetesimals must decrease correspondingly (e.g. Thommes et al, 2003). As the growing protoplanet is itself embedded in the gravitational field of the star, one finds by studying the restricted three body problem that a growing body can only accrete planetesimals which are within its gravitational reach (in its feeding zone), i.e. in an annulus around the body which has a half width which is a multiple (~ 4) of the Hill sphere radius $R_H = (M/3M_*)^{1/3} a$ of the protoplanet. Without radial excursions (migration), a protoplanet can therefore grow in situ only up to the so-called isolation mass (Lissauer, 1993).

The outcome of this growth stage is the inner part of the planetary system with a high number of small protoplanets, with masses between 0.01 and $0.1 M_{\oplus}$, which are called *oligarchs*. When the gas disk is present, growth is stalled at such masses since gas damping hinders the development of high eccentricities which would be necessary for mutual collision between these bodies (Ida and Lin, 2004a). In the outer part of the planetary system, i.e. beyond the iceline, a few 1 to $10 M_{\oplus}$ protoplanets form.

2.2.4 From protoplanets to giant planets

For the formation of the most massive planets, the gaseous giants, two competing theories exist. The most widely accepted theory is the so-called core accretion - gas capture model. However, we will first discuss the direct gravitational collapse model.

Direct gravitational collapse model. In this model, giant planets are thought to form directly from the collapse of a part of the gaseous protoplanetary disk into a gravitationally bound clump. As we will see below, this requires fairly massive disks, so that it is thought that this mechanism should occur early in the disk evolution. For the mechanism to work, two requirements must be fulfilled:

1. The self-gravity of the disk (measured at one vertical scale height) must be important compared to the gravity exerted by the star (D'Angelo et al, 2010). The linear stability analysis of Toomre (1981) shows that a disk is unstable for the growth of axisymmetric radial rings if the Toomre parameter $Q < 1$. The disks become unstable when they are

cold and massive. Hydrodynamical simulations show that disks become unstable to non-axisymmetric perturbations (spiral waves) already at slightly higher Q values of about 1.4 to 2 (Mayer et al, 2004). At the orbital distance of Jupiter, the surface density of gas must be about 10 times larger than in the minimal mass solar nebula² (MMSN), in order for the disk to become unstable.

2. In order to allow for fragmentation into bound clumps, the time-scale on which a gas parcel in the disk cools and thus contracts must be short compared to the shearing time scale, on which the clump would be disrupted otherwise, which is equal to the orbital timescale (Gammie, 2001). If this condition is not fulfilled, only spiral waves develop leading to a gravoturbulent disk. The spiral waves transport angular momentum outward, and therefore let matter spiral inward to the star. This process releases gravitational binding energy, which increases the temperature, and reduces the gas surface temperature, so that the disk evolves to a steady state of marginal instability only, without fragmentation.

From the time-scale arguments, we see that the correct treatment of the disk thermodynamics is of central importance to understand whether the direct collapse model can operate. Radiation hydrodynamic simulations give a confused picture, where different groups find for similar initial conditions both fragmentation (Boss, 2007) and no fragmentation (Cai et al, 2010). This illustrates that the question whether bound clumps can form is still being debated. It is usually thought that it is unlikely that disk instability as a formation mechanism can work inside several tens of AU. This is due to the fact that the two necessary conditions discussed above lead to the following dilemma, as first noted by Rafikov (2005): a disk that is massive enough to be gravitationally unstable is at the same time too massive to cool quickly enough to fragment, at least inside say 40-100 AU. Outside such a distance, the situation might be different as the orbital time scales become long (Boley, 2009).

In contrast to the subsequently discussed core-accretion model, giant planet formation is extremely fast in the direct collapse model, as it occurs on a dynamical time scale.

Core-accretion model. The basic setup for the core-accretion model is to follow the concurrent growth of a initially small solid core consisting of ices and rocks, and a surrounding gaseous envelope, embedded in the protoplanetary disk. This concept has been studied for over thirty years (Perri and Cameron, 1974; Mizuno et al, 1978; Bodenheimer and Pollack, 1986). Within the core-accretion paradigm, giant planet formation happens as a two step process: first a solid core with a critical mass (of order $10 M_{\oplus}$) must form, then the rapid accretion of a massive gaseous envelope sets in.

The growth of the solid core by the accretion of planetesimals is modeled in the same way as described in Sect. 2.2.3. The growth of the gaseous envelope is described by one-dimensional hydrostatic structure equations similar to those for stars, except that the energy released by nuclear fusion is replaced by the heating by impacting planetesimals, which are the main energy source during the early phases. The other equations are the equation of mass conservation, of hydrostatic equilibrium, of energy conservation and of energy transfer. Boundary conditions (Bodenheimer et al, 2000; Papaloizou and Nelson, 2005) are required to solve these equations. We have to distinguish two regimes:

- At low masses, the envelope of the protoplanet is attached continuously to the background nebula, and the conditions at the surface of the planet are just the pressure and

² In the MMSN model (Weidenschilling, 1977; Hayashi, 1981) it is assumed that the planets formed at their current positions, and that the solids found in all planets of the solar system today correspond to the amount of solids available also at the time of formation. The total disk mass is then found by adding gas in the same proportion as observed in the star.

temperature in the surrounding disk. The radius of the planet is given in this regime approximately by the Hill sphere radius. The gas accretion rate is given by the ability of the envelope to radiate away energy so that it can contract and in turn new gas can stream in.

- When the gas accretion obtained in this way becomes too high as compared to the externally possible gas supply, the planet enters the second phase and contracts to a radius which is much smaller than the Hill sphere radius. This is the detached regime of high-mass, runaway (or post-runaway) planets. The planet now adjusts its radius to the boundary conditions that are given by an accretion shock on the surface for matter falling onto the planet from the Hill sphere radius, or probably more realistically, by conditions appropriate for the interface to a circumplanetary disk. In this phase, the gas accretion rate is no more controlled by the planetary structure itself, but by the amount of gas which is supplied by the disk and can pass the gap formed by the planet in the protoplanetary disk (Lubow et al, 1999).

Pollack et al (1996) have implemented the aforementioned equations in a model that we may call the baseline formation model. They assumed a constant pressure and temperature in the surrounding disk, and a strictly fixed embryo position, i.e. no migration. Figure 1 shows the formation and subsequent evolution of a Jupiter mass planet fixed at 5.2 AU for initial conditions equivalent to case J6 in Pollack et al (1996). In the calculation shown here the core density is variable, the luminosity is spatially constant in the envelope, but derived from total energy conservation (Papaloizou and Nelson, 2005). The limiting maximum gas accretion rate is simply set to $10^{-3} M_{\oplus} \text{ yr}^{-1}$, and accretion is completely stopped once the total mass is equal to one Jupiter mass. In a full simulation (Alibert et al, 2005a), the maximum limiting accretion rate, as well as the termination of gas accretion is given by the decline of the gas flux in the disk caused by the evolution of the protoplanetary nebula.

The top left panel shows that three phases can be distinguished. In phase I, a solid core is built up. The solid accretion rate is large, as shown by the top right panel. The phase ends when the planet has exhausted its feeding zone of planetesimals, which means that the planet reaches the isolation mass, which is of order $11.5 M_{\oplus}$. In phase II, the accretion rates are low, and the planet must increase the feeding zone. This is achieved by the gradual accretion of an envelope: an increase in the gas mass leads to an increase of the feeding zone of solids. Therefore the core can grow a little bit. This leads to a contraction of the external radius of the envelope. Gas from the disk streams in, leading to a further increase of the envelope mass. In phase III, runaway gas accretion occurs. It starts at the crossover mass, i.e. when the core and envelope mass are equal (about $16.4 M_{\oplus}$ in this simulation). At this stage, the radiative losses from the envelope can no more be compensated for by the accretional luminosity from the impacting planetesimals alone. The envelope has to contract, so that the new gas can stream in (note the quasi exponential increase of the gas accretion rate), which increases the radiative loss as the Kelvin-Helmholtz time scale decreases strongly with mass in this regime, so that the process runs away, quickly building up a massive envelope.

The existence of such a critical mass is intrinsic to the core-envelope setup and not dependent on detailed physics (Stevenson, 1982; Wuchterl, 1993). The critical core mass is typically of the order of $10-15 M_{\oplus}$, but it can amount to $1-40 M_{\oplus}$ in extreme cases (Papaloizou and Terquem, 1999).

Shortly after the beginning of runaway gas accretion phase, the limiting gas accretion rate is reached. The collapse phase starts which is actually a fast, but still hydrostatic contraction (Bodenheimer and Pollack, 1986; Lissauer et al, 2009) on a time scale of $\sim 10^5$

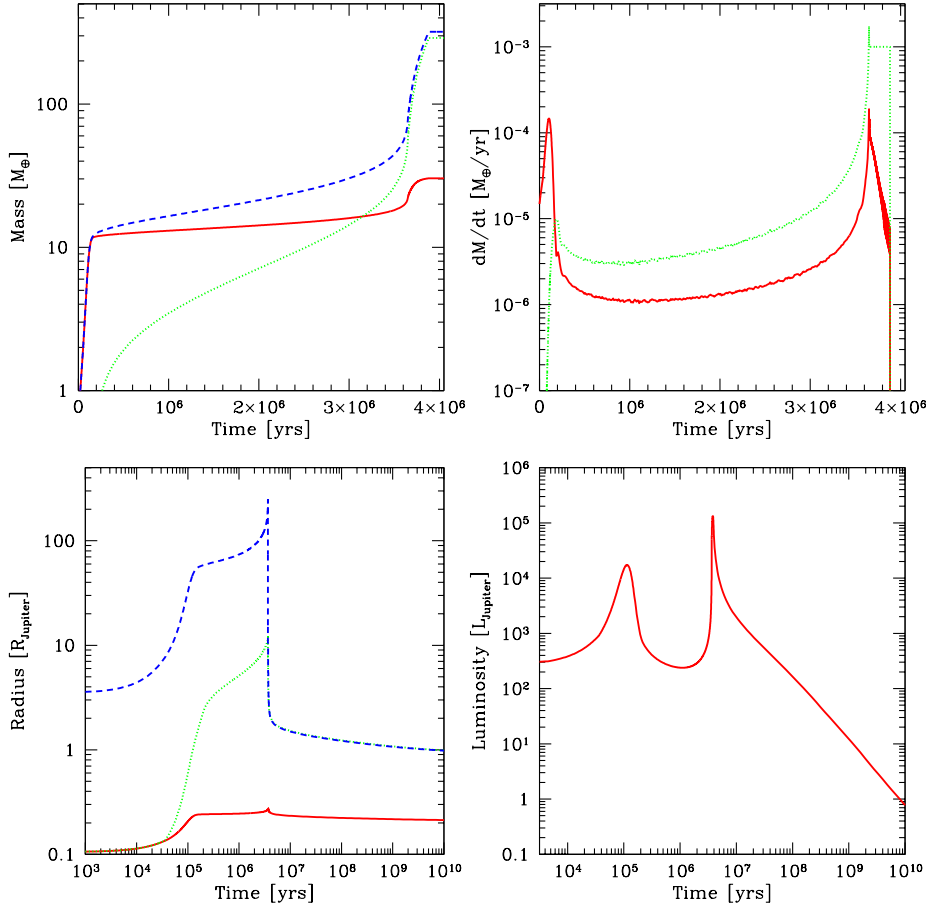


Fig. 1 Simulation for the in-situ formation of Jupiter. The top left panel shows the evolution of the core mass (red solid line), the envelope mass (green dotted line) and the total mass (blue solid line). The top right panels shows the accretion rate of solids (red solid line) and of gas (green dotted line). The limiting gas accretion rate is set to $10^{-3} M_{\oplus} \text{ yr}^{-1}$. Note that the model is allowed to overshoot this value for a few time steps. The bottom left panel shows the evolution of the core radius (red solid line), the total radius (blue dashed line) and the capture radius (green dotted line). The latter radius is relevant for the capture of planetesimals. It is larger than the core radius due to the braking effect of the envelope. The outer radius is initially (during the attached regime) very large, as it is equal to the Hill sphere radius. At about 4 Myrs, it detaches from the nebula and collapses to a radius of initially about 2 Jupiter radii. Afterwards, there is a slow contraction phase. The bottom right panel shows the internal luminosity of the planet. The first peak in the curve is due to the rapid accretion of the core, and the second to the runaway gas accretion/collapse phase.

years. The planet surface detaches now from the surrounding nebula. The contraction continues quickly down to an outer radius of about 2 R_{Jupiter} (bottom left panel).

Over the subsequent billion years, after the final mass is reached, slow contraction and cooling occurs. The different phases can also be well distinguished in the luminosity of the planet (bottom right curve), in particular the two maxima when a significant amount of gravitational binding energy is released during the rapid accretion of the core and during the runaway gas accretion and collapse phase.

The baseline formation model has many appealing features, producing a Jupiter-like planet with an internal composition similar to what is inferred from internal structure model in a four times MMSN in a few million years. Note that in the calculation shown here it was assumed that all planetesimals can reach the central core. In reality, the shielding effect of a massive envelope prevents planetesimals of 100 km in radius as assumed here to reach directly the core for core masses larger than about $6 M_{\oplus}$ (Alibert et al, 2005b), and the planetesimals get dissolved in the envelope instead.

The largest part of the evolution is spent in phase II. The length of this phase becomes uncomfortably close to protoplanetary disk lifetimes for lower initial solid surface densities, or for higher grain opacities in the envelope (Pollack et al, 1996). This is the so-called time-scale problem. However, once migration is included, this problem can be overcome (Alibert et al, 2004).

2.2.5 From protoplanets to terrestrial planets

For terrestrial planets, the requirement that they form within the lifetime of the gaseous protoplanetary disk (≤ 10 Myrs) can be dropped. Indeed, we recall the final outcome of the planetesimal to protoplanets stage discussed in Sect. 2.2.3 in the inner part of the protoplanetary nebula, i.e. inside the iceline: a large number of oligarchs with masses between 0.01 to $0.1 M_{\oplus}$.

Once the eccentricity damping caused by the gas disk or by a sufficiently large population of small planetesimals is finished, these oligarchs start to mutually pump up their eccentricities, and eventually the orbits of neighboring protoplanets cross, so that the final growth stage up to the final terrestrial planets with masses of order of the mass of Earth starts. The system of large bodies evolves through a series of giant impacts to a state where the remaining planets have a configuration close to the smallest spacings allowed by long-term stability over Gyr timescales (Goldreich et al, 2004). This long term stability manifests itself in the form of a sufficiently large mutual spacing of the bodies in terms of mutual Hill spheres, with typical final separation between the planets of a few ten Hill radii (Raymond et al, 2008). Interestingly, such basic architectures now become visible in the recently detected multi-planet extrasolar systems consisting of several low-mass planets (Lovis et al, 2011).

In the inner solar system, simulations (now based on direct N-body integration) addressing this growth stage must concurrently meet the following constraints (Raymond et al, 2009): the observed orbits of the planets, in particular the small eccentricities (0.03 for the Earth); the masses, in particular the small mass of Mars; the formation time of the Earth as deduced from isotope dating, about 50-100 Myrs; the bulk structure of the asteroid belt with a lack of big bodies; the relatively large water content of the Earth with a mass fraction of 10^{-3} and last but not least, the influence of Jupiter and Saturn.

Figure 2 shows as an example six snapshots in time for the terrestrial planet formation in the inner solar system by Raymond et al (2009). This simulation starts with roughly 100 0.01 to $0.1 M_{\oplus}$ oligarchs, plus additional background planetesimals, as well as Jupiter and Saturn. One notes in the first panel the well defined eccentricity excitations at the places of mean motion resonances with the giant planets. In panel two and three, this resonant excitation spreads out. During the stage of chaotic growth (until about 100 Myr), substantial radial mixing occurs, bringing water-rich bodies in the inner system, as visible in the last three panels. At the end, four terrestrial planets with masses between about 0.6 and $1.8 M_{\oplus}$ have formed. The orbital distances, eccentricities, masses, formation time scales, and water content found in this simulation are approximatively in agreement with the actual solar system,

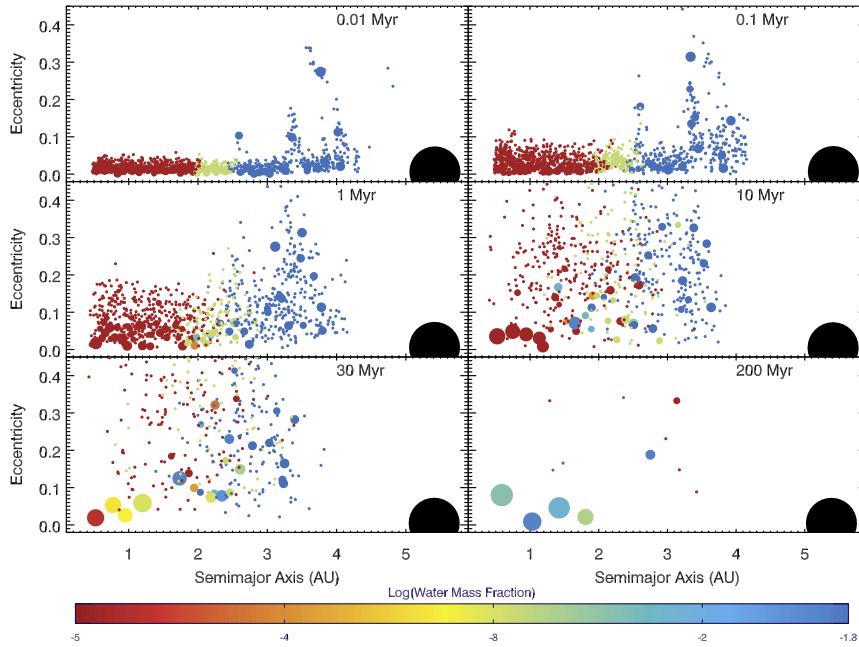


Fig. 2 Six snapshots in time for an N-body simulation of terrestrial planet formation by Raymond et al (2009). The size of each body is proportional to its mass, while the color corresponds to the water content by mass, going from red (dry) to blue (5% water). Jupiter is indicated as a large black circle while Saturn is not shown. (Reprinted with permission from Elsevier)

but the Mars analogue is too massive, and there are three additional bodies in the asteroid belt. This simulation thus reproduces many important observed aspects, but not all of them. A main complication arises: the positions, eccentricities and masses of the giant planets at each moment in time are not exactly known, but significantly influence the formation of the terrestrial planets.

2.2.6 Orbital migration

Orbital migration occurs through the gravitational interaction of the planet with the protoplanetary disk. If the resulting torques exerted by the different parts of the disk onto the planet do not sum up to exactly zero, the planet will react on them by adjusting its angular momentum, i.e. its semimajor axis. Two major types of migration have been identified:

1. Low-mass planets migrate in so-called type I migration (Goldreich and Tremaine, 1980; Tanaka et al, 2002).
2. Massive planets which can open a gap in the gaseous disk migrate in type II migration (Lin and Papaloizou, 1986).

Migration can be both a threat and a benefit for planet formation: on the one hand, if migration happens on a time scale shorter than the growth time scale, planetary cores fall into the star before they can significantly grow (e.g. Mordasini et al, 2009b). On the other hand, it allows planetary cores to grow beyond the isolation mass as cores always get into

new regions of the disk where there are still fresh planetesimals to accrete, which reduces the formation time of giant planets, as the lengthy phase II in core accretion is skipped (Alibert et al, 2004). Numerical simulations of the migration process (e.g., Paardekooper et al, 2010; Kley et al, 2009; Crida and Morbidelli, 2007) have shown that depending on the local disk properties like the temperature and surface density gradients, both in- and outward migration can occur. The disk model is therefore of very high importance. It was also found that migration and accretion can strongly interact: For example, inward migration without significant gain in planetary mass occurs when a planet migrates through a part of the disk which it has previously emptied from planetesimals while migrating outward. On the other hand, gas runaway accretion and the associated mass growth can cause the switch to another migration regime. Note that hot Jupiters form as the isolation mass limitation in the inner system can be overcome thanks to migration.

2.3 Selected key questions

2.3.1 *Surface density distribution?*

As mentioned above, understanding angular momentum transport is critical to understanding how protoplanetary disks evolve, and without detailed knowledge of the processes of angular momentum transport all of our models are necessarily idealized. We can tune the free parameters of viscous accretion models to match observed time scales and accretion rates, but such models are necessarily phenomenological and are consequently rather lacking in predictive power.

The single most important observation we could make in this area would be to determine the (gas) surface density distribution $\Sigma(R)$. Coupled to a measurement of the accretion rate, this would allow one to determine directly the efficiency of angular momentum transport as a function of radius (as $\dot{M} = 3\pi\nu\Sigma$ in a quasi-steady disk). Deriving $\nu(R)$ would provide us with critical insight into how angular momentum is transported, and would also allow a significant refinement of the disk evolution models.

Directly observing $\Sigma(R)$ in gas in the potential planet-forming region is likely to be beyond our capabilities for some years yet, but recent observations have made significant progress in determining spatially resolved dust surface density profiles on scales of tens of AU (Andrews et al, 2009; Isella et al, 2009; Andrews et al, 2010). Extending these results down to AU scales would be of significant interest, both in terms of disk evolution and for models of planet formation. Recent attempts to measure the turbulent velocity field in T Tauri disks may also provide important insight into this problem (Hughes et al, 2011).

2.3.2 *Resolve transitional disks?*

In addition, spatially resolved studies of the so-called transitional disks are likely to be key to understanding the processes that drive both planet formation and disk clearing. Current IR observations allowed one to resolve some transitional disk structures on scales of a few AU (Eisner et al, 2006; Ratzka et al, 2007; Olofsson et al, 2011; Tatulli et al, 2011), and similar observations of small numbers of objects have also been made at mid-infrared to millimeter wavelengths (Hughes et al, 2007, 2009; Brown et al, 2009; Gräfe et al, 2011). Extending these results to large, unbiased samples of transitional disks will potentially allow one to distinguish between different models for disk clearing, and perhaps even directly detect newly formed planets (Wolf and D'Angelo, 2005).

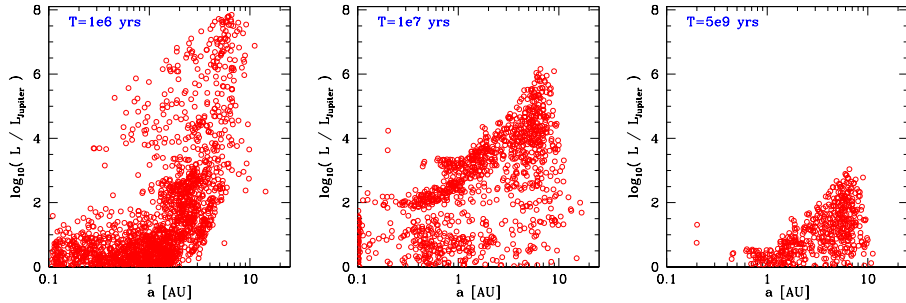


Fig. 3 Luminosity for a population of synthetic planets forming and evolving around a solar like star. The luminosity in units of Jupiter's luminosity today ($8.7 \times 10^{-10} L_\odot$) is shown as a function of distance, for three moments in time. The left panels is during the formation epoch, the middle panel soon after the protoplanetary disks have disappeared, and the right panels shows the situation after 5×10^9 yrs. Note that outward migration, or outward scattering is impossible in these simulation by construction, which likely leads to an underestimation of giant planets at large semimajor axes (from Mordasini et al. in prep.).

2.3.3 Luminosities of young planets?

A key property for several detection methods of extrasolar planets like direct imaging or interferometric methods is the luminosity of (young) giant planets (Absil et al, 2010). As outlined in Sect. 2.2.4, the luminosity is a strong function of time (and of planetary mass?). The highest luminosities occur during the gas runaway accretion and collapse phase. For fast gas accretion one finds very high peak luminosities, up to $\sim 0.1 L_\odot$ for a Jupiter mass planet, but the phase of high luminosity is only very short, about 10^4 yrs. Lower peak luminosities are found if the gas accretion rate is low, but the duration of the phase is longer (Lissauer et al, 2009). This local energy input into the disk leads to the formation of a hot blob ($T \sim 400 - 1500$ K) around the planet, with a size equal to a few Hill spheres of the planet, corresponding to 0.1-1 AU for a growing giant planet a 5 AU. Such a feature should be detectable in the mid-IR, and might even cast shadows (Klahr and Kley, 2006; Wolf, 2008a).

For observational surveys looking for planetary companions, it is relevant to know the distance-luminosity distribution as a function of time. Figure 3 (Mordasini et al., in prep.) shows this for a synthetic population of planets forming around a solar like star. Note that outward migration is not yet possible by construction in this set of models, which might be relevant in the context, as it leads to an underestimation of giant planets at large semimajor axes which are prime targets for such surveys. Note further that the luminosity of young giant planets is in general a topic which is still being debated (Fortney et al, 2005). The left panel shows the distance-luminosity plane at an age of the protoplanetary disks of 10^6 yrs. There are some very bright planets with luminosities up to about $0.06 L_\odot$. They are found somewhat outside the current position of Jupiter, at 6-7 AU. These are massive planets forming in solid rich disk, which get early in the gas runaway accretion/collapse phase, so that high gas accretion rates are possible. The much lower luminosities of the planets at smaller distances (inside about 1 AU) is caused in contrast by the accretion of planetesimals. The middle plot shows the situation at 10 million years, thus after all gaseous protoplanetary disks have disappeared. Gas accretion onto the planets has therefore ceased, but the planets are still quite luminous in this early phase of contraction. At the present age of the solar system (as shown in the right panel) luminosities have decreased by several orders of mag-

nitude. The highest luminosities are caused by some ~ 30 Jupiter mass objects. Two massive planets relatively close to the star are also visible.

2.3.4 Where in the disk do giant planets form?

The rate equations for solid accretion (Sect. 2.2.3) indicates that a position not far outside the iceline is the sweet spot for giant planet formation within the core-accretion paradigm, as massive cores can form still relatively quickly. This is confirmed by more complete simulations (Mordasini et al, in prep.), which compute the initial location of planets that eventually grow more massive than $300 M_{\oplus}$ (about 1 Jupiter mass) relative to the position of the iceline in their parent protoplanetary disk: the typical position from where giant planet come is indeed a few AU outside the iceline, especially for low and medium [Fe/H] disks. At high [Fe/H], giant planets can form both inside, as well as clearly outside the iceline (see also Ida and Lin, 2004a).

The location of the iceline itself is set, at least initially, by the energy production due to viscous dissipation in the disk, and its radiation at the disk surface. Fits to the location of the iceline as a function of disk and stellar mass in this regime can be found in Alibert et al (2011). For a solar-type star, it lies between roughly 2 to 7 AU. At later stages, when the disk becomes optically thin, the location of the iceline becomes determined by the energy input from the star (Ida and Lin, 2004a), and lies at about 3 AU. In the observed semimajor axis distribution of the extrasolar planets, there is an upturn in the frequency at a semimajor axis of about 1 AU, which could be caused by this preferred starting position close to the iceline, and subsequent orbital migration (Mordasini et al, 2009b; Schlaufman et al, 2009). This would thus be a direct imprint of disk properties on planetary properties. But one should keep in mind that the temperature and solid surface density structure in the disks might be in reality much more complicated (Dzyurkevich et al, 2010) than assumed in the simple models used here.

3 Observing disks and exoplanets

One of the immediate goals in planet formation research is to determine the statistics, properties, and large- and small-scale structures of circumstellar disks and exoplanets. Ultimately, the study of disks spanning across the pre- to the post-planet formation phases over a range of stellar masses will help identifying the most profound trends, hence the relevant physics, that are central to planet formation. In this section, we briefly outline the current state-of-the-art in spatially resolved observations of circumstellar disks and exoplanets (see also Absil and Mawet, 2010). In particular, we aim at outlining the specific observing methods that are available and the extent to which they can be used to infer the properties of an individual disk or exoplanet.

3.1 Circumstellar disks

Spatially unresolved photometry is by far the easiest way to assess the presence and determine some of the properties of a circumstellar disk. Over the last three decades, this approach has been used to determine the typical ~ 5 Myr time scale for disk survival (Fedele et al, 2010), hence planet formation, as well as to assess the presence of dust grains 1 mm in size or larger in the majority of protoplanetary disks (Natta et al, 2007). Similarly, recent

Spitzer surveys have established that 10–50% of young main sequence stars host a debris disks (Trilling et al, 2008; Meyer et al, 2008; Lestrade et al, 2009), confirming that the formation of planetesimals is a very common outcome of disk evolution, in line with the high proportion of detected exoplanets around nearby stars (Udry and Santos, 2007).

However, analyses of spectral energy distributions of these objects are limited to some very simple questions (Is the disk present or absent? Is it optically thin or thick?) as a result of numerous ambiguities between the various physical parameters that describe a given disk (Chiang et al, 2001). To give a simple example, determining that a debris disk system is characterized by a black-body excess emission only firmly establishes the temperature of this dust population. Its physical location around the star, which could then be compared to an exoplanetary system or to planet formation theories, can only be inferred by making an assumption about the distribution of size and composition of the dust grains.

3.1.1 Observing Circumstellar Disks

Before addressing particular observing techniques, it is useful to discuss the ways in which disks can be studied if they can be spatially resolved. This will help to highlight the complementarity of the various observing techniques and to identify the areas in which long-baseline interferometry can provide a unique contribution.

Scattered light imaging At optical wavelengths, circumstellar disks are not significant emitters since their temperature does not exceed the dust sublimation temperature (typically ~ 1500 K). At these wavelengths, a disk can only be imaged in scattered light, i.e. stellar photons that have scattered off a dust grain in the disk prior to reaching the observer. As demonstrated by McCabe et al (2003), disks can be imaged in scattered light up to the mid-IR regime. However, depending on the stellar effective temperature and luminosity as well as the dust properties, the relative contribution of the thermal emission becomes important at near- to mid-IR wavelengths (e.g., Pinte et al, 2008a), i.e., the main source of scattered photons is the hot dust in the innermost disk regions itself. Consequently, not only the stellar photosphere, but also these inner regions have to be hidden from direct view if the goal is to obtain large-scale disk images in the optical to mid-IR wavelength range.

Scattered light images are powerful tools to determine the *overall geometry* of a disk. First of all, an image usually provides a direct estimate of the disk *inclination*. Furthermore, it provides a lower limit to the disk *outer radius*. Because it does not rely on intrinsic disk emission, scattered light can be detected up to large distances from the central star (up to 1000 AU) with sensitive enough detectors. In the case of debris disks, which are optically thin, scattered light images directly trace the structure of disks with surface brightness enhancements in regions of higher density. In fact, surface brightness profiles can be inverted into *surface density profiles*, making it possible to infer the presence of planets through gaps, asymmetries or resonant trapping of dust particles. On the other hand, protoplanetary disks are optically thick and scattered light only probes the upper surface of the disk. Indeed, surface brightness profiles inform us on the geometry of the disk surface: a flat or shadowed disk does not produce substantial scattered light, for instance. In the specific case of edge-on disks, it is possible to infer the *vertical scale height* of the dust component. If the vertical extent of the dust component is deemed too small compared to the prediction for a disk in hydrostatic equilibrium, this can be interpreted as a sign of settling compared to the gas component. Scattered light images of optically thick disks, however, suffer from ambiguous interpretation: lateral asymmetry can be either due to an intrinsic large-scale asymmetry in

the disk or an illumination disparity, possibly because of asymmetry in the innermost regions of the disk.

Because of the nature of scattering, optical and near-IR images of disks also inform on the nature of the dust grains: grains much smaller than the observing wavelength scatter isotropically while large grain are strongly forward-throwing. Dust properties, especially the possibility of porous or non-spherical grains, also play a role in setting the scattering “phase function”. If the viewing geometry of a system, hence the scattering angle at each position in the disk, can be determined, it is possible to map the phase function. This can in turn be used to probe the *grain size distribution*, under some assumption about the dust composition. While multiple combinations of dust compositions (including porosity) and size distributions can yield the same scattering asymmetry, one can take advantage of a multi-wavelength approach to map this asymmetry as a function of wavelength, which can help disentangle the effects of *dust composition* and grain size distribution. Finally, if the dust grains have a sufficiently strong spectral feature in their albedo function (such as the water ice feature around $3\ \mu\text{m}$), it is possible to use scattered light imaging to constrain the dust composition independently of the phase function and of the disk optical depth.

In optically thin disks, *grain sizes* can also be constrained by the observed color of the disk relative to the central star. Indeed, very small grains have an albedo function that drops significantly towards longer wavelengths, making the disk “blue”, whereas disks containing larger grains are typically neutral or slightly “red”. The intensity scattered off a dust grain is actually the product of the albedo and the phase function, so it is critical to obtain a resolved image to disentangle the two effects.

As a final note, scattered photons are generally highly linearly polarized, with details depending on the photon wavelength, dust size, shape and composition. Therefore, maps of linear polarization vectors or, second-best as this induces a loss of information, polarized intensity images also convey insight on the dust properties. Polarized imaging offers the added benefit that the central star is essentially unpolarized, which alleviates dramatically the high-contrast problem posed by scattered light imaging.

Thermal Emission Mapping At near- and mid-IR and longer wavelengths, disks are imaged via their dust thermal emission. Dust grains are heated by the central star and re-emit as gray bodies depending on their equilibrium temperatures. The inner few AUs of a disk emit mostly in the near- and mid-IR range whereas the outer regions (beyond 10 AU) emit primarily in the far-IR and (sub)millimeter wavelength regimes. Therefore, it is possible to discern details in the immediate vicinity of the central star in the mid-IR regime if the spatial resolution is high enough, gaining insight on the disk *inner radius*, as well as the geometry of the inner regions of the disk.

At the longest wavelengths, most of the disk is optically thin, so that the surface brightness of a disk is a direct measure of the $\kappa_\nu \Sigma(r) B_\nu(T)$ product, where κ_ν is the dust opacity, $\Sigma(r)$ the surface density and $T(r)$ the dust temperature. A surface brightness map can therefore be used to determine the *surface density profile* of a disk if its temperature profile can be estimated or assumed. Furthermore, the ratio of surface brightnesses at independent wavelengths is only dependent on the opacity ratio, which itself is a function of the *grain size distribution*. This method has first been used with unresolved observations to probe the presence of dust grains as large as 1 mm. If the wavelength-dependent resolution can be accounted for properly, resolved maps can be used to study spatial variations in the grain size distribution.

Because debris disks are optically thin at all wavelengths, it is possible to take advantage of the inescapable rule of thumb that observables are most sensitive to grains whose size is

comparable to the observing wavelength. If grains of various sizes have different spatial distributions as a consequence of size-dependent forces exerted on the grains, this can translate into significantly different morphologies as a function of wavelength for a given disk, for instance from mid-IR to millimeter wavelengths.

As a final note, it is worth emphasizing that the scattered light and thermal emission regimes overlap in wavelength which, in the case of optically thick disks, leads to a combination of different “photon histories” that contribute to the observed image and must be disentangled, generally by comparing observations to predictions of complex radiative transfer models. Debris disks offer the possibility of more straightforward interpretations as all photons received by the observed only interact once with the disk.

Other approaches In addition to these two generic approaches, there are several other methods that can provide spatially resolved information about disks. First of all, disks around some Herbig Ae/Be stars have been spatially resolved in near- to mid-IR PAH³ observations. PAH grains are stochastically heated by the UV radiation of early-type stars and emit in a few bands between 3 and 12 μm . Comparing the morphology of disks in these bands and in adjacent continuum bands has revealed that PAH grains can be excited up to very large distances (well beyond 100 AU in some cases) in the surface layers of flared disks. As such, they provide key information regarding the *global structure* of disks on the large scale (vertical height, flaring), akin to scattered light images.

An unexpected source of *spatial* information about protoplanetary disks comes from photometric time series, which reveal variability from the optical to the to mid-IR on time-scales of a few days to a few months. At least some of these variations arise from inhomogeneities and/or asymmetries in the inner regions of disks, at a distance from the star determined by the observed time scale via Keplerian rotation. This approach can be used to probe the structure of disks within a few AU at most of the central star.

The various approaches outlined so far focus on the dust component of disks, which is the common element to protoplanetary and debris disks. However, most of the mass of protoplanetary disks is in gaseous form which can also be spatially resolved. For instance, the rotational lines of many molecular species lie in the (sub)millimeter regime, so that they can be mapped with the same instruments as their adjacent continuum. While this is currently limited to the most massive disks because of sensitivity limitations, this method can be used to study the chemical structure of disks as well as to measure the Keplerian rotation of circumstellar disks, hence the mass of the central star. At much shorter wavelengths, it is possible to apply the “spectro-astrometric” method to near-IR molecular emission lines. The objective is then to measure a spatial displacement of a source photocenter across a spectral emission line, revealing the emission from the hot gas component of the disk, which is located in the inner few AU.

Observational techniques Protoplanetary disks are too distant to be imaged with simple, ground-based imaging techniques at optical or IR wavelengths. Diffraction-limited devices (adaptive optics on large ground-based telescopes, or the Hubble Space Telescope) are necessary to image disks, providing a typical linear resolution of 5–10 AU, insufficient to discern details in the innermost regions of disks. Furthermore, except in the special cases of edge-on disks or polarized imaging, a coronagraph is required to block the light of the central star which, with the unwanted side effect of masking out the inner 50–100 AU of the disk as well. Nonetheless, an increasingly number of disks (currently about three dozens)

³ Polycyclic aromatic hydro-carbons

has been imaged in scattered light using these techniques. Debris disks, which are located much closer (down to a few pc from the Sun), can be imaged with very high linear resolution, up to 1 AU, and as close as a few AU from their parent star in favorable cases. Such images, typically dominated by scattered light can typically be obtained from the near-UV to the near-IR regime (2–5 μ m). Also, it is possible to use a back-end spectroscopic instrument (long-slit or integral field unit) to search for spectro-astrometric signatures of hot gas in the inner region of disks.

In the far-IR to millimeter regime, the spatial resolution afforded by single-dish telescopes is insufficient to resolve any protoplanetary disk, and only a handful of nearby debris disks have been resolved⁴. Long-baseline interferometers working in the (sub)millimeter range (VLA, IRAM Plateau de Bure, CARMA, ATCA, SMA) provide subarcsecond resolution, sufficient to resolve disks. Such instruments have been used to map the continuum thermal emission of protoplanetary disks in the outer regions of disks, specifically in the disk midplane which contains the highest density of dust particles. With the exception of rare cases, these interferometers are not sensitive enough to detect debris disks, however.

Long-baseline interferometric techniques in the optical, near- and mid-IR regimes have also been used extensively in recent years to map the innermost regions of protoplanetary and debris disks. The spatial resolution achieved by an interferometer is defined as λ/B where λ is the wavelength and B the *baseline*, that is the distance between the telescopes. For a typical baseline of 100m, the interferometric spatial resolution is ~ 4 mas and ~ 20 mas for the K and N bands, respectively, thus in adequacy with the angular sizes involved in our science case. The exquisite resolution these interferometers provide allows one to resolve the inner radius of many protoplanetary disks, although in most cases analyses are limited to comparison of interferometric data with synthetic model images of disks with simple morphological structures. In all cases, because of their intrinsically small field-of-view, as well as the use of an observing wavelength $\lambda \leq 15 \mu$ m, only the inner few AU of disks can be studied through such observations.

3.1.2 Inner disk regions: Observational findings

To date, well over 100 protoplanetary disks and over two dozen debris disks have been spatially resolved at one or more wavelengths⁵. We summarize some of the main findings resulting from these images for protoplanetary and debris disks, with a focus on findings that are related to planet formation.

Herbig Ae/Be stars: thermal emission of the dusty inner rim: Monnier et al (2005); Vinković and Jurkić (2007) have shown on a sample of Herbig Ae/Be stars that the interferometric size of the K band emission was correlated with the star luminosity, as illustrated on Fig. 4 (left). From this correlation they have demonstrated that the near-IR excess of such stars was – with at the exception of the most luminous ones – arising from the thermal emission of the inner part of the dusty circumstellar disk, located at the dust sublimation radius (roughly $T \sim 1500$ K for silicates), assuming that the dust is in equilibrium with the radiation field. If this scenario works well for Herbig Ae stars and late Be, it however fails to interpret the size of the IR excess emission region for the early Be, the inner rim being too close to the star regarding their high luminosity. In this case, one likely interpretation is that the gas inside the dust sublimation radius is optically thick to the stellar radiation, hence shielding a fraction of the stellar light and allowing the dusty inner rim to move closer to the star.

⁴ It must be noted that the *Herschel Space Observatory* is now rapidly expanding this list.

⁵ An up-to-date list is maintained at the <http://www.circumstellardisks.org/> website.

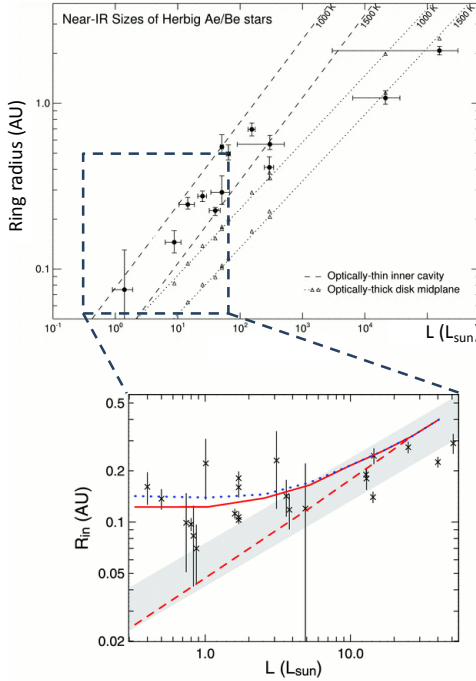


Fig. 4 K band interferometric size-luminosity relationship for intermediate (top, adapted from Monnier et al, 2005) and low (bottom, adapted from Pinte et al, 2008b) mass young stars. We can see that for the T Tauri regime, considering the thermal emission only (dashed line) does not reproduce the correlation whereas taking into account both the thermal and scattered light emission with the same disk model (solid line) does. (Reproduced by permission of the AAS)

T Tauri stars: a strong contribution of the scattered light. Together with the last improvements of interferometers in terms of sensitivity, it is only recently that the same kind of study could have been performed on the less luminous T Tauri stars. And the results that have been obtained were somewhat surprising, the size of the near-IR emission being *larger* than predicted (Akeson et al, 2005; Eisner et al, 2007b, 2005). Many hypotheses were invoked such as lower sublimation temperature $T_{\text{sub}} \sim 1000\text{K}$, fast dissipation of the inner disk, magnetospheric radii bigger than dust sublimation ones hence defining the location of the inner rim; until Pinte et al (2008b) had shown that when the luminosity of the star decreases, the contribution of the scattered light, in addition to that of the thermal emission, could not be neglected anymore. As a consequence these authors have convincingly demonstrated that the model of the inner disk located at the dust sublimation radius was holding for the T Tauri regime as well, and that no alternative scenario was required as long as the radiative transfer in the disk was thoroughly studied (thermal + scattered light).

The shape of the dusty inner rim: As it is directly and frontally irradiated by the star, it was quickly suggested that the inner rim would be probably thicker than the disk straight behind it which at the contrary only receives a grazing star light. As a result, the inner rim is expected to be “puffed-up”, hence casting a shadow on the outer part of the disk. However,

how big and sharp the puffed-up rim is and how pronounced the shadow behind appears remain open questions. In the past years, various models with increasing complexity have been developed to address this issue. After the first simple models by Natta et al (2001) and Dullemond et al (2001) in which the rim was assumed to exhibit a vertical wall, approximate 1-D (e.g. D'Alessio et al, 2004; Isella and Natta, 2005) and full 2-D radiative transfer models (e.g. Dullemond and Dominik, 2004a; Tannirkulam et al, 2007; Kama et al, 2009) have progressively shown that the rim was most likely rounded off, although the true vertical profile of the rim is hard to determine as it is highly dependent on dust and gas properties.

From an observational point of view, provided that the source is seen under a large enough inclination angle, images of its near-IR emission should all the more deviate from axisymmetry than the inner rim is sharp. Using three telescopes simultaneously, interferometry enables to measure such a level of asymmetry through the so-called “closure phase” observable (Monnier, 2000), the bigger the closure phase, the bigger the departure from axi-symmetry. In this framework, observations with the 3-telescope IOTA interferometer of a sample of 16 young stars (Monnier et al, 2006) have mostly revealed sources with small closure phases, hence ruling out the sharp vertical wall hypothesis and favoring a smooth rounded off structure for the inner rim. New observations with higher closure phase accuracy should be extremely fruitful to further constrain the shape of the inner rim.

The hot gas inside the dusty inner rim: Though dust is mostly dominating the near-IR continuum emission of young stars, there are some cases where the dust rim cannot account for the entire near IR excess observed in the SED. Particularly, in the case of stars where the accretion rate is high enough (roughly $> 10^{-7} - 10^{-8} M_{\odot} \text{ yr}^{-1}$) the contribution of the hot gaseous component to the near-IR excess cannot be neglected. Since the hot gas is located between the star and the dust sublimation radius, we expect its region of emission to be *hotter* and *more compact* than that of the dusty inner rim. As a consequence, observing at shorter wavelengths or longer baselines appears to be well suited to probe this region. This was first achieved by Isella et al (2008) which have observed the Herbig Ae star MWC 758 with the AMBER instrument on the VLTI, both in the H and K bands. They have shown that, if the K band observations alone are well interpreted by the classical dusty puffed-up inner rim (Isella and Natta, 2005), it fails to reproduce the H band observations for which the emission is less resolved than expected by this model. Furthermore, with this single model, the SED cannot be fitted successfully, showing a lack of energy in the H band. Conversely, by adding an unresolved hotter component (of $T = 2500\text{K}$) to the model, they managed to reproduce both the H and K bands measurements jointly. Given the temperature and the size ($\leq 0.1\text{AU}$) of this emission region, the unresolved component was then interpreted as arising from the hot gas accreting close to the star, an hypothesis reinforced by models of accreting gas (Muzerolle et al, 2004) which allowed for a satisfactory fit of the shape of the SED by filling the lack of energy in the H band. A somewhat similar strategy was used by Eisner et al (2007a) who observed different Herbig Ae/Be stars with the Keck interferometer (KI), using moderate spectral dispersion ($R=25$) within the K band. They have found that for several stars of their sample, single-temperature ring could not reproduce the data well, and that models incorporating radial temperature gradients or two rings should be preferred, supporting the view that the near-IR emission of Herbig Ae/Be sources can arise both, from hot circumstellar dust and gas. For example, the interferometric data of AB Aur require the presence of one dust inner rim together with a more compact and hotter component ($T \sim 2000\text{K}$) interpreted as coming from the hot dust-free inner gas. And as a matter of fact, this scenario was also proposed by Tannirkulam et al (2008) who observed the same star with the very long baselines (300m) of the CHARA interferometer, hence probing

smaller emission region and showing the need of adding smooth hot ($T > 1900\text{K}$) emission inside the dust inner rim, contributing to 65% of the K band excess.

However, as an increasing number of interferometric observations led to the direct detection of gas inside the dust sublimation radius, a careful analysis of the expected gas continuum emission shows that such a conclusion is eventually not straightforward. In the specific case of the Herbig Ae star HD 163296, Benisty et al (2010) have indeed pointed that neither gas LTE⁶ opacities – which produce strong molecular bands absent in the observed spectrum – nor H[–] non-LTE opacity – where the resulting continuum emission is too weak and presents an inconsistent wavelength dependence – could account for the extra IR excess not filled by the emission of the (silicate) dusty rim. Conversely, the presence of refractory grains inside the inner rim, such as iron, corundum, or graphite which can survive at much higher temperatures could be a satisfactory alternate interpretation. Similarly, the supposedly detection by interferometry of hot water molecular emission (MWC 480, Eisner, 2007) inside the dust sublimation radius was soon after invalidated by high-resolution spectroscopy single-dish observations of the same source which did not show the strong molecular lines expected (Najita et al, 2009). In one case, the young Be star 51 Oph, Tatulli et al (2008) confirmed that the strong observed CO overtone emission was originating from a region located at 0.15AU from the star – that is in the gaseous rotating disk –, but it seems that in a general manner this inner gaseous disks may be poorer in molecules than expected and the composition of the matter responsible for the continuum emission from inside the dusty rim remains unclear and more complex than first contemplated. The above puzzling examples emphasize the need to accompany interferometric measurement with (as long as possible) simultaneous high-resolution spectroscopic observation in order to avoid misinterpretation of the interferometric data. Whenever possible, directly recording dispersed interferograms with the appropriate spectral resolution obviously remains the best-suited solution, at it is discussed in the next section.

Accretion/ejection phenomena with gas line observations. One major achievement in interferometry in the past years is the capacity of spectrally dispersed the interferogram across the wavelength range, with resolution high enough (AMBER/VLTI: $R=1500$, see Petrov et al (2007), and KI: $R=250, 1700$, see e.g. Wizinowich et al (2004); Ragland et al (2008)) to spatially resolve the lines emission regions and separate them from that of the continuum, that is to directly probe – through their emission lines – the gaseous species which constitute 99% of the mass of the circumstellar matter. Among all the IR emission lines that are seen in young stars, the atomic transition of the hydrogen Br γ is by far the most observed in spectro-interferometry for it is the brightest and can therefore be studied with rather good signal to noise ratio (SNR). Two main scenarios are commonly in balance to interpret the origin of this emission line, scenarios for which the extension of the emission region will differ:

- *Magnetospheric accretion:* If the line is emitted in accreting columns of gas (Hartmann et al, 1994), then the region of emission lies roughly between the star and the corotation radius, that is *the line emission region is much more compact than that of the continuum* which comes from the dust sublimation radius.
- *Outflowing winds/jets:* At the contrary, if the line arises from outflows (Shu et al, 1994; Casse and Ferreira, 2000; Sauty et al, 2004), one expects the *line emitting region to be of the same size or bigger than that of the continuum*.

⁶ Local thermal equilibrium

By measuring the size of the emitting regions responsible for both the emission line and the surrounding continuum and compare their relative size, IR spectro-interferometry enables to disentangle between both scenarios and to constrain the origin of Br γ in young stars. Such an effect was investigated in parallel by both spectro-interferometric IR instruments AMBER and KI, first on single young stars (Tatulli et al, 2007; Malbet et al, 2007) and subsequently on surveys (Kraus et al, 2008; Eisner et al, 2009, 2010), and these author have found a large variety of spatial scales for the Br γ emission region, both smaller and bigger than that of the adjacent continuum. A complete comprehension of the phenomena at stake yet remains to be elaborated. However, these results have already suggested two distinct trends for the low- and intermediate-mass young stars respectively: if the correlation between magnetospheric-accretion and Br γ emission seems well established for T Tauri stars, it appears that for Herbig Ae/Be stars we are mostly probing outflows phenomena, the Br γ line being probably in this case an indirect tracer of accretion through accretion-driven mass loss (Kraus et al, 2008). Spectro-interferometry thus enables to spatially locate the emitting regions of IR lines in young stars, although in practice only the brightest one, Br γ , has been deeply investigated so far. With the regular increase in sensitivity of interferometers, this promising field is expected to move one step forward along two main axes:

1. The observation of weaker lines such as Pa β to probe the geometry of the region at the interface between accretion and the stellar surface, the structure of this interface playing a crucial role in mass loss and angular momentum regulation phenomena (Dougados et al, 2003), the iron line [FeII] to put further constraints on the MHD models on jets and their launching region (Pesenti et al, 2003), or several other lines directly tracing the hot rotating gas such as the CO molecule;
2. The interferometric observation at very high spectral resolution (typically $R \sim 8000$) in order to spatially *and spectrally* resolve the lines, thus tracing the various emitting regions along the lines from the wings towards the central part and accessing the kinematics and velocity maps of these regions, in order to directly measure the rotation at the base of the jets (Bacciotti et al, 2003; Dougados, 2009) as well as quantify the (Keplerian?) disk rotation of the hot gas around young stars.

The size of the 10 μ m region as a proxy for the disk vertical structure: Following through the circumstellar disk further away from the star than the inner rim, the middle disk – located roughly from one to few AUs and radiating at temperatures of a few ~ 100 K – is adequately probed by interferometry at mid-IR wavelengths. Particularly, such a technique has enabled to unveil its vertical structure as well as the composition of its surface layer.

By observing a sample of Herbig Ae/Be stars with the MIDI/VLTI instrument, Leinert et al (2004) have measured the radius of the 10 μ m emission region of the whole young stars and compared them with their mid-IR color. It was shown that the more red objects were displaying more extended emission than that of the more blue sources. Such a result is consistent with the classification of Meeus et al (2001) where the group I flared disks are redder and which mid-IR emission appears larger, whereas the group II flat self-shadowed disks present a more compact mid-IR emission.

Radial evolution of the disk mineralogy: Mid-IR interferometry can also provide spectrally dispersed interferograms (e.g. MIDI/VLTI, $R \sim 230$) in a wavelength range perfectly suited to study the silicate feature at $\sim 10 \mu$ m, which allows one to probe the radial composition of the disk atmosphere. One finds that the surface of the inner disk has larger and more crystalline (crystallinity fraction of 40% to 100%) silicate grains than that of the outer part,

being smaller and more amorphous. Remarkably enough, such a property holds for a large range of stellar masses, from the intermediate Herbig Ae/Be stars (van Boekel et al, 2004) to less massive T Tauri stars (Ratzka et al, 2007; Schegerer et al, 2008, 2009).

The connection to the outer disk regions Scattered light images and thermal emission maps have confirmed that many disks have outer radii beyond 100 AU although there is a large object-to-object scatter (Watson et al, 2007). In a handful of disks in which the inner regions have been depleted of small dust grains, millimeter mapping with interferometers has provided sufficient resolution to resolve the inner radius of the disk at a few tens of AU, typically (Pi  tu et al, 2006; Sauter et al, 2009; Hughes et al, 2009). This came as a direct confirmation of the prediction based on the peculiar SED of “transition” disks. In one case, the inner region has also been tentatively imaged in scattered light (Thalmann et al, 2010). It is generally believed that the inner hole in at least some transition disks is the result of carving by a forming planet, although this remains to be confirmed. More surprisingly, inner holes have been discovered in disks in which no prior evidence existed for such a structure (Isella et al, 2010a). Once again, this emphasizes the crucial importance of high-resolution observations in the analysis of any particular disk.

The outer structure of protoplanetary disks imaged in scattered light is flared (Burrows et al, 1996; Lagage et al, 2006; Perrin et al, 2006b; Okamoto et al, 2009), in accordance with simple models based on hydrostatic equilibrium, implying that stellar illumination is the only significant source of heating for the outer disk regions. It must be emphasized, however, that more than half of all known protoplanetary disks around T Tauri stars in nearby star-forming regions have *not* been detected in scattered light, despite multiple surveys using the Hubble Space Telescope or adaptive optics devices (Stapelfeldt & Ménard, priv. comm.). Because our current knowledge is biased towards flared disks which are much easier to detect since they intercept more starlight, it is possible that undetected disks represent a more advanced, settled state in disk evolution. In the specific case of intermediate-mass Herbig Ae stars, SED analyses have led to a picture in which, for so-called “group II” (Meeus et al, 2001), the outer disk lies in the shadow cast by the inner regions, reducing the chances to detect the disk in scattered light. Indeed, only two of the 10 disks imaged in scattered light around Herbig stars pertain to the group II discussed above. However, it remains unclear whether this phenomenon is related to the non-detection of many disks around T Tauri stars, for which no clear-cut distinction is seen in SED analyses. If confirmed, this could indicate strong evolution towards a geometrically thin, dense midplane which would provide appropriate conditions for planet formation.

The small number of resolution elements across the disk offered by currently operating (sub)millimeter interferometers prevents detailed studies of their surface density profile. Fitting power-law models to data indicates that the global density profile is typically $\Sigma(r) \propto r^{-0.5..-1}$, significantly flatter than the Minimum Mass Solar Nebula model (Kitamura et al, 2002; Andrews and Williams, 2007). Typical surface densities at a radius of 100 AU are on the order of a few g cm^{-3} . Recent work at the highest achievable resolution supports a picture in which the density profile is not well described by a single power law (Wolf et al, 2008), but is tapered towards the outermost regions (Isella et al, 2009; Guilloteau et al, 2011). Because none of these observations actually probe the region in which planets are thought to form (inside of 10 AU), current estimates of the actual surface density in the inner regions are strongly dependent (by more than two orders of magnitude) on inward extrapolation of the outer density profile, so that it remains impossible to directly assess whether the density in the midplane of a given disk is high enough to sustain planet formation.

Beyond these global characteristics, spatially resolved observations of disks have revealed a slew of asymmetries and small-scale structure in many disks (Mouillet et al, 2001; Fukagawa et al, 2004; McCabe et al, 2011). Spiral arms and gaps may be related to the presence of embedded protoplanets, although their interpretation is often ambiguous due to the large optical depth of the disks. Density perturbations induced by an outer stellar companion or a self-gravitating disk are equally plausible in many cases (Reche et al, 2009). Lateral large-scale asymmetries are generally thought to trace the inhomogeneous structure of the inner disk that affects the illumination pattern of the outer disk. The clearest illustration of this phenomenon is the variability seen in the images and integrated polarization signal of the HH 30 edge-on disk (Watson and Stapelfeldt, 2007; Durán-Rojas et al, 2009). This phenomenon may be related to the quasi-periodic shadowing observed in AA Tau, in which the inner wall of the disk is warped and the base of the accretion column onto the star periodically occults our line of sight to the star (Bouvier et al, 2007). Recent photometric timeseries obtained with the *CoRoT* telescope revealed that this phenomenon may indeed be common among T Tauri stars, with a frequency as high as 30% (Alencar et al, 2010).

While millimeter observations of disks have unambiguously established that the largest dust grains in the midplane are at least millimeter-sized, it is still extremely challenging to probe their radial dependencies. Early attempts indicate little-to-no differences as a function of radius (Isella et al, 2010a; Guilloteau et al, 2011). In the disk upper layers, scattered light images indicate that their optical properties are grossly similar to those of interstellar grains, although in several cases, power law size distributions have to be extended up to a maximum grain size of a few micron to better reproduce the data (Burrows et al, 1996; Stapelfeldt et al, 1998; McCabe et al, 2003; Duchêne et al, 2004; Sauter et al, 2009). Nonetheless, power-law distributions with a maximum grain size of $10\ \mu\text{m}$ or larger are systematically excluded, indicating that the dust properties are significantly different from those of the midplane (Duchêne et al, 2002; Wolf et al, 2003; Pinte et al, 2008c). Polarization mapping of protoplanetary disks has also revealed high degrees of polarization, typical of small dust grains (Silber et al, 2000; Glauser et al, 2008; Perrin et al, 2009). A stratified structure is a common prediction to models of grain growth and settling, whereby larger grains reside much lower than small ones due to their weaker coupling to the gas. Detailed multi-wavelength studies of at least a handful of disks have confirmed such a settled disk structure (Duchêne et al, 2004; Pinte et al, 2008c). In some disks, this picture is also supported by a dust scale height that is smaller than expected based on an hydrostatic equilibrium gas structure (Watson et al, 2007). Finally, water ice coating of dust grains in the disk outer regions has been confirmed in scattered light imaging taken in and out of the $3\ \mu\text{m}$ absorption band for several disks (Terada et al, 2007; Honda et al, 2009; McCabe et al, 2011) or spatially resolved spectra (Schegerer and Wolf, 2010). In all cases, these conclusions apply to the outer disk, tens of AU away from the star. It is natural to assume that this is also true in the inner disk, but it cannot be confirmed directly with current observations.

Debris disks As discussed above, the closer distance to many debris disks enables much higher linear resolution, down to sub-AU scales. At this resolution, many disks show significant departures from smooth, axisymmetric structures: gaps, warps, dual midplanes, lateral density asymmetries have all been identified (Mouillet et al, 1997; Goliowski et al, 2006; Fitzgerald et al, 2007a; Kalas et al, 2007b; Schneider et al, 2009). Some of these structures, namely gaps and warps, are frequently interpreted as evidence for the presence of undetected planetary objects. This interpretation has recently been strikingly confirmed in two debris disks, whose structure led to a correct prediction of the semimajor axis of the putative planet, which was subsequently directly imaged (Kalas et al, 2008a; Lagrange et al, 2009).

Several other debris disks show similar structures although no planet has been found to date (Koerner et al, 1998; Schneider et al, 1999). Furthermore, some disks have shown to be eccentric or off-centered, which is most easily explained by the influence of an unseen massive body on an eccentric orbit (Kalas et al, 2005; Buenzli et al, 2010).

Scattered light images of many disks, especially when coupled with SED analyses, have allowed one to locate precisely the location of a “parent” body ring. Semimajor axes range from a few AU to up to 100 AU from the central star, indicating that planetesimal formation can occur over a broad range of radii or, alternatively, that migration mechanisms, along with resonance trapping with full-size planets, can carry planetesimals over large distances after their formation.

In the parent body ring, planetesimals constantly collide with each other, producing vast amounts of small dust grains which are subsequently carried away from the ring via radiation pressure or stellar wind pressure. Only grains smaller than \sim mm/cm can be directly detected, so studies of debris disks are limited to the analysis of this secondary dust population. In the rare cases where the same disk has been imaged over two or more orders in wavelengths (any combination of scattered light imaging, mid-IR imaging and submillimeter mapping), striking differences in morphology have been observed, indicating that grains of different sizes follow different spatial distributions (Fitzgerald et al, 2007b; Maness et al, 2008). When coupled with a dynamical model of the disk, this can be used to infer more robustly the location of the various components of the disk.

As is the case for protoplanetary disks, scattered light images of a debris disk allow one to constrain the grain size distribution, most notably the size of the smallest grains in the disk. Generally speaking, these are in the $0.1\text{--}5\,\mu\text{m}$ range and in good agreement with the expected blow-out size given the central star luminosity and/or stellar wind (Boccaletti et al, 2003; Clampin et al, 2003; Golimowski et al, 2006; Kalas et al, 2007a). It is arguable whether a strict power-law size distribution should be expected in a collisional cascade (Thébault and Augereau, 2007). Here, scattered light images at multiple wavelengths can provide constraints for the grain size distribution. Most importantly, departures from spherical compact grains has been identified in one disk and suggested in at least another one (Schneider et al, 2006). In particular, polarimetric imaging of the debris disk surrounding AU Mic has revealed that the smallest dust grains are highly porous (Graham et al, 2007; Fitzgerald et al, 2007a). It is likely that this property was inherent to the colliding parent bodies, raising the question of the efficiency of grain compaction during the growth phase of dust grains. Because porous grains have a much smaller density, they react differently to the various forces exerted on them during the evolution of disks, so this property could be important for planet formation theories. Unfortunately, it is extremely challenging to demonstrate that small dust grains are indeed porous in earlier stages of disk evolution (Pinte et al, 2008c; Perrin et al, 2009).

3.2 Exoplanets

The analysis of the structure of extrasolar planetary systems and the analysis of basic characteristics of exoplanets since the mid-1990s allow one now to approach the question of planet formation from the perspective of the “results” of this process. For this reason, a brief overview about the current state of planet detection capabilities and results is summarized in this section.

A recurrent feature in the field of exoplanet observation is that model expectations have been repeatedly challenged and overhauled by observations. The majority of planetary sys-

tems detected to date have turned out to be strikingly different from the Solar System in several fundamental ways. However, before briefly evoking these results in more details below, it is important to keep in mind that our present knowledge is strongly constrained by the detection biases of the observing techniques, and that it is still possible that our Solar System is representative of the most common types of planetary systems.

About 700 planets are known with a radial-velocity signature, spanning periods between less than a day and several years, and masses from the brown dwarf limit to a few Earth masses (see exoplanets.org, exoplanet.eu). More than 1000 transit candidates, a majority of them probably bona fide planets, have been identified by the Kepler mission, down to sizes of 1 Earth radius (see, e.g., Lissauer et al, 2011). Other techniques have identified planets in lower numbers, but in interesting regions of parameter space: very light planets around pulsars, distance planets with microlensing, free-floating planets and wide systems with imaging.

Planet diversity The planets detected today practically fill all the volume in parameter space allowed by physical constraints and detection limits, and this is arguably the most impressive and unexpected result of the first ~ 15 years of exoplanet research. The Solar System features three types of planets, cold gas giants and ice giants, and warm rocky planets, all orbiting on relatively circular orbits, aligned with the rotation plane of the Sun, and with internal compositions compatible with accumulation of condensate material and accreted gas at or near their present orbital distance.

By contrast, *a*) the eccentricity distribution of exoplanet orbits is very broad, much closer to that of binary stars than of the Solar System, with circular orbits being exceptional (except very close to the star where tidal forces had time to circularize the orbit), *b*) close-in planets are common, down to the shortest orbital distances allowed by tidal destruction, *c*) the orbit of many close-in planets is not aligned with the rotation plane of the star, *d*) giant planets with much higher masses than Jupiter exist, all the way to the Brown Dwarf limit around $12 M_{Jup}$ and higher, *e*) many close-in gas giants are much larger than predicted by models, *f*) planets with masses between ice giants and rocky planets are not uncommon, and *g*) the composition of planets does not correlate much with the material available in the protoplanetary disk at their present orbital distance.

The one point of agreement between observations and previous expectation is the basic prediction of core-accretion theory. A clear link is observed between the presence of heavy planets around a star and the host star's content of heavy elements (Santos et al, 2004; Fischer and Valenti, 2005), thus presumably the abundance of dust in the protoplanetary disk. Furthermore, high-density planets with masses below the critical mass of accretion of hydrogen and helium are abundant. The ensemble features of the planet population confirm the basic tenets of the core-accretion models. Although the competing scenario for giant planet formation – formation by disk gravitational instability – has not been ruled out entirely, it seems to be confined to a minority of cases, at least in the regions of parameter space probed by present surveys.

Giant planets Because of their enhanced detectability, the most extensively studied category of giant planets is the so-called “hot Jupiters”, gas giants on close orbits (inside 0.1 AU). Their statistical properties are now well known and outlined in the next paragraphs. Hot Jupiters accompany around one Solar-type star in 200 (Gould et al, 2006; Howard et al, 2010). At larger orbital distances, gas giants get more common as the orbit get wider, reaching a frequency of about 5 % of solar-type stars out to radii of 2-3 AU (Marcy et al, 2005). As radial-velocity surveys do not seem to have reached the mode of the gas giant frequency

distribution yet, the actual frequency including Jupiter analogues could be comparable or much higher. At the other extreme in orbital distance, imaging surveys show that giant planets are also present at distances larger than the Neptune orbit (Marois et al, 2008; Kalas et al, 2008b). The statistics of this population will emerge in the coming years as imaging surveys like GPI and SPHERE get in full swing. One intriguing early indication from the HR8799 system is that cold gas giants are not analogous to brown dwarfs of the same temperature, but differ drastically in colors, a possible indication of different cloud coverage (Bowler et al, 2010).

Hot Jupiters are found at all orbital distances down to a few multiple of the distance at which the planet would fill its Roche lobe ($P=1\text{--}3$ days depending in the mass), and seem to accumulate against this limit. A “pile-up” of orbits is observed near $P=3$ days for gas giant lighter than Jupiter, with a mass dependence leading to periods near 1–2 days near masses of $2 M_{\text{Jup}}$ (Mazeh et al, 2005). The pile-up seems absent for higher masses (Pont, 2009). The angle between stellar spin and planetary orbit – measured for transiting planets by the radial-velocity anomaly observed during the transit, the “Rossiter Mc Laughlin effect” – shows a very wide distribution, all the way from aligned orbit to polar or entirely retrograde orbits, again with the exception of very close orbits which are generally aligned (Winn et al, 2010). Because of these last two observations, the balance of evidence to explain the presence of hot Jupiters and close-in planets generally has recently been tilting away from explanations involving inward migration in the protoplanetary disk, towards dynamical evolution after the disk has dissipated. The leading explanation now invokes planet–planet dynamical interactions and planet–star tidal interactions to bring planets inward and explain where they end up (Naoz et al, 2011). Only violent dynamical interactions seem able to account for the high level of disorder in the distribution of spin-orbit angles, although scenarios invoking disk–planet interactions have also been invoked (Lai et al, 2011).

Many hot Jupiters have a much larger radius – as measured by the depth of the brightness dip during transits – than predicted by structure models. Several explanations have been proposed, and as more transiting planets have been discovered it is now clear that the size anomaly is closely related to the amount of incoming irradiation received from the host stars. Hot Jupiter atmospheres seem able to transfer a significant fraction of the incoming radiative energy into internal entropy, via one or several processes that may or may not include ohmic dissipation (Batygin and Stevenson, 2010), or eddy dissipation (Showman and Guillot, 2002; Youdin and Mitchell, 2010). Other explanations have been proposed for the anomalous radii but do not account for the observed dependence with stellar irradiation.

Observations have been gathered on the atmospheres of hot Jupiters during transits, secondary eclipses or phase variations, and it appears that there is more than one type of hot Jupiter atmosphere. This field is still in its infancy and there are few robust observations. For most objects, the data consist of a series of secondary eclipse depth measurements in a subset of the *Spitzer* telescope channels of $3.6\text{--}24\,\mu\text{m}$, giving a broad outline of the energy distribution of the day-side thermal irradiation of the planet. Tentative indications from these observations include the following: some atmospheres have a temperature inversion in the lower layers and others do not (Fortney et al, 2008a), the general atmospheric circulation is dominated by eastward jets (Knutson et al, 2009), some hot Jupiters are very dark and others reflective (Cowan and Agol, 2011), the fate of the incoming stellar light can be dominated by alkali metal absorption (Na and K) (Sing et al, 2008), or by scattering from a haze layer. Explanations for these features are yet very tentative, including the presence of a layer of titanium oxide vapor for the temperature inversion, and silicate dust grains for the high-altitude haze.

Spectra are now being collected for much colder planets discovered by direct imaging, and the study of gas giant atmospheres at the other end of the temperature range can be expected to blossom soon. Already, as mentioned earlier, the preliminary indication that the clouds on the planets of HR8799 do not behave like those on brown dwarfs of the same temperature is very tantalizing.

Terrestrial planets The NASA Kepler mission is bringing a quantum leap in our knowledge of lower-mass exoplanets. The veil on statistical properties of $10\text{-}20 M_{\oplus}$ planets, that was slowly moving one planet at a time, was lifted in one sweep by the results of the first year of Kepler data.

The initial Kepler results indicate that the abundance of planets keeps increasing towards smaller masses and towards larger orbital distance. From around 0.5% for hot Jupiters orbiting sun-like stars, the frequency of planets increases tenfold towards masses in the $10\text{-}20 M_{\oplus}$ range, and tenfold again from short orbital distances to 1 AU. These results offer, qualitatively, strong support for the standard core-accretion scenario of planet formation, although they differ markedly in detail. Population synthesis using core-accretion models and disk migration predicted a gap in mass between gas giants and planetary embryos near the critical mass for runaway accretion of hydrogen and helium ($15 M_{\oplus}$), but such a gap is not observed. The size distribution of more than 1000 planet candidates from Kepler is rather smooth, suggesting that the neat separation in the Solar System between gas giants, ice giants and terrestrial planets is not a universal outcome of planet formation.

With apparently continuous distributions in mass and orbital distance, it is tempting to extrapolate the present distribution towards Earth analogues. If the power-law parametrization of the presently observed distributions are extrapolated to approximately $1 M_{\oplus}$ and 1 AU, they amount to a star-to-planet ratio near unity (obviously counting the fact that a single star can have more than one planet) – a very remarkable result that would imply that terrestrial planets are an extremely common outcome of star formation. The Kepler mission will soon reach this regime and be able to provide a solid answer.

The sparser results from microlensing surveys, probing large orbital distances, and even the few known cases of terrestrial planets orbiting pulsars, are also broadly supporting these abundance estimates.

Planetary systems Another remarkable outcome of radial-velocity and transit surveys is the finding that systems with more than one planet are common. The Kepler mission has discovered more than one hundred systems with two or more transiting planets, and up to six transiting planets in the same systems. Given the geometric bias requiring alignment of the orbital planes with the line of sight for the transits to be observable, the high occurrence rate of systems with multiple transits is remarkable and was not expected. Radial-velocity surveys have also uncovered systems with more than four planets, although the exact number is often difficult to establish given the sparse data sampling and the superposition of all the orbital signals, and the lowest-mass candidates are usually doubtful.

When the selection effects are taken into account, it appears that planets are very commonly found in systems. Interestingly, it seems that many systems are quite close to the stability limit, “dynamically full” in the sense that the addition of one major planet would lead to short term instability and catastrophic dynamical evolution. This, together with the misaligned spin-orbit angles of many hot Jupiters, has lent support to the speculation that planet formation was in some sense “too efficient” and initially leading to over-crowded systems which would later evolve by dynamical interaction, possibly leading to the formation of close-in planets and the ejection of free-floating planets. This is a powerful constraint from

planet formation model, which struggle to understand how the formation process clears all the hurdles between dust grain and full-fledge planet, let alone the problem to form planets in such abundance.

Some known planetary systems exhibit orbital resonance between two or more planets, but as an exception rather than a rule, perhaps suggesting that violent dynamical interactions are more common than orderly inward migration of several planets together.

Habitability The concept of habitable planets has generated an abundant literature, but based on a single example and few data, it has yet to demonstrate its relevance. While there is general agreement as to which orbital ranges are favorable to the presence of liquid water on the surface of a terrestrial planet, there is much variation in the details, and clear determinations of habitability are difficult to achieve in specific cases (Selsis et al, 2007). It is not clear that the concept of habitability extends to non-solar stellar types in a straightforward manner. For example, M stars are strong sources of UV radiation which may be a second important parameter aside of temperature for the permanence of liquid water and a substantial atmosphere (Raymond et al, 2007). Furthermore, it is not obvious if a mild temperature, resulting from equilibrium with the stellar radiation is the only or even the main source of habitability (the greenhouse and anti-greenhouse effects can maintain surface temperatures very far from the equilibrium temperature on a planet with a thick atmosphere, and geothermal or tidal energy are able to keep a surface ocean liquid even with low stellar irradiation). Therefore, even though the $M \sim 1 M_{\oplus}$, $T_{\text{eq}} \sim 300$ K region is obviously a soft spot for planet searches from the point of view of habitability and from a parochial perspective, there is nothing in our present knowledge that makes compelling the belief that this is very tightly connected to habitability or astrobiological interest (see also Lammer et al, 2009).

4 Scientific potential of optical to mid-IR interferometers

With the background of the theoretical models for the disk evolution and planet formation and corresponding observational findings, we now discuss the role of near-future long-baseline interferometers working from optical to the mid-IR wavelengths.

In this section, we will first review quickly the capabilities of coming interferometric instruments (Sect. 4.1) before outlining selected science cases in Sect. 4.2. These discussions are complemented by an outlook on synergy effects expected from observations with near-future large observatories and interferometers both in the IR and the (sub)millimeter domain in the subsequent section (Sect. 5).

4.1 Selected near-future interferometric instruments

To a great extent, the current knowledge about the inner part of protoplanetary disks has been obtained with interferometric instruments that are presently in operation: AMBER⁷ (Petrov and The AMBER Consortium, 2003) and MIDI⁸ (Leinert et al, 2003) on the VLTI (Glindemann et al, 2003), MIRC⁹ (Monnier et al, 2004), CLIMB¹⁰ and VEGA¹¹ (Mourard

⁷ Astronomical Multi-beam Combiner: the near-infrared/red focal instrument of the VLTI

⁸ Mid-infrared interferometric instrument

⁹ Michigan Infrared Combiner

¹⁰ Classic Infrared Multiple Beamcombiner

¹¹ Visible spectrograph and polarimeter

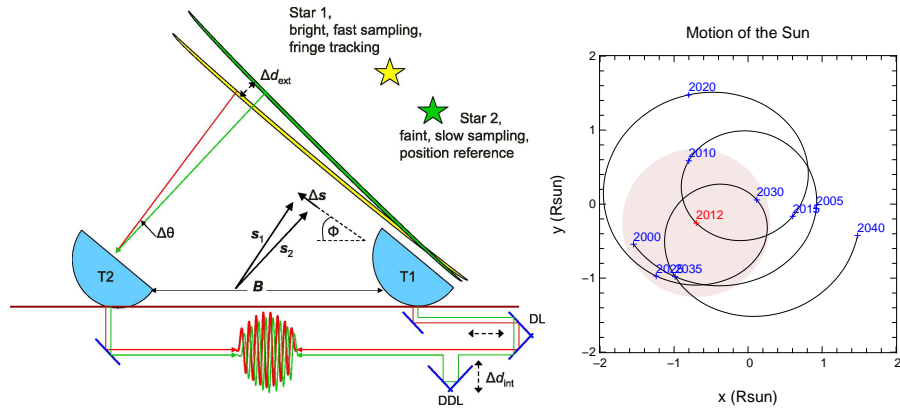


Fig. 5 Left: Schematic principle of dual-star narrow-angle astrometry (from Launhardt 2009). Right: Astrometric wobble of the Sun under the influence of solar system planets (in solar radii). (Reproduced with permission from Elsevier)

et al, 2010) on CHARA¹² (ten Brummelaar et al, 2005), and SPR¹³ and the N band nullder (Millan-Gabet et al, 2011) on the KI (Perrin et al, 2006a). Furthermore, the PTI¹⁴ (Pedretti et al, 2008) and IOTA¹⁵ (Pedretti et al, 2008) have been used for circumstellar disk studies until recently. For selected results obtained with these interferometers and instruments, we refer to Sect. 3. Here, we present the near-future instruments that will be available on the VLTI, the Keck telescopes, and will discuss, exemplarily, the new optical/infrared interferometer MROI.

4.1.1 VLTI/PRIMA

PRIMA is a facility that will soon provide the VLTI both with a new instrumental capability and an enhancement of the existing instruments AMBER and MIDI (Delplancke, 2008). It results from the joint effort of ESO and the ESPRI¹⁶ (Launhardt, 2009). It will offer the following new observing functionalities:

1. Astrometric detection with accuracy expected to be down $\sim 50 \mu\text{as}$;
2. Faint object observation with MIDI and AMBER;
3. Phase-referencing imaging with MIDI and AMBER;

PRIMA implements a narrow-angle dual-star astrometric capability to the VLTI. The schematic principle of narrow-angle astrometry can be seen in Fig. 5 (see also Shao and Colavita, 1992). Two telescopes are used to observe interferometrically and simultaneously two objects in the sky. By using internal metrology and a proper knowledge of the telescope array localization it is possible to provide a measurement of the astrometric distance between the two objects.

¹² Center for High Angular Resolution Astronomy

¹³ Self-phase referencing

¹⁴ Palomar Testbed Interferometer

¹⁵ Infrared Optical Telescope Array

¹⁶ ESPRI is a consortium led by the Observatoire de Genève (Switzerland), Max Planck Institute for Astronomy, and Landessternwarte Heidelberg (Germany)

PRIMA's success relies on the inclusion of several new subsystems at VLTI and their joint operation. These subsystems are the building blocks of a proper astrometric system. They include:

1. Star Separator Systems at each Auxiliary Telescope focus (possibly extended to the Unit Telescope array). This system will allow one to observe simultaneously two objects in the isoplanatic sky patch: the science target and a reference object.
2. Two Fringe Sensing Units (FSU A and B). These instruments allow one to track simultaneously interference fringes on two objects.
3. Differential Delay Lines (DDL) that compensate for the optical path difference between the two objects therefore allowing one their simultaneous observation.
4. A Metrology System (PRIMET) that allows the angular distance between the science target and the reference to be measured.

With all these systems in place, PRIMA should be able to track on a reference star and monitor the astrometric wobble of the science target. As of July 2011 all PRIMA subsystems that have been installed on the mountain are almost all individually operational. Their common operation is now the focus of all the efforts. Once ready, PRIMA will be offered to the astronomical community.

4.1.2 VLTI/GRAVITY

GRAVITY (Gillessen et al, 2010) is a second generation instrument for the VLTI. It has been designed specifically to observe highly relativistic motions of matter close to the Galactic Center where a massive black hole gravity reigns.

To reach its final purpose, observing the astrometric motion of the faint near-IR flare at the center of the Milky way, GRAVITY will have to reach an unprecedented sensitivity. It will offer the possibility to observe with four telescopes in imaging and narrow-angle astrometric mode. It will add to the VLTI infrastructure near-IR sensitive adaptive optics and the capability to fringe track on a reference object within one telescope field-of-view (i.e. 2" for the UTs). GRAVITY will allow objects of magnitude up to $K \sim 18$ to be observed as long as a suitable off-axis reference object is available ($K \sim 10$). In on-axis mode the sensitivity will be $K \sim 10$.

In its imaging mode GRAVITY/VLTI will offer the measurement of interferometric observables (visibility, differential phases, closure phases, and triple amplitudes) on six baselines with \sim mas resolution. With time and earth-induced projection effects the uv plane can be properly sampled, therefore paving the way for conventional aperture synthesis image reconstruction. Three spectral resolution modes in the K band will be accessible i.e. $R \sim 22,500,4000$.

In its astrometric mode, using a newly implemented metrology system, GRAVITY will allow the measurement of angular distances with accuracies as low as $10 \mu\text{as}$. Detecting a displacement of $10 \mu\text{as yr}^{-1}$ corresponds to $\sim 7 \text{ m/s}$ at 150 pc, a typical distance for star-forming regions.

4.1.3 VLTI/MATISSE

MATISSE¹⁷ (see, e.g., Lopez et al, 2009; Wolf et al, 2009) is a mid-infrared spectro-interferometer combining the beams of up to four UTs or ATs of the Very Large Telescope

¹⁷ Multi Aperture Mid-Infrared SpectroScopic Experiment

Interferometer (VLTI). MATISSE will measure closure phase relations and thus offer an efficient capability for image reconstruction. In addition to this, MATISSE will open two new observing windows at the VLTI: the L and M band in addition to the N band. Furthermore, the instrument will offer the possibility to perform simultaneous observations in separate bands. MATISSE will also provide several spectroscopic modes. In summary, MATISSE can be seen as a successor of MIDI by providing imaging capabilities in the mid-infrared domain. The extension of MATISSE down to $\sim 3\ \mu\text{m}$ as well as its generalization of the use of closure phases makes it also an extension of AMBER. Thus, in many respects MATISSE will combine and extend the experience acquired with two first generation VLTI instruments – MIDI and AMBER.

MATISSE will extend the astrophysical potential of the VLTI by overcoming the ambiguities often existing in the interpretation of simple visibility measurements. The existence of the four large apertures of the VLT (UTs) will permit to push the sensitivity limits up to values required by selected astrophysical programs such as the study of AGNs and extra-solar planets. Moreover, the existence of ATs which are relocatable in position in about 30 different stations will allow for the exploration of the Fourier plane with up to 200 meters baseline length. Key science programs using the ATs cover for example the formation and evolution of planetary systems, the birth of massive stars as well as the observation of the high-contrast environment of hot and evolved stars.

The primary goal of MATISSE is to allow image reconstruction in the mid-infrared wavelength range with an unprecedented spatial resolution of $\sim 10\ \text{mas}$. A sufficient *uv* coverage will be reached on the basis of 3-5 different AT configurations (with 1 night of observation per AT configuration). Constrained by the dynamical evolution of MATISSE targets on $\sim \text{mas}$ scale, the different AT configurations (i.e., a complete set of observations for a given target) should be scheduled within a period of two-four weeks. The comparison between models and visibility points and phases in the Fourier plane is considered as an alternative approach for the data analysis. This approach will profit from the combination of the experience gained with MIDI (data analysis in the N band) and radio interferometry (simultaneous analysis of many *uv* data points).

In the N band, the sensitivity of MATISSE depends on the number of combined beams but is in general comparable to MIDI. The type and number of astronomical sources per object class is therefore comparable to those of MIDI. MATISSE will allow one to investigate the expected complex nature of the small-scale structures traced with MIDI. These observations are expected to significantly improve our understanding of fundamental astrophysical processes in various classes of objects (e.g., planet formation / planet-disk interaction, structure of AGN tori).

In the L&M bands, observations will allow one to trace regions with higher characteristic temperatures. The physical conditions and chemical environment can therefore be studied in different regions (e.g., in protoplanetary disks, or stellar winds). While N band observations are clearly dominated by the thermal emission of warm and cool dust, L/M band continuum images are expected to be dominated by the scattering and thermal emission of radiation of hot dust grains. Thus, MATISSE will provide complementary information about the structure of the dusty environment of the various astrophysical objects, but also about the dust properties. Furthermore, in L band the highest sensitivity is expected due to the reduced background emission.

MATISSE will provide a spectral coverage from the L band ($\sim 3\ \mu\text{m}$) to the N band ($\sim 13\ \mu\text{m}$) with spectral resolutions of $R \sim 30$ (L/N), 100–300 (L/N), and 500–1000 (L). Beside an individual analysis of measurements in different bands, the combination of data from multiple bands is expected to provide much stronger constraints on models of science targets

than data from a single band alone. This is due to the different regions (spatial resolution), different physical conditions and processes (temperature), and origin of the radiation (re-emission, scattering) of the MATISSE targets that can be traced in L to N band the wavelength range.

4.1.4 VLTI/VSI

The VLTI Spectro Imager (VSI; Malbet et al, 2008) instrument has been proposed in 2006 to ESO as a possible VLTI 2nd generation instrument dedicated to spectro-imaging at the milli-arcsecond scale of various compact astrophysical sources in the near-infrared. Compared to GRAVITY, it would bring the *J* and *H* bands, high spectral resolution and the possibility to use 6 VLTI beams at the same time offering an imaging snapshot capability within a night.

VSI will provide the astronomical community with spectrally resolved near-infrared images at angular resolutions down to 1.1 mas and spectral resolutions up to $R = 10000$ to 30000. Targets as faint as $K = 13$ will be imaged without requiring a brighter nearby reference object; fainter targets can be accessed if a suitable off-axis reference is available. This unique combination of high-dynamic-range imaging at high angular resolution and high spectral resolution for a wide range of targets provides the opportunity for breakthroughs in many areas at the forefront of astrophysics, especially for the formation of stars and planets.

VSI will probe the morphology of the dusty close environment of pre-main-sequence stars at NIR where the temperature of the emitting material is close to the dust sublimation temperature. Therefore it will focus on the central radiation field in the environment structure, i.e. the exact shape of the sublimation surface/rim and inner cavity. It will permit to correlate the morphology with dust properties, but also to detect possible planetary orbiting companions which open cavities in the central disk region. This information is important to understand the influence of planetary companions on the planet formation and migration scenarios. The structure of the inner disk revealed by the capacity of image reconstruction with VSI can help to understand the initial conditions for planet formation.

The most remarkable feature of VSI is its capacity to get snapshot images of these environments within a night, opening the path to time-dependent morphology. At Taurus distance, the Earth orbit is located at 7 mas. Therefore, all motions within this radius will have time constants of the order of months and even less. For the first time a systematic study of the orbital evolution of the dusty environment will be feasible and compared to numerical simulations. By comparing objects at different evolutionary stages, the time scales for the morphological evolution and dissipation can be addressed. With VSI, a considerable advance in PMS stellar evolution models is expected and more precise timing of the central stars will be available. The spectral capacity of VSI in the NIR domain will allow the estimation of the stellar mass. This mass directly affects the central radiation field and the dusty environment via sublimation/heating and radiation pressure.

4.1.5 KI/ASTRA

The KI¹⁸ combines the two 10m Keck telescopes with a baseline separation of 85m. The resulting resolution of $\lambda/2B \sim 2.7$ mas at $2.2 \mu\text{m}$ is about a factor 3 better than the diffraction limit of the planned ~ 30 m class next generation of ground-based telescopes currently

¹⁸ Unfortunately, NASA has currently decided to cease operations funding for the KI for budgetary reasons. Please check for more up-to-date information the Keck Interferometer support page: <http://nexsci.caltech.edu/software/KISupport/>

under development. The opto-mechanical complexity of the imaging process of 30 m telescopes (Gilmozzi and Spyromilio, 2008) will make it difficult to match and outperform the high precision of *interferometric* astrometry with *imaging* astrometry. Recent developments include the addition of nulling interferometry and improved sensitivity (Colavita et al, 2008).

ASTRA, which stands for the *ASTrometric and phase-Referenced Astronomy*, is a major development effort to broaden the astrophysical applications of the KI (Woillez et al, 2010). There are three modes of ASTRA which implement continuous corrections for phase distortions by increasing degree of complexity: the self-referenced spectroscopy (SPR) stabilizes fringes *on-axis* directly on the science target and enable higher spectral resolution up to a few thousands; dual-field phase-referenced visibility measurements (DFPR) stand for integration beyond the atmospheric coherence time to reach $K=15$ mag on science targets while locking the fringe tracker on an offset guide star; the narrow-angle astrometry mode (AST) eventually will measure distances between a pair of stars within the isopistonic patch to a precision of $50\ \mu\text{as}$. The three ASTRA steps, or modi of operation, gradually increase the technological complexity. The SPR mode (Woillez et al, 2010; Pott et al, 2010) is already in operation and we focus here in the two other coming developments.

Dual-field operation. The dual-field operation is a natural extension of the SPR mode. Two fringe cameras run in parallel. The first one tracks the fringes for good piston and vibration correction, enabling much longer integration times at the second camera to increase the SNR. But in contrast to SPR, the dual-field phase-referencing mode focuses on increasing the limiting magnitude of the low-dispersion mode by about 5 magnitudes to allow one pointing the second fringe camera on a faint star within the isopistonic patch around a bright star. The key difference in the implementation between these first two phases is that for the dual-field operation the light has to be split already in the image plane at the Nasmyth foci of the telescopes. After this field separation, the light travels along two separate beam trains down to the beam combining laboratory, thus a doubled delay line infrastructure is needed. The additional delay lines are already in regular use for the operation of the KI nullder instrument. The advantage of the dual-field operation is two-fold. The atmospheric differential piston, as measured on the bright star in the primary field, can be applied to both fields to stabilize the fringe motion. This correction is effective as long as the star separation is smaller than the isopistonic angle. But monitoring helper systems are needed to ensure that the non-common path after the beam separation does not suffer from vibration induced decorrelation and differential tip-tilt. DFPR operation will also allow one to use the one (unresolved) star as phase reference against the other. An unresolved star, used as phase reference, has no intrinsic visibility phase, so the measured phase derives entirely from the atmosphere and the instrument. This knowledge can be used to calibrate and retrieve the intrinsic phase information from the (fainter) companion in the second field. This will allow the measurement of imaging information about the object in the second field, as long as its position and the related astrometric phase is known. For instance asymmetric dust distributions would produce intrinsic phase signals. First on-sky tests validated the ASTRA dual-field hardware during the summer 2010, separate fringes on two stars were recorded.

Astrometry For the phase-referenced visibility measurement (DFPR), the absolute fringe location does not matter, as long as the geometrical delay is corrected for well enough to ensure that the fringe pattern stably ends up on the detector. The visibility information is encoded in the *contrast* of the interference signal. But astronomical information is also contained in the differential fringe *location* which encodes the absolute separation between two

stars. ASTRA-AST (Pott et al, 2009; Woillez et al, 2010) is designed to measure the differential optical path difference (OPD) between both stars. ASTRA-AST will provide the KI with an internal laser metrology system precise enough to measure Δ OPD at the 10 nm level, which transforms into a precision better than 50 μ as for stars separated closely enough that the differential atmospheric phase distortions do (nearly) cancel out, i.e. for two stars from within the isopistonic angle. Note that the actual *astrometric* baseline of the observation is defined by the endpoints of the internal metrology system used to measure the precise differential fringe delay. This astrometric baseline typically does not exactly coincide with the conventionally calibrated wide-angle baseline. Since the astrometric baseline is typically not defined in the primary space of the telescope, it is difficult to measure it at a precision of about 50 μ m, which is required to achieve the goal of 50 μ as astrometry. To avoid the difficulty of knowing the astrometric baseline, the technique of differential narrow-angle astrometry (DNA) was developed for ASTRA-AST. This technique relaxes the requirements on the precision of the astrometric baseline to a few millimeter, and still achieves the goal of 50 μ as astrometry when observing nearby calibrator binaries of similar orientation and separation on the sky (Woillez et al, 2010). Such a precision level is provided by the KI due to the stability of the Keck telescope pivots over the night.

Laser guide star aided interferometry The second of the two Keck telescopes will be equipped with a powerful sodium layer laser beacon to allow for adaptive optics correction independent of a bright visible guide star (Chin et al, 2010). This will put the KI in the unique position of being able to offer laser guide star-AO aided operations of targets too faint in the visible to feed the current wave front sensor. In the context of young stellar objects (YSO) and their disks, this is particularly interesting for deeply dust embedded objects and edge-on disk systems, which delivered no or poor AO-correction so far.

4.1.6 MROI/SIRCUS

The Magdalena Ridge Observatory Interferometer (MROI) is an optical/near-IR interferometer being built west of Socorro, New Mexico, on a mountain at 3,500 m and overlooking the site of the EVLA (Fig. 6). The entire interferometer has been optimized for a high-sensitivity imaging mission. The baselines for MROI range from roughly 8 to 345 meters, allowing it to access angular resolutions of 30 mas down to 0.3 mas. First fringes for the facility are scheduled for 2013, with more telescopes coming online shortly thereafter and production of rudimentary images beginning in 2015. When complete, the facility will consist of ten 1.4 m diameter relocatable telescopes laid out in an equilateral-Y configuration, with 28 separate telescope pads to accommodate array reconfiguration (Creech-Eakman et al, 2010b). Full descriptions of the MROI capabilities and progress have been presented recently by Santoro et al (2010), Jorgensen and Mozurkewich (2010), Farris et al (2010), and Fisher et al (2010).

In broad terms, the MROI will utilize two separate beam combiners running simultaneously: one, a pairwise correlator optimized for faint source fringe tracking, will monitor the atmospheric perturbations between nearest-neighbor telescopes (in either the H or K_s near-IR band), while the other, a multi-beam closure phase combiner, will collect science data in another bandpass of interest. The current design is for two different science combiners, one optimized for the near-IR windows with another offering a capability in the *R* and *I* optical bandpasses. The goal for the science combiners is to permit full sampling of all possible interferometer baselines within 8 minutes, allowing the MROI to deliver deep images with high dynamic range in a *snapshot* mode routinely.



Fig. 6 A recent photograph of the MROI beam combining facility. To the left in the photograph extends the single pass delay lines in a 190m long building. To the right in the photograph is the location of the center of the array arms to be laid out in an equilateral-Y with the longest baseline attaining nearly 345m (adapted from Creech-Eakman et al, 2008).

MROI IR science instrument, SIRCUS (Creech-Eakman et al, 2010b), will come online in about 2014, and will be capable of spectral resolutions of $R \simeq 30$ and $R \simeq 300$ on objects as faint as $H=14$, with dynamic range of at least 5 more magnitudes within the image itself. A snapshot image with SIRCUS could be produced about every 8 minutes (where about 2 minutes of this is actual on-source integration) using beams from six of the MROI telescopes.

The Key Science Mission for the MROI is targeted on three main areas of astrophysical interest, all of which would be revolutionized were very high angular resolution imaging routinely achievable (Creech-Eakman et al, 2010a). For all three core areas, many of the physical processes occurring remain poorly understood, requiring complex imaging to be better understood. One of the cornerstones of the MROI Key Science mission is the study of star formation in low- and high-mass molecular clouds and the evidence of the earliest stages of planetary formation during this period of the star early life. In order to make a substantial contribution to our understanding of these YSOs, the MROI has been designed to be capable of making images of targets in the nearest star formation regions (for the northern hemisphere) on AU and sub-AU scales.

The MROI will be able to access hundreds of YSOs, not only due to the long baselines, unprecedented sensitivity and baseline bootstrapping capabilities of the reconfigurable array, but also because of MROI ability to offset point from optical objects down to about $V = 16$ within a few tens of arcseconds from objects for which fringes are to be tracked. This is crucial for YSOs due to their heavy dust enshrouding and because YSO cores are often just becoming observable in the IR/optical for only the most evolved objects.

4.2 Exemplary sciences cases

While the observations described in Sect. 3 have been key in confirming and improving current theories of planet formation, much is left to understand and characterize about circumstellar disks. Key questions that need to be addressed concern the surface density profile and three-dimensional dust distribution in the inner regions of protoplanetary disks prior to planet formation, and the presence of, e.g., planet-induced asymmetries in the inner few AU of any type of disks (see Sect. 2.3). To unambiguously address these issues, resolved images at the highest possible resolution are a necessary step forward.

Obtaining high-resolution images of the inner regions of protoplanetary disks can hardly be achieved with the next generation of large telescopes. For example, with a 42m ground-based telescope providing diffraction-limited images in the near-IR, the highest linear resolution that can be achieved in a distance of 140 pc is about 1 AU, so that only a few resolution elements will cover the entire planet-forming region. Furthermore, the disk will remain em-

bedded in the glare of the central star. Only long-baseline interferometry offers the promise of imaging of disks with a linear resolution on the order of 0.1 AU.

4.2.1 The diversity of planet-forming regions

With milliarcsecond angular resolution long-baseline interferometry has proven to be an ideal tool to study protoplanetary disks (see e.g. Millan-Gabet et al, 2007). It has refined the vision of the inner astronomical unit structure of a disk, revealing the emission discontinuity at the dust sublimation distance, the putative presence of hot gas accreting onto the star and/or wind emission and refractory dust (Benisty et al, 2010). The current sensitivity of VLTI instruments limits the exploration of protoplanetary disks to the brightest ones and therefore mainly intermediate-mass stars. The essential limitation comes from (1) the availability of a reference in the isopistonic field and (2) the fact that there are only two Fringe Sensing Units that will limit the observations to one spatial frequency visibility (one baseline) per observation. PRIMA opens the possibility to use a reference star close to the young star to phase the interferometer. This opens the way to longer integrations on fainter targets or with increased spectral resolution.

One of the most evident interesting things would be to increase the sample of solar-mass pre-main sequence stars (T Tauri stars) for which disks near-IR size and inclination can be estimated. As shown by Pinte et al (2008a), sampling the emission from disks around low-mass stars would certainly bring significant constraints on disk energy balance through radiative transfer modeling. Also, astrometric detection of multiplicity among young stars for which radial-velocity surveys are less efficient (e.g. because of line veiling) would allow one to probe the properties of disks in binary/multiple environments.

As outlined in Sect. 3.1.2, most of the disk studies published so far have been focused on intermediate-mass pre-main sequence stars and few interferometric studies have been sensitive enough to observe protoplanetary disks around T Tauri stars. GRAVITY's sensitivity should allow the sample of observed young-stellar objects to be increased considerably and span the entire range of stellar masses. This will therefore open the way to statistical studies on disk morphologies and their relation with the central stars properties. On the favorable case where the disks are largely spatially resolved by the VLTI, image reconstruction of the K band emission in the continuum and in the lines will be the source of important information. This has already been carried by several authors (Renard et al, 2010; Kraus et al, 2010) with AMBER but the addition of a new telescope significantly increases the mapping efficiency. The predominant lines for disk studies in the K band are $\text{Br}\gamma$ and CO overtone. Several questions will be addressed thanks to the GRAVITY ability to map the K band emission with a certain dynamical range:

1. What is the nature of the disk inner rim (dust distribution vs. gas distribution)?
2. Can we constrain the inner disk vertical structure (e.g. flaring, inner edge width, temperature radial dependance)?
3. Can we use the CO emission lines to constrain disk dynamics at the astronomical unit level?
4. Can we detect structures in the emission that can be related to the planet formation mechanisms (density waves, clumpiness)?
5. Can we relate the $\text{Br}\gamma$ emission to the accretion ejection mechanisms?
6. Can we constrain the mass loss morphology (wind/jet) and therefore constrain the physical mechanisms at play at planetary formation spatial scales? Does mass loss affect planetary formation?

GRAVITY's contribution should be seen as complementary to MATISSE and the combination of the two should be a powerful tool to constrain the disk physical conditions within the central astronomical unit of a protoplanetary disk.

At KI, the high differential precision of visibilities and phases in spectroscopic operation (currently offered as SPR, but DFPR spectroscopy is also conceivable) allows one to distinguish different constituents of circumstellar disks, and measure their (differential) kinematic properties. Earth rotation and repeated observations will minimize the limitations of the single-baseline on full two-dimensional kinematics and astrometry. Furthermore, the ASTRA upgrade provides the single baseline KI with a series of new observing capabilities. In particular, the sensitivity of the KI fringe tracker and LGS-AO operation open up for the first time the observation of faint and red targets at the 10-15 mag level (K band) to the tool of long-baseline interferometry in the near-IR. Due to the increased sensitivity in DFPR (off-axis fringe tracking) mode, the current exemplary studies of the brightest nearby targets can be extended to more systematic surveys of larger samples of circumstellar disks.

4.2.2 The potential of interferometric imaging of the planet-forming region

The importance of simultaneous multi-baseline observations In terms of spatial resolution, a major progress has been achieved with MIDI and AMBER in the recent years. Given the typical distance of nearby star-forming regions of \sim 140-200 pc and the spatial resolution achievable with the *Very Large Telescope Interferometer* (VLTI) in the 8-13 μ m atmospheric window of 10-20 mas, these instruments are best suited to study the planet-forming region in circumstellar disks. One of the first exciting results achieved with MIDI was to show the difference in the dust grain evolution between the “inner” disk (represented by the correlated flux) and the outer disk (net flux), using the low-resolution spectroscopy observing mode (van Boekel et al, 2004). However, given the intrinsic limitations of the analysis of single-baseline observations (interpretation of visibilities, such as in the case of MIDI), one has only weak constraints on the structure and size of the emitting region: The interpretation is based on models, which in turn are weakly constrained in the inner disk region because of the lack of adequate observations since the main constraints are given at best by mid-infrared SEDs in a few cases. The situation becomes even more difficult if visibilities are used to constrain more than the geometrical parameters, such as the inner emissivity profile of circumstellar disks. High angular resolution images at infrared wavelengths are of decisive importance to distinguish between various existing disk models.

True surface brightness profile in circumstellar disks around T Tauri / HAe/Be stars Two-telescope interferometers allow one to derive the “mean” disk size and the approximate inclination of the disk. In this data analysis it is usually assumed that iso-brightness contours are centered on the location of the central star. In contrast, multi-baseline interferometers will allow studies of circumstellar disks that are not exactly seen face-on, and show a brightness profile which cannot be described by iso-brightness contours centered on the star.

In the mid-infrared, this will allow one to derive the radial temperature profile of the hot dust on the disk surface and the inner disk rim. This profile will provide information about the radial and vertical structure of the disk, and thus also about the importance of viscous heating (in addition to the stellar heating) and hence on the interior density structure in the potential planet-forming region of the disk.

Complex structures on large and small scale Thanks to the increasing spatial resolution of optical to mid-infrared images of young circumstellar disks it becomes more and more evident that these disks are highly structured. Moreover, the inner region of circumstellar disks is expected – but not yet proven – to show large-scale (sub-AU – AU sized) density fluctuations / inhomogeneities. Locally increased densities and the resulting locally increased disk scale height have direct impact on the heating of the disk by the central star and are expected to show up as local brightness variation (due to increased absorption / shadowing effects) in the mid-infrared images.

Evidence for dust grain growth and sedimentation The most reliable conclusions about grain growth - as the first stage of planet formation - are based on the millimeter slope in the SED of circumstellar disks (Beckwith et al, 1990) and more recently on images of dust disks provided by millimeter interferometry, such as the Butterfly Star in Taurus (Wolf et al, 2003) and CQ Tau (Testi et al, 2003)). These images reveal grain growth up to particles of cm size. Clearly missing, however, are *a*) observational constraints on the region, where dust grain growth is presumably fastest, and *b*) a detailed knowledge of the vertical distribution of the dust particles. The scattering parameter of dust grains significantly changes from sub-micron to micron-size (or larger) grains in the wavelength range of stellar emission. Together with the dust density structure, the forward- vs. backward-scattering behavior of dust grains determines the temperature structure of the disk which in turn controls the vertical structure of the disk.

As simulations of dust settling in circumstellar disks show that the disk flaring and thus the ability to absorb stellar radiation even at large distances from the star depend on the grain size distribution in the upper disk layers (e.g., Dullemond and Dominik, 2004b). Conclusions about the importance of this effect may be derived by comparing the average intensity profile for a large sample of sources (see e.g., Sauter and Wolf, 2011).

Evidence for the presence of planets Once (proto-)planets have been formed, they may significantly alter the surface density profile of the disk and thus cause signatures that are much easier to find than the planets themselves (e.g., Wolf, 2008b). The appearance and type of these signatures depend on the mass and orbit of the planet, but even more on the relevant physical processes (e.g., turbulence) and the disk properties (e.g., mass, viscosity, magnetic fields) and thus on the evolutionary stage of the circumstellar disk.

Status of disk clearing within the inner few AU Depending on the temperature and luminosity of the central star, the sublimation radius for dust grains is of the order of 0.1 - 1.0 AU (T Tauri - Herbig Ae/Be stars) – a spatial resolution which can be approximately reached with MATISSE in the L band in the case of nearby YSOs. However, inner cavities in disks – dust depletion regions with radii which are much larger than the sublimation radius of interstellar medium-like grains – have been found (see Sect. 2.3.2).

Imaging: An MROI case study In the following, we present a case study which illustrates the potential of next-generation interferometers in the domain of imaging through adequate sampling of the uv plane and state-of-the-art image reconstruction. As described in Sect. 3.1.1, YSOs have flared disk geometries with puffed-up inner walls at the location where the accretion disk makes its closest approach to the star (Millan-Gabet et al, 2007; Pinte et al, 2008a). These flared disk models tend to imply that most of the near-IR continuum emission comes from a narrow annular region where dust is sublimating. As a consequence, there is a large

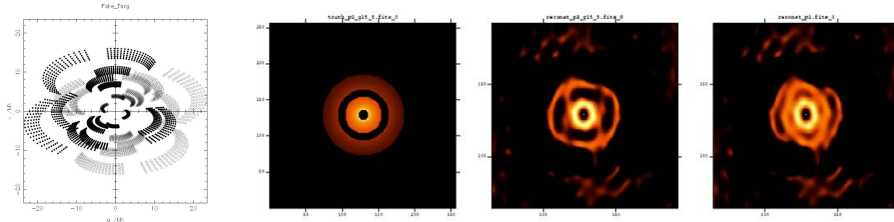


Fig. 7 From left to right the panels show: a) UV coverage of the simulation for a YSO at a distance of 140 pc using a 6-telescope configuration of MROI with SIRCUS during a 6-hour observation. b) The original image on which the simulations are modeled with a 0.7 AU gap present and employing an intensity fall-off of r^{-2} . c) A six-telescope SIRCUS image of the YSO with the gap, and d) The same six-telescope YSO image without the gap. The color scale is logarithmic and covers only the range of intensities in the disk, whereas the central point source is actually 130 times brighter than the brightest pixels in the reconstructed disk images.

contrast between the brightness of the central star to that of the outermost parts of the disk, causing the detection of gaps within the disk to be challenging. In particular, we refer the reader to the models of Wolf et al (2002) in which radiative transfer images of disks around YSOs were derived (for much longer wavelengths) using hydrodynamical simulations and various intensity fall-offs were derived assuming the presence of a Jupiter-mass planet at $\simeq 5$ AU around a solar-mass protostar. Using these models, simulated data has been generated for the near-IR continuum emission from a Herbig Ae/Be star in a face-on presentation with a central cavity due to dust sublimation. For comparison, in some simulations a gap of 0.7 AU was superimposed in the dust at 2.1 AU from the star, putatively due to the presence of a Jupiter-mass planet. The ratio of disk to stellar flux was 3.35.

The simulated dataset was prepared by evaluating the discrete Fourier transform of the model image at spatial frequencies corresponding to the measured projected baselines, converting to MROI observables (squared visibilities and bispectra), and adding Gaussian noise appropriate for bright ($K \simeq 5$) targets. These simulated dataset were used as input to the BSMEM maximum entropy imaging code (Baron and Young, 2008) and a point source image was used as the default. A six-telescope MROI was used with telescopes place at stations West 0, 1, and 4, North 1 and 3 and South 2, which resulted in a baseline range of 7.8 to 32 meters. The lowest spectral resolution of SIRCUS ($R \simeq 30$) was used with assumed uncorrelated visibility calibration errors of $\Delta V/V = 0.02$. A six hour observation duration was assumed for a target at $+25^\circ$ and MROI at 33.98° latitude such that a set of 42 visibility amplitudes and 70 closure phase measures was obtained every 20 minutes (Fig. 7).

As can be seen in the images, the uv coverage for the MROI on such a target is excellent, and the performance of SIRCUS on MROI results in reconstructed images with a dynamic range of 1000:1. Further, a degree of super-resolution has been obtained, as is demonstrated by the resolution of the 7 mas diameter inner cavity. The presence of the dust gap, indicative of a putative Jupiter-mass planet, is clearly evident from the reconstructed images. This type of work will be very complimentary to similar work done with e.g. ALMA, where MROI is highly suited to imaging the inner hot disk, and ALMA to the outer, cooler disk regions. For the nearest seven star-forming regions observable from the northern hemisphere, the MROI will be able to resolve structures down to the 0.15 to 1 AU scales in the IR.

In phase II implementation of MROI, the facility will deploy optical capabilities (in the R and I bandpasses) and bring online the final four telescopes of the array. Once optical imaging is possible, angular resolutions of less than a milliarcsecond will be routinely possible, and in particular, emission line imaging to trace shocked regions and magnetically

channeled accretion in YSOs will become feasible. No other facility-class optical interferometers current or planned are expected to work at optical wavelengths, therefore MROI will deliver a unique capability unparalleled by ELT employing adaptive optics or space-based facilities.

4.2.3 Analysis of the mineralogy and gas in protoplanetary disks with MATISSE

In L band ($\sim 3.0 - 4.1 \mu\text{m}$), interferometric observations of the H_2O ice broad band feature ($2.7-4.0 \mu\text{m}$) and PAHs: $3.3 \mu\text{m}$, $3.4 \mu\text{m}$; nano-diamonds: $3.52 \mu\text{m}$ will become possible, while in M band ($\sim 4.6 - 4.8 \mu\text{m}$) CO fundamental transition series ($4.6-4.78 \mu\text{m}$), CO ice features $4.6-4.7 \mu\text{m}$ and recombination lines, e.g., $\text{Pf}\beta$ at $4.65 \mu\text{m}$, can be investigated with “interferometric resolution”. In N band ($\sim 8 - 13 \mu\text{m}$), spectral features to be investigated with MATISSE will be very similar to those of studied with MIDI. However, MATISSE will allow one to constrain the spatial distribution in much more detail.

4.2.4 Disks around massive stars

While several prominent low-mass star-forming regions can be found at distances of $150 \text{ pc} - 300 \text{ pc}$ from the Sun, most of the currently active high-mass star-forming regions are located at distances beyond 1 kpc , distances of 3 to 7 kpc are quite common. Furthermore, massive stars predominantly form in the densest regions of young stellar clusters. Recent investigations estimate typical number densities of $5 \times 10^4 \text{ stars}/\text{pc}^3$ (Orion Trapezium Cluster, McCaughrean and Stauffer, 1994) or even higher values (Eisenhauer et al, 1998; Stolte et al, 2002). Although more and more theoretical investigations point towards the formation of high-mass stars by disk accretion (e.g., Yorke, 2004), clear observational evidence for the existence of such disks remains rather scarce. Convincing cases were mainly found by radio interferometry (e.g., Shepherd et al, 2001; Cesaroni et al, 2005; Schreyer et al, 2006). Disks around young massive stars are probably short-lived since they are ablated by the strong UV flux and winds of the central star on time scales of $\leq 10^5$ years (Hollenbach et al, 1994). Thus, the best chance to detect such disks is to catch those systems in an early phase of evolution. As high-mass star formation is associated with high extinction, mid-infrared interferometry is the ultimate tool for investigating such disks.

In general, disks around massive stars are expected to be relatively massive themselves (e.g., Yorke and Bodenheimer, 1999). As a consequence, they are increasingly susceptible to gravitational instabilities. Numerical simulations, including realistic cooling conditions (e.g., Durisen et al, 2001; Johnson and Gammie, 2003) and MHD turbulence (e.g., Fromang et al, 2004; Fromang, 2005) show that sufficiently massive disks tend to form dense spiral arms, arclets, ridges and similar kinds of surface distortions. For disk-star systems with a mass ratio $M_{\text{disk}}/M_* > 0.3$, the disk might even begin to fragment into distinct blobs. As it is impossible to constrain these predicted complex structures on the basis of simple visibility measurements, high-resolution imaging is essential to make progress.

With the success of the mission for characterizing star-forming regions in the IR, there is a tremendous number of new objects available for studying with interferometry as identified in the GLIMPSE surveys in particular (Churchwell et al, 2009). An area in which interferometry has only recently shown success is the study of massive YSOs, for which competing theories of formation scenarios are still strongly debated (Zinnecker and Yorke, 2007). The existence of the so-called “green-band emission” at the IRAC $4.5 \mu\text{m}$ band, a possible tracer of shocked gaseous regions, could readily be compared with the locations of pre-forming stellar cores. Identification of massive YSOs is being accomplished in the

submillimeter and radio where the YSO shocked gases are evident and extinctions are much lower (Araya et al, 2007; Hofner et al, 2007; Beuther et al, 2002), and so the complementarity of these IR and radio techniques is again quite promising. Nevertheless, studies of core multiplicities, which could help sort among competing formation mechanisms, are still in their early stages as they require very high angular resolution in the IR.

Cyganowski et al (2011) have catalogued nearly 300 possible massive YSOs candidates from the GLIMPSE survey. In their Table 1 they list 97 *likely* candidates. Of these candidates which are north of -10° declination and therefore readily available to the MROI, 19 (67%) have integrated fluxes above 11.5 magnitudes at IRAC 3.6, 4.5 and $5.8\mu\text{m}$ bands. If these sources suffer less than 2.5 magnitudes extinction between the IRAC bands and the MROI tracking wavelengths of H and K_s , there is a high likelihood that the MROI will be able to image these regions and help contribute to our understanding of multiplicity and therefore help sort among competing formation scenarios. Such success has recently been demonstrated using VLTI AMBER in the near-IR (Kraus et al, 2010) and MIDI in the mid-IR (Vehoff et al, 2010) on two massive YSOs using instruments much less sensitive than MROI is predicted to perform by $\simeq 2015$.

4.2.5 Astrometric detection of exoplanets

As an astrometric instrument, PRIMA is designed to measure the displacement of the star on the sky plane due to the gravitational influence of companions, hopefully of planetary nature (see, e.g., Fig. 5). The expected reflex motion of a host star of mass M_* located at a distance d from earth and orbited by a planetary companion of mass M_P with orbital radius a_P is given by the following formula:

$$\Delta\alpha = 0.33 \left(\frac{a_P}{1\text{AU}} \right) \left(\frac{M_P}{1\text{M}_\oplus} \right) \left(\frac{M_*}{1\text{M}_\odot} \right)^{-1} \left(\frac{d}{10\text{pc}} \right)^{-1} \mu\text{as.} \quad (2)$$

The astrometric detection parameter space of PRIMA brings evident complementarity to radial-velocity observations. The further away from the star, the stronger the astrometric signal (with a longer period to sample). As presented by Launhardt (2009) PRIMA can be used to address several issues:

1. Obtain the inclination of the planetary orbit to derive the planetary mass (constrained by radial-velocity surveys only),
2. Confirm long-period planets candidates in radial-velocity surveys,
3. Measure the relative orbit inclinations in multiple planetary systems,
4. Perform an inventory of planets around stars with different mass and age, in particular planets around young stars (age < 300 Myr).

A preliminary list of 900 candidates has been selected by the ESPRI consortium while the final list will be probably much reduced. Indeed, the final planetary mass detection performance will be directly linked to the ability to find a reference star at $10''$ to $30''$ and to the astrometric precision. Astrometric accuracies of $100\mu\text{as}$ have been demonstrated at the Palomar Tested Interferometer (Colavita et al, 1999) with the PHASES program (Muterspaugh et al, 2006). It is hoped that PRIMA will be able to track on $K \sim 9$ stars on a routine basis as it was done during commissioning (Sahlmann et al, 2009). The precision of $10\mu\text{as}$ was the initial goal but this was done with an incomplete description of the instrument. A precision of a few $10\mu\text{as}$ would already permit significant contributions such as the detection of Jupiter mass planets at a distance of 1-5 AU.

As an astrometric device, GRAVITY will be sensitive to the wobble of a star under the gravitational influence of its planetary system. Given its sensitivity, detecting Jupiter and Saturn mass planets at ~ 1 AU from their parent star should be within reach. The strength with respect to PRIMA is the redundancy provided by the simultaneous six baselines observation. However, the limited 2" field-of-view will restrict such studies to those objects having a suitable fringe tracking reference.

As an interferometer, GRAVITY provides the capability to measure precise closure phases. It has been shown (Renard et al, 2008) that using four UT telescopes with GRAVITY one can reach a sufficient closure phase precision to directly detect hot-Jupiters with favorable stellar to planet brightness ratio. Moreover, a moderate spectral resolution capability might allow the detection of molecular features such as methane/water absorption in the planet spectrum to be detected.

At KI, the envisaged precision level of $50 \mu\text{as}$ of the ASTRA astrometry mode will allow for the detection of on-sky reflex motion of exoplanet hosting stars. While large astrometric exoplanet surveys such as ESPRI (Launhardt et al, 2008) are most efficiently done with two orthogonal baselines and smaller apertures, ASTRA-AST observations will have a high impact with the detailed study of fainter and complex multi-planet systems aligned with the KI baseline.

4.2.6 Direct imaging of Exoplanets: A challenge for interferometry

Direct imaging and observations of exoplanets with optical interferometers are inherently challenging due to the very large contrasts between the star and exoplanet. However, interferometry offers access to measurements impossible with conventional telescopes. CHARA has recently contributed to our understanding of fundamental physical scales in confirmed exoplanet systems by making accurate measurements of the host star diameters (Baines et al, 2009). As interferometers continue to characterize planet-bearing stars, and in particular features such as stellar spots and limb-darkening, we will gain better understanding of basic parameters associated with planet transits and the environments in which these planets exist. More challenging yet would be the actual characterization of the exoplanets themselves via spectroscopy, which could in principle be accomplished using differential closure phase techniques.

Studies have been undertaken to determine the feasibility of such measurements, including investigations of the potential of existing interferometric instruments: VLTI using AMBER (Joergens and Quirrenbach, 2005) and PIONIER (Absil et al, 2011), and CHARA using MIRC (Zhao et al, 2010). These studies suggest that characterization of closure phases with milli-radian level precision will yield information on both orbital geometries and spectral energy distributions in the exoplanetary atmospheres. These measurements are presently limited by interferometric systematics which presently prevent these facilities from attaining required closure phase precisions. Other potential complications include the need for adequate models for the host stars, which are most likely resolved by the interferometers, and how to adequately address changes in the orbital geometries of the star-exoplanet systems which are likely on the order of Earth rotation synthesis time scales for so-called hot Jupiter candidates. The MROI will have advantages over existing interferometers, in particular in that the array telescopes can be deployed and optimally baseline bootstrapped in order to match MROI intrinsic angular resolution to the systems being measured. Further, the high dynamic range and fidelity in SIRCUS images (with 10 telescopes it collects 36 independent closure phases every 8 minutes), will be produced via stabilized fringes delivered as a matter of course. With MROI planned observing scenarios, it may be possible to produce

useful closure phase measurements on these systems, but this will certainly require more study and simulations once the MROI is operational.

It is clear that interferometry will remain the only feasible method to obtain sub-mas angular resolutions in the optical and IR on these types of object for at least the next decade. Because circumstellar environments of YSOs are expected to be complex, and exoplanets will likely require high-precision differential closure phases, imaging interferometers in particular are likely the only viable tools to make any significant progress understanding the contiguous environments of nearby systems.

5 The role of selected complementary observatories

One caveat of optical/infrared measurements is that protoplanetary disks are extremely optically thick in this wavelength range, so that it will remain impossible to *directly* probe the midplane in the inner regions of the disk. Over the next few years, ALMA will greatly expand our ability to spatially resolve protoplanetary and debris disks at (sub)millimeter wavelengths. For protoplanetary disks, this will allow one to extend the study of surface density profile and dust segregation down to the inner few AU.

Another shortcoming inherent to existing and planned optical/infrared long-baseline interferometers is the low sensitivity compared to that of large-aperture telescopes operating at the same wavelengths. Both, planned large-aperture ground-based (e.g., E-ELT¹⁹) and space-based observatories (e.g., JWST²⁰, SPICA²¹) are therefore essential to achieve a comprehensive understanding of circumstellar disk physics by tracing the low-luminosity outer disk regions. In turn, interferometric observations – both at optical/infrared and (sub)millimeter wavelengths – will reduce the uncertainties related to the inward extrapolation of the outer surface density profile.

5.1 ALMA: the Atacama Large Millimetre Array

The Atacama Large Millimeter/submillimeter Array (ALMA) has been designed to be the leading ground-based observatory at millimeter and submillimeter wavelengths in the foreseeable future. ALMA will initially be composed of $54 \times 12\text{-m}$ and $12 \times 7\text{-m}$ diameter antennas located on the Chajnantor Altiplano at an altitude of 5000 m in Northern Chile. The plateau offers a relatively constant altitude site for arranging the ALMA antennas in several different configurations. In the most compact configuration the longest available baseline will be of only ~ 150 m, in the most extended it will be up to ~ 15 km. To fully exploit the excellent conditions on the site for submillimeter observations, ten receiver bands covering all the atmospheric transparency windows from 30 GHz to 1 THz are planned. The six highest priority bands will be available from the start of full science operations in early 2013. The remaining frequency bands will be added later to the array. Detailed descriptions of the ALMA system and performances have been published in Kurz et al (2002) and Haupt and Rykaczewski (2007). When fully operational, ALMA will be 10-100 more sensitive and have 10-100 times better angular resolution than existing (sub-)millimeter instruments.

One of the three high-level science requirements by which the design of the ALMA system is determined is directly related to the observation of protoplanetary disks: Imaging the

¹⁹ European Extremely Large Telescope (Ramsay et al, 2010)

²⁰ James Webb Space Telescope (Mather, 2010)

²¹ Space Infrared Telescope for Cosmology and Astrophysics (Nakagawa, 2011)

gas kinematics in protostars and protoplanetary disks around young Sun-like stars at a distance of 150 pc, enabling the study of their physical, chemical and magnetic field structures and to detect the tidal gaps created by planets undergoing formation in the disks. Protoplanetary disks feature prominently in the high-level ALMA science goals and in the ALMA DRSP²² and are a key science theme where ALMA is expected to provide a significant step forward, both for the study of the solid and gas components.

5.1.1 *Dust in protoplanetary disks*

At submillimeter and especially millimeter wavelengths, the dust thermal emission in protoplanetary disks is mostly optically thin to its own emission. The only possible exception being the innermost regions of the disk close to the star. Observing at these wavelengths offers the possibility of probing the bulk of the solids in the disks, especially at the disk midplane where most of the material is located and where planet formation is thought to occur. This methodology has been applied with success to estimate the total disk mass, the distribution of the material in the disk and to put constraints on the evolution of dust, in particular grain growth towards the formation of planetesimals (Beckwith et al, 1990; Beckwith and Sargent, 1991; Dutrey et al, 1996; Wilner et al, 2000; Testi et al, 2001; Natta et al, 2007; Hughes et al, 2008; Isella et al, 2009; Andrews et al, 2009).

ALMA will also allow one to study of disk properties as a function of the central star parameters (age, mass), the evolution of disk structure and the relationship with planet formation processes and environment, and a proper understanding of the dust evolution processes. The presence and properties of circumstellar disks in the sub-stellar mass domain and around the higher mass protostars are still debated. These systems are currently difficult to probe but ALMA is expected to overcome the current limitations (Natta and Testi, 2008; Testi and Leurini, 2008). Simulations show that ALMA will allow one to probe the diversity of disk properties at the bottom of the mass function, but it will still be hard to resolve spatially these disks and probe their structure. In the high-mass regime, ALMA should clarify the role of disk in the formation of these objects by detecting and resolving the disk structure (Cesaroni, 2008; Krumholz et al, 2007).

5.1.2 *Protoplanets*

In the solar-mass stars regime, ALMA will provide the sensitivity and resolution to detect forming protoplanets if they do exist in nearby star-forming regions (Wolf and D'Angelo, 2005). Current observations show that grain growth is a relatively common process and many disks show evidence for very large grains in the midplane (e.g. Lommen et al, 2009; Ricci et al, 2010a,b), suggesting also that large grains can remain on the disk for long times. These findings are at odds with model predictions of grain growth and migration in disks, which suggest that large grains should be efficiently removed from the outer regions of disks (Brauer et al, 2008b). Observations and theory could be reconciled if large grain migration is halted or slowed down (e.g. Birnstiel et al, 2010). To constrain theoretical expectations it is necessary to resolve grain growth as a function of radius in disks and to observe the possible patterns in disks that may be responsible for slowing inward grain drift. Initial attempts in

²² ALMA Design Reference Science Plan; a collection of the science projects that can be expected to be carried over during the initial years of ALMA full science operations. The latest version of the DRSP is available on the ESO webpages: <http://www.eso.org/sci/facilities/alma/science/drsp/>; for a high-level analysis of the DRSP content, see Hogerheijde (2006) and Testi (2008).

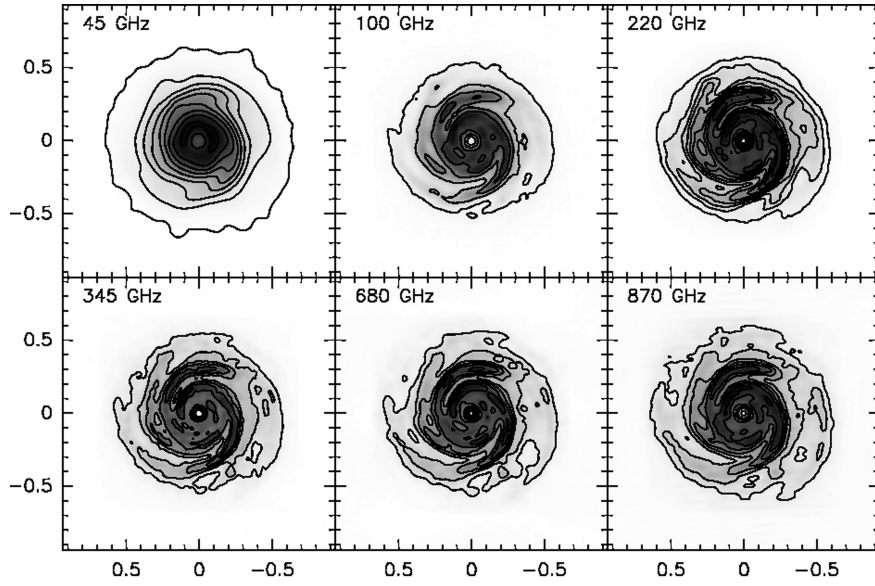


Fig. 8 Simulated ALMA observations of a self-gravitating circumstellar disk in the Taurus Star Forming Region. Axis scales are in arcseconds (adapted from Cossins et al, 2010).

this respect are being performed with current instruments (Isella et al, 2010b; Banzatti et al, 2011; Guilloteau et al, 2011), but ALMA will put the initial findings on a firmer ground. As an example, Cossins et al (2010) simulated ALMA observations of a self-gravitating disks which develops a pattern of spiral structures that trap large grains and slow or halt migration (see Fig. 8). The simulations demonstrate that, once completed, ALMA will not only allow one to detect such features in protoplanetary disks, but also to derive the dust properties in the high and low density regions of the disk constraining selective dust trapping.

5.1.3 Tracing the spatial distribution and kinematics of molecules

One major unknown in planet formation scenarios is the radial and vertical distribution of the gas and its evolution with time in the regions $< 20 - 50$ AU. Furthermore, the mass and dynamics of disks surrounding young low-mass stars are gas dominated²³ but the main gas component, H₂, remains difficult to observe. The quadrupolar H₂ rotational transitions in the mid-IR only trace the warm material which is located at the disk surface. Hence, there is no simple way to get a reliable estimate of the cold gas mass. One has to rely on indirect tracers such as CO or rarer molecules whose observations are sensitivity limited. This situation will drastically improve with ALMA, thanks to its very large collecting area.

In the early 1990's, CO J=1-0 and J=2-1 maps not only revealed that disks are in Keplerian rotation around T Tauri (Koerner et al, 1993) and Herbig Ae stars (Piétu et al, 2005) but led to the first quantitative studies of the physical conditions of the gas in disks, provided an adequate data analysis is used (e.g. Dutrey et al, 2007). Multi-line multi-isotope study of CO can unveil the vertical structure of gas disks, in particular the temperature. This has been illustrated by Dartois et al (2003) and Piétu et al (2007) who showed that the “CO disk

²³ The gas-to-dust ratio is supposed to be of the order of 100 in a disk of 1 Myr.

surface”, traced by an opacity of ~ 1 in the ^{12}CO $J=2-1$ transition located at about 3-5 scale height, is significantly warmer than the mid-plane. This method using higher CO transitions would sample the disk atmosphere (Qi et al, 2004, 2006) revealing the impact of X-rays and UV irradiation on the disk properties. The disk surface can be reasonably approximated by models of photo-dissociation regions, while the colder disk interior reflects a chemistry close to that of dense clouds. In all T Tauri disks where CO has been mapped, the gas temperature in the mid-plane appears to be below the CO freeze out point (17 K), suggesting that the vertical turbulence should play an important role by providing chemical mixing between the vertical molecular layers. Direct studies of the turbulence will also be possible with ALMA by quantifying the non-thermal component of molecular line broadening.

Rarer molecules are more difficult to detect. Moreover, most of them may have transitions which are in non-LTE conditions, contrary to first rotational lines of CO. These molecules can provide invaluable information on disk density structures provided the excitation conditions are understood and properly modeled (Dutrey et al, 1997). Several groups (Kastner et al, 1997; van Zadelhoff et al, 2001) have conducted molecular surveys, but they are sensitivity limited to the most abundant molecules found in molecular clouds. In addition to CO, ^{13}CO and C^{18}O , only HCO^+ , H^{13}CO^+ , DCO^+ , CS, HCN, HNC, DCN, CN, H_2CO , N_2H^+ and C_2H have been firmly detected. As soon as the full ALMA array is operational, the number of detected and mapped molecules will increase revealing the complexity of the disk molecular chemistry and the vertical stratification of molecules (Semenov et al, 2008). For example, mapping of molecular ions such as N_2H^+ or HCO^+ and its isotopomers should provide the first quantitative information on the ionization fraction, one key element to characterize the dead zone.

5.2 Infrared Space Observatories

Space observatories benefit from a much more stable image quality, with no seeing-degradation point spread function (PSF), and also usually better sensitivities for a given size of the primary mirror. To illustrate the potential of near-future infrared observations from space to provide complementary insights on the topic of circumstellar disks and planets, we make use of the well-advanced preparatory science studies for the JWST which is designed to replace the Hubble Space Telescope.

The JWST primary mirror will be larger in size than that of the Hubble Space Telescope (6.5 m compared to 2.4 m) and its range of wavelength coverage will shift towards the IR (0.6-28 μm). While ground-based instruments suffer in this wavelength range from an incomplete coverage due to the atmospheric absorbing bands as well as a limited sensitivity with a large thermal background beyond $\sim 2 \mu\text{m}$, JWST will have access to any wavelength in the range mentioned above and will be limited by zodiacal light up to 16 μm . Beyond this wavelength, its sensitivity will be constrained by the sunshield thermal radiation and the telescope proper emission. More information concerning the telescope and its specificities can be found in Gardner et al (2006).

The JWST comprises a suite of three instruments and a Fine Guidance Sensor (FGS) that can be also used to obtain scientific observations. The FGS features narrow band Fabry-Perot spectro-imaging (Doyon et al, 2008) and pupil interferometry by a Non Redundant Mask (NRM) (Sivaramakrishnan et al, 2009). Occulting masks are also available and can be combined with apodization masks to produce 10^{-4} (at an angular distance larger than 2") contrast ratio coronagraphic images in the near-IR range. The NIRCam instrument is in principal an imager observing in the near-IR range (0.6-5.0 μm) with a set of broad, inter-

mediate, and narrow band filters. It is equipped with a set of coronagraphic occulters (three apodized spots and two apodized wedges with sizes ranging from 2 to $6 \lambda/D$) that allow the NIRCam instrument to conduct high-contrast imaging observations (Krist et al, 2007). In addition, NIRCam offers also the possibility to produce slitless spectra using a set of grisms (2.4-5 μm) with $R \sim 2000$ spectral resolution. The NIRSPEC instrument features a multi-object spectrometer, an integral field unit (IFU), and a long-slit mode. The spectral resolutions range from $R=100$ to $R=2700$. Finally, MIRI is the mid-IR instrument (5-28 μm) observing both in imaging and spectroscopic modes. The MIRI imager sub-instrument is equipped with focal plane coronagraphic masks, three four-quadrant phase masks and one Lyot mask (Baudoz et al, 2006) particularly designed to observe exoplanets and circumstellar disks, respectively, at wavelengths of 10.65/11.4/15.5/23 μm . It offers also slit and slitless prism modes ($R=100$); the spectrometer sub-instrument is an IFU with higher spectral resolution ($R=3000$).

5.2.1 Protoplanetary disks

Its remarkable sensitivity to faint diffuse objects coupled with a good angular resolution at IR wavelength comparable to that of ground-based instruments make the JWST a first choice facility for the study of protoplanetary and debris disks. Its high-level spectroscopic capabilities at medium resolution ($R \sim 2500$) will allow one to study the gas chemistry in protoplanetary disks and the dust content in protoplanetary and debris disks in detail, and to search for leftover warm gas in debris disks. Furthermore, some spatial information will also be obtained in the case of the closest objects ($d \lesssim 50 \text{ pc}$).

Important science questions regarding the physical state and evolution of protoplanetary disks can be tackled using the JWST capabilities in order to constrain the physical conditions (depending on the star mass) that lead to planet formation. In the case of the JWST, at least three science cases/questions can be identified. The first one deals with the large scale (50-500 AU) vertical structure of protoplanetary disks. The second one is the dust sedimentation process, which is a prerequisite to planet formation through core accretion. Finally, MIRI and NIRCAM have both, and for the first time ever, the angular resolution, the sensitivity and the stability to directly detect thin/weak structures imprinted in the disks by already formed giant planets.

In relatively short integration sequences, the IFU spectrometer in MIRI will be able to measure the abundances and temperatures of species in gaseous form with an amazing precision. The observations of atomic line like the [NeII], [NeIII] and possibly [Si] (Gorti and Hollenbach, 2008) signatures at 12.81 and 15.55 and 17.4 μm , respectively, will allow one to trace the physical state (e.g., temperature, heating mechanism) of the upper tenuous layers of the disks. At deeper levels in the inner few AUs, the molecular layer contains among others H₂ (the major constituent of giant exoplanets), water, OH, C₂H₂ and HCN molecules. The observation of water lines in non-LTE state (Salyk et al, 2008; Pontoppidan et al, 2010) provides an important diagnostic of the layers where the gas and the dust start to couple in the disks. In parallel, MIRI's high-sensitivity imaging capabilities coupled with an excellent inner working angle (IWA=1 λ/D) of the 4QPM coronagraph, will be particularly efficient to angularly resolve the disks in the mid-IR range. At these wavelengths the thermal emission dominates. However, given MIRI extreme sensitivity, the (unresolved) inner rim light scattered by the dust particles at the surface of the will start dominating at distances from the star fixed by the stars luminosity (see Fig. 9). MIRI will have a major role to expand our knowledge concerning the lower-mass stars disks. The intermediate-mass stars have a pure thermal emission that dominates up to more than $\sim 2''$ from the star at 10 μm ($r \gg 2$

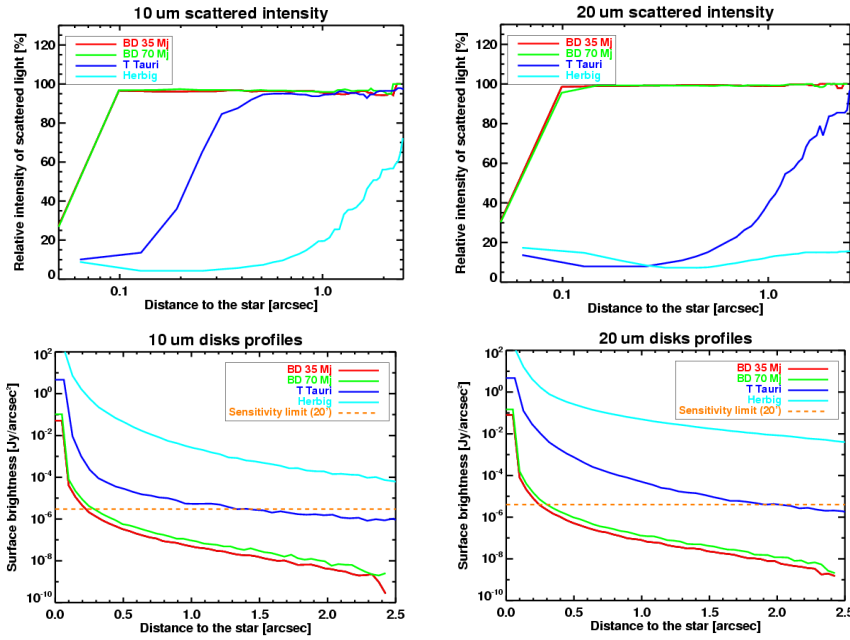


Fig. 9 Upper panel: relative proportions of (inner rim) scattered light (10 and 20 μm) with respect to the total emission. The lower panel displays the protoplanetary disks total emission (10 and 20 μm) as a function of the angular distance to the star for an object at 140 pc. Different types of star are considered: an Herbig Ae star (A0e, $L=40 L_\odot$), a T-Tauri star ($T_{\text{eff}}=3900$ K, $R_*=3 R_\odot$), and two brown dwarves (70 and 35 Jupiter masses, respectively).

at 20 μm respectively). The lower-mass T-Tauri stars have a scattered light emission that starts to dominate above a distance of $\sim 0.2''$ at a wavelength of 10 μm ($\sim 1.2''$ at 20 μm respectively). Finally, MIRI observations of disks around brown dwarves (BD) will be dominated by the scattered light emission at any distance/wavelength. However, if the extended disk emission should be easily detectable in relatively short integration times ($t\sim 1\text{h}$) in the cases of Herbig and T-Tauri stars, brown dwarf disks extended emission will require fairly long integration times ($\sim 3\text{h}$ at the most favorable wavelength of 23 μm ; see Fig. 9). Albeit so that a fairly large observing time will be needed in the latter case, it will be worth spending it as JWST/MIRI will be the unique facility able to detect and resolve BDs disks emission at these wavelengths in the next decade. Observing a mixture of star and inner rim scattered light, the NIRCAM imager will typically achieve in coronagraphic mode at 2.5 μm a 230/70 $\mu\text{Jy/arcsec}^2$ ($\sim 16.2/17.5 \text{ arcsec}^{-2}$) surface brightness magnitude sensitivity, respectively, at distances of 0.3 and 0.5'' from a 10th magnitude star (0.3'' corresponds to the IWA ($4 \lambda/D$) of the NIRCAM wedge coronagraphic mode at a median wavelength of 2.5 μm). These detection limits will allow one to easily detect and resolve protoplanetary disks around Herbig and T-Tauri type stars in the closest star-forming regions. However, in the case of disks around brown dwarves it will remain extremely difficult. Nonetheless, there is some hope that in the most favorable cases (closest and brightest ones e.g. around TW Hya) they should be resolved at a level of few spatial resolution elements; given the very red color of the disks, the multi-color PSF subtraction should be particularly interesting to apply in this case. The resolved images of the disks will be used to derive several physical

parameters. The first and most immediate ones are the physical size (outer radius, or a least an lower limit on it), the disks inclination and position angle by measuring them directly on the images. Using a slightly more evolved analysis of the isophots centering w.r.t. the star position, one can also derive the disks thickness and their flaring angle as a function of the distance to the star (Lagage et al, 2006).

The inner zones of disks ($a \leq 10$ AU) have a surprisingly rich chemistry, as revealed in recent years by mid-IR spectroscopy (Lahuis et al, 2006; Carr and Najita, 2008; Salyk et al, 2008). Features from H_2O , OH, HCN, C_2H_2 and CO_2 have been detected, implying abundances that are orders of magnitude higher than in the outer disk or in protostellar clouds which indicates an active high-temperature chemistry. There is evidence for differences in the observed spectra between disks around Herbig Ae, T-Tauri stars and brown dwarves as well as among disks around T-Tauri stars themselves which can be partly understood in terms of stellar irradiation. A complete inventory of their content in ingredients (e.g. NH_3 , CH_4 , C_6H_6 , HCO^+ or HCN) to form prebiotic molecules will be established in a *large number of targets* by the MIRI instrument. At shorter wavelengths, the NIRSpec instrument will observe the forests of rovibrational ^{12}CO , ^{13}CO and C^{18}O line emission allowing one to establish accurate excitation diagrams and determine with precision the vibrational temperature(s). Finally, even with the moderate resolution of NIRSPEC and MIRI spectrally resolved observations (e.g. by spectro-astrometry technique; Pontoppidan et al, 2008) will be also a source of valuable information.

Based on numerical simulations of the dynamical evolution of the disk structure, one expects that massive planets embedded into disks strongly modify their appearance, sculpting and structuring them: inner voids, gaps, walls, asymmetries (Nelson et al, 2000; Edgar and Quillen, 2008, see also Sect. 3.1.2). There are more and more indirect convincing indications e.g. from the modeling of the SED, from velocity-resolved observations of the gas phase (Acke et al, 2005), or interferometric measurements (Fedele et al, 2008) that many protoplanetary disks are structured. Some disks display inner depleted regions (the so-called transitional disks, see e.g. Brown et al, 2009; Sicilia-Aguilar et al, 2009; Muze-Rolle et al, 2010). Some others have or are believed to feature intermediate large walls (as opposed to the inner rims at the dust sublimation radius, typically a fraction of an AU) at the limit between an inner and an outer massive, optically thick disk (Bouwman et al, 2003; Thalmann et al, 2010; Verhoeff et al, 2011). Finally, dynamical simulations show that giant planets embedded in disks would not only carve a gap but also launch large-scale spiral waves (Edgar and Quillen, 2008). Since the density waves induce a local heating of the disk they produce in turn thermal emission features that can be best detected in the mid-IR range. The JWST instruments do not in general have the required angular resolution to directly image these gaps, walls, and spiral structures. However, given their extreme sensitivity and stability it will be possible to obtain indirect indications of the presence of e.g. a spiral structure or a wall at projected distances larger than $\sim 0.2''$ by searching for surface brightness asymmetries in the disk.

5.2.2 Debris disks

Due to the complexity and aberrations in the JWST PSF, the ultimate contrast achieved with the NIRCam coronagraph is expected to be about 10 times worse than that achieved by the coronagraphs on the Hubble Space Telescope (for instance the ACS coronagraph). Therefore, the JWST is not meant to search for and resolve previously unseen debris disks in scattered light, as most of the candidate targets have already been observed with the Hubble Space Telescope at better contrast levels. In non-thermal emission imaging, JWST's

primary contribution will be the characterization of known debris disks at previously unobtainable wavelengths (2.5-5 μm). This characterization shall probably mainly be focused on the sizes/shapes/composition of the dust grains and the study of structures in the surface density produced by giant planets. On the other hand, the MIRI instrument will map the debris disks in the thermal (and possibility scattering far away from the star) IR regime with an angular resolution and sensitivity by far better than anything that will have been achieved before. MIRI will be for instance able to map at 23 μm with an angular resolution ($\sim 0.9''$) 7 times better than *Spitzer* the VEGA archetype, a disk which is currently unobservable from the ground given its low surface brightness. This disk appears featureless at modest spatial resolutions ($\sim 7''$; Su et al, 2005; Sibthorpe et al, 2010). This will offer the possibility to search for planet footprints at an ~ 7 AU spatial scale in the disk.

5.2.3 Exoplanets studies

One of the major science cases for the JWST is that of the exoplanet studies. The JWST is particularly well adapted for this task because of an extreme sensitivity, a very stable point spread function, and covers the IR 1-28 μm wavelength range where numerous molecular emission features are found. Besides, observations are generally easier in the IR range where the thermal emission of the planet dominates, because of a reduced star-planet contrast ($10^5 - 10^7$ in the case of giant planets) in comparison with the visible range ($10^9 - 10^{11}$).

Given the very high contrast to deal with in the IR range, direct imaging observations of exoplanets with the JWST will require the use of coronagraphic modes to efficiently reject the starlight. Multi-wavelength/multi-epoch observations using the different instrument will have to be combined to unambiguously confirm the planetary nature of the sources discovered. However, even though the JWST segmented-mirror producing considerable additional diffraction structures is not primarily designed to conduct coronagraphic observations, the very high stability of its point spread function combined with superb sensitivity performances at wavelengths where the thermal emission of giant exoplanets emerges make the JWST a very good competitor to specifically designed instruments on ground-based larger telescopes. This stability can be efficiently exploited to achieve better rejection performances through multi-wavelength observations using e.g. the TFI coronagraphic mode. As a general rule, the niche for JWST imaging programs lies in searching and characterizing giant planets on fairly large orbits around faint late-type stars (M and later). One of the major scientific goal will be to disentangle between hot-start (Baraffe et al, 2003) and core-accretion proposed models (Fortney et al, 2008b) for giant planets formation. Simulated performances of the NIRCAM coronagraphic mode show that old (1 Gyr and more), narrow orbit ($a \geq 5$ AU), self-luminous giant exoplanets detection/characterization will best conducted at 4.5-5 μm around close-by late type (M and brown dwarves) stars (Green et al, 2005). Self-luminous giant planets of age younger than 100 Myr will be observable at orbital radii larger than 25 AU around a few hundred young stars within 25-150 pc. Using Monte-Carlo simulations, Beichman et al (2010) have computed the success rate in terms of detectability for 2 representative samples: around nearby (age ≤ 100 Myr, 25-140 pc) young stars and around nearby M stars (ages between several Myr and 5 Gyr, $d \leq 15$ pc). Concerning telluric planets, although typical super-Earth exoplanets should not be detectable by the JWST because their emission is weak and they are probably found at narrower angular separations from the star, two “non-classical” cases appear to be favorable for direct imaging detection. First, the presence of a dusty circumplanetary ring should boost the mid-IR flux by an order of magnitude around late-type stars. A second interesting case deals with high-temperature telluric planets after a major catastrophic impact event. Depending on the

presence (or not) or a residual atmosphere, the cooling time shall be long enough (several Myr) for such exoplanets to be observed by direct imaging around $3.8\text{ }\mu\text{m}$ (Miller-Ricci et al, 2009). Finally, one should also mention the possibility provided by MIRI and NIR-Spec IFUs spectrometers to perform spectral deconvolution (Thatte et al, 2007), a starlight rejection technique which is complementary to coronagraphic imaging.

While direct imaging of exoplanets will deal with large separation objects ($d \gtrsim 1''$), a very larger amount of information will come from the study of transiting objects. Transit spectroscopy of these objects on relatively narrow orbits by essence, will provide a unique set of information to characterize them. The main advantages of JWST observations over ground-based ones lie in the stability (no variable atmospheric absorption) and access to longer wavelengths where molecular signatures are numerous. Typical relative precisions achievable from the ground are of the order of 0.1 % and are limited by systematic errors due to the atmosphere. In the case of space-born observatories, systematic errors also exist and limit the relative precision achievable to a few 10^{-4} , so well above the photon noise limit still. When *Spitzer*/IRS or *Spitzer*/IRAC observations of exoplanets were limited to bright objects and low-resolution spectra, JWST observations of fainter targets or at higher spectral resolution should be possible. All things remaining equal, a crude estimate based on the ratio of telescope apertures (6.5 m vs 90 cm) shows that high-resolution ($R = 3500$) spectroscopic observations will be possible on targets for which *Spitzer* was limited to photometric or low-resolution spectroscopic observations. Two JWST instruments include slitless spectroscopic modes (grisms mode in NIRCAM, low-resolution spectroscopy in MIRI imager). While shorter wavelengths (1-5 μm) are best suited for primary eclipse observations, longer wavelengths are more adequate to determine the effective temperature of exoplanets by means of secondary transit or detect phase modulation signals in the case of tidally locked out-of-plane exoplanets. Also even though emission spectra produce potentially larger signals than transmission spectra, features in transmission spectra will always be present whatever is the structure of the exoplanet atmosphere. As opposed to that, isothermal atmospheric profiles would produce featureless emission spectra. Depending on the size of the planet, its distance to the star, and the star brightness, NIRSpec and NIRCam can be used to obtain spectra (narrow band photometric measurements) in a spectral range where signatures of H_2 , H_2O , CH_4 , CO and CO_2 are present. MIRI imager and spectrometer will probe slightly cooler objects in a wavelength range where NH_3 , CO_2 , H_2O , CH_4 , and O_3 signatures are present. Simulated observations by the JWST show that a significant SNR of 3 is achievable on a single primary transit observation with NIRSpec ($\lambda = 3\text{ }\mu\text{m}$, $R=100$) of a Jupiter-sized planet. The same detection limit is reached at $3\text{ }\mu\text{m}$ on Neptune-sized planets up to a distance of 10 pc (Belu et al, 2011). Around $10\text{ }\mu\text{m}$, MIRI low-resolution spectrometer ($R = 100$) achieves a $3\text{-}\sigma$ detection limit on Neptune-sized exoplanets ($d = 10\text{ pc}$) by combining few transits. In the case of telluric planets, by combining 20 transit observations with NIRSpec, a 10^{-5} relative precision is achieved at a spectral resolution of $R \sim 100$ which allows the characterization of the atmosphere of a hydrogen rich super-Earth exoplanet (Clampin, 2009). CO_2 $4.3\text{ }\mu\text{m}$ ($15\text{ }\mu\text{m}$ respectively) signatures of super-Earths at 10 pc are detectable by NIR-Spec (MIRI resp.) if *all* its primary transits (~ 50) are combined over the JWST lifetime. In this case, planets in the habitable zone are found around stars with spectral types later than M2. Maybe more interesting, the ozone feature at $9.6\text{ }\mu\text{m}$ of a super-Earth planet around a M4V (or later type) star 6.7 pc away is detectable again by summing the signals of all the transit events (Belu et al, 2011). However, the expected number of planets in such a favorable configuration is only on the order of 1 when considering all the M stars of the solar neighborhood. Finally, the TFI mode of the FGS allows one also to obtain spectro-imaging ($1.5\text{-}5\text{ }\mu\text{m}$, $R = 100$) data; its (NRM) sub- λ/D imaging capability and its relatively simple

coronagraphic mode could provide in some cases very useful complementary data to the instruments already cited.

6 Concluding remarks

The major limitation of the current studies of the planet formation process is the insufficient spatial resolution of existing imaging telescopes, at optical to millimeter wavelength range. High-resolution imaging as it will be possible with the next generation of multi-baseline interferometers is therefore of essential importance for planet formation and evolution studies. The ability to investigate the inner regions of protoplanetary and debris disks in unprecedented detail will provide insight into planetary systems at various stages of their evolution. Questions about disk evolution and planet formation belong to the key science cases for the presented interferometers which are therefore designed also to meet the requirements in sensitivity and accuracy.

The presented tasks for the next generation of long-baseline optical to infrared interferometers and exemplary case studies are by no means comprehensive, but illustrate the potential of these type of astronomical observations. Moreover, as pointed out, the combination of individual interferometers with those operating at other wavelengths and single telescopes which provide significant higher sensitivity and field-of-view is essential to connect small and large scales and to trace the complex interplay of different physical processes in protoplanetary disks. From this point of view, currently existing and planned large ground-based telescopes and (sub)millimeter interferometers in combination with space observatories provide the perfect frame for the next-generation long-baseline optical to infrared interferometers.

Acknowledgements The work on this article was initiated during the workshop “Circumstellar disks and planets – Science cases for the second generation VLTI instrumentation” (University of Kiel, 2010), funded through the “Optical Interferometry Networking Activity” (European Community’s Seventh Framework Programme under Grant Agreement 226604). RDA acknowledges support from the Science & Technology Facilities Council (STFC) through an Advanced Fellowship (ST/G00711X/1). CM acknowledges the valuable discussions with H. Klahr, Y. Alibert, W. Benz, Ch. Ormel, K.-M. Dittkrist, and A. Reufer during the preparation of Sect. 2.2. CM acknowledges financial support by the Swiss National Science Foundation and the financial support as a fellow of the Alexander von Humboldt Foundation. The realization of the KI-ASTRA upgrade is supported by the NSF MRI grant, AST-0619965. The W.M. Keck Observatory is operated as a scientific partnership among the California Institute of Technology, the University of California and the National Aeronautics and Space Administration. The Observatory was made possible by the generous financial support of the W.M. Keck Foundation. The authors wish to recognize and acknowledge the very significant cultural role and reverence that the summit of Mauna Kea has always had within the indigenous Hawaiian community. The KI is funded by the National Aeronautics and Space Administration as part of its Exoplanet Exploration program Funded by NASA, the KI is developed and operated by JPL²⁴, NExSci²⁵ and the W. M. Keck Observatory (WMKO²⁶). ASTRA is funded by the National Science Foundation (NSF) Major Research Instrumentation (MRI) program²⁷. Besides the NSF engagement, a number of science institutes contribute to the ASTRA collaboration to advance and profit from large-aperture OLBI (UC Berkeley, UCLA, Caltech, NExSci, JPL, University of Arizona). The design and deployment of the MROI facility is being directed from a Project Office at the New Mexico Institute of Mining and Technology. The MROI main collaborator on the project is the former COAST interferometer group at the Cavendish Laboratory, University of Cambridge, UK. SW acknowledges the tremendous work done by the MATISSE Science Group (Phase A); selected parts

²⁴ Jet Propulsion Laboratory; http://planetquest.jpl.nasa.gov/Keck/keck_index.cfm

²⁵ NASA Exoplanet Science Institute; <http://nexsci.caltech.edu>

²⁶ <http://keckobservatory.org>

²⁷ Wizinowich, P., Graham, J., Woillez, J., et al. NSF-MRI Award Abstract #0619965

of this article are based on the “MATISSE, Sciences Cases” (Doc. No. VLT-TRE-MAT-15860-432, Wolf et al., 2007). We wish to thank W. Brandner, T. Herbst, F. Ménard, and K. Stapelfeldt, for fruitful discussions during the preparation of this article.

References

Absil O, Mawet D (2010) Formation and evolution of planetary systems: the impact of high-angular resolution optical techniques. *A&A Rev.*18:317–382, DOI 10.1007/s00159-009-0028-y, 0912.3915

Absil O, Le Bouquin JB, Lebreton J, Augereau JC, Benisty M, Chauvin G, Hanot C, Mérand A, Montagnier G (2010) Deep near-infrared interferometric search for low-mass companions around β Pictoris. *A&A*520:L2, DOI 10.1051/0004-6361/201015156, 1009.1245

Absil O, Le Bouquin JB, Berger JP, Lagrange AM, Chauvin G, Lazareff B, Zins G, Hague-nauer P, Jocou L, Kern P, Millan-Gabet R, Rochat S, Traub W (2011) Searching for faint companions with VLTI/PIONIER. I. Method and first results. *A&A*535:A68, DOI 10.1051/0004-6361/201117719, 1110.1178

Acke B, van den Ancker ME, Dullemond CP (2005) [O I] 6300 Å emission in Herbig Ae/Be systems: Signature of Keplerian rotation. *A&A*436:209–230, DOI 10.1051/0004-6361:20042484, arXiv:astro-ph/0502504

Akeson RL, Boden AF, Monnier JD, Millan-Gabet R, Beichman C, Beletic J, Calvet N, Hartmann L, Hillenbrand L, Koresko C, Sargent A, Tannirkulam A (2005) Keck Interferometer Observations of Classical and Weak-line T Tauri Stars. *ApJ*635:1173–1181, DOI 10.1086/497436

Alencar SHP, Teixeira PS, Guimarães MM, McGinnis PT, Gameiro JF, Bouvier J, Aigrain S, Flaccomio E, Favata F (2010) Accretion dynamics and disk evolution in NGC 2264: a study based on CoRoT photometric observations. *A&A*519:A88+, DOI 10.1051/0004-6361/201014184, 1005.4384

Alexander R (2008a) From discs to planetesimals: Evolution of gas and dust discs. *New A Rev.*52:60–77, DOI 10.1016/j.newar.2008.04.004, 0712.0388

Alexander RD (2008b) [NeII] emission-line profiles from photoevaporative disc winds. *MNRAS*391:L64–L68, DOI 10.1111/j.1745-3933.2008.00556.x, 0809.0316

Alexander RD, Armitage PJ (2009) Giant Planet Migration, Disk Evolution, and the Origin of Transitional Disks. *ApJ*704:989–1001, DOI 10.1088/0004-637X/704/2/989, 0909.0004

Alexander RD, Clarke CJ, Pringle JE (2004) On the origin of ionizing photons emitted by T Tauri stars. *MNRAS*348:879–884, DOI 10.1111/j.1365-2966.2004.07401.x, arXiv:astro-ph/031276

Alexander RD, Clarke CJ, Pringle JE (2005) Constraints on the ionizing flux emitted by T Tauri stars. *MNRAS*358:283–290, DOI 10.1111/j.1365-2966.2005.08786.x, arXiv:astro-ph/0501100

Alexander RD, Clarke CJ, Pringle JE (2006a) Photoevaporation of protoplanetary discs - I. Hydrodynamic models. *MNRAS*369:216–228, DOI 10.1111/j.1365-2966.2006.10293.x, arXiv:astro-ph/0603253

Alexander RD, Clarke CJ, Pringle JE (2006b) Photoevaporation of protoplanetary discs - II. Evolutionary models and observable properties. *MNRAS*369:229–239, DOI 10.1111/j.1365-2966.2006.10294.x, arXiv:astro-ph/0603254

Alibert Y, Mordasini C, Benz W (2004) Migration and giant planet formation. *A&A*417:L25

Alibert Y, Mordasini C, Benz W, Winisdoerffer C (2005a) Models of giant planet formation with migration and disc evolution. *A&A*434:343

Alibert Y, Mousis O, Mordasini C, Benz W (2005b) New jupiter and saturn formation models meet observations. *ApJ*626:L57

Alibert Y, Mordasini C, Benz W (2011) Extrasolar planet population synthesis. III. Formation of planets around stars of different masses. *A&A*526:A63, DOI 10.1051/0004-6361/201014760, 1101.0513

Andrews SM, Williams JP (2005) Circumstellar Dust Disks in Taurus-Auriga: The Submillimeter Perspective. *ApJ*631:1134–1160, DOI 10.1086/432712, arXiv:astro-ph/0506187

Andrews SM, Williams JP (2007) High-Resolution Submillimeter Constraints on Circumstellar Disk Structure. *ApJ*659:705–728, DOI 10.1086/511741, arXiv:astro-ph/0610813

Andrews SM, Wilner DJ, Hughes AM, Qi C, Dullemond CP (2009) Protoplanetary Disk Structures in Ophiuchus. *ApJ*700:1502–1523, DOI 10.1088/0004-637X/700/2/1502, 0906.0730

Andrews SM, Wilner DJ, Hughes AM, Qi C, Dullemond CP (2010) Protoplanetary Disk Structures in Ophiuchus. II. Extension to Fainter Sources. *ApJ*723:1241–1254, DOI 10.1088/0004-637X/723/2/1241, 1007.5070

Araya E, Hofner P, Sewiło M, Goss WM, Linz H, Kurtz S, Olmi L, Churchwell E, Rodríguez LF, Garay G (2007) An H₂CO 6 cm Maser Pinpointing a Possible Circumstellar Torus in IRAS 18566+0408. *ApJ*669:1050–1057, DOI 10.1086/521576, 0708.3832

Armitage PJ (2007) Lecture notes on the formation and early evolution of planetary systems. ArXiv Astrophysics e-prints arXiv:astro-ph/0701485

Armitage PJ (2010) *Astrophysics of Planet Formation*. Cambridge, UK: Cambridge University Press

Armitage PJ, Livio M, Pringle JE (2001) Episodic accretion in magnetically layered protoplanetary discs. *MNRAS*324:705–711, DOI 10.1046/j.1365-8711.2001.04356.x, arXiv:astro-ph/0101253

Bacciotti F, Testi L, Marconi A, Garcia PJV, Ray TP, Eislöffel J, Dougados C (2003) Unveiling the Launching Region of YSO Jets with AMBER. *Ap&SS*286:157–162, DOI 10.1023/A:1026151304959

Baines EK, McAlister HA, ten Brummelaar TA, Sturmann J, Sturmann L, Turner NH, Ridgway ST (2009) Eleven Exoplanet Host Star Angular Diameters from the Chara Array. *ApJ*701:154–162, DOI 10.1088/0004-637X/701/1/154, 0906.2702

Balbus SA (2009) Magnetohydrodynamics of Protostellar Disks. In: Garcia, P (ed) *Physical Processes in Circumstellar Disks Around Young Stars*, arXiv0906.0854

Balbus SA, Hawley JF (1991) A powerful local shear instability in weakly magnetized disks. I - Linear analysis. II - Nonlinear evolution. *ApJ*376:214–233, DOI 10.1086/170270

Balbus SA, Hawley JF (1998) Instability, turbulence, and enhanced transport in accretion disks. *Reviews of Modern Physics* 70:1–53

Banzatti A, Testi L, Isella A, Natta A, Neri R, Wilner DJ (2011) New constraints on dust grain size and distribution in CQ Tauri. *A&A*525:A12+, DOI 10.1051/0004-6361/201015206, 1009.2697

Baraffe I, Chabrier G, Barman TS, Allard F, Hauschildt PH (2003) Evolutionary models for cool brown dwarfs and extrasolar giant planets. The case of HD 209458. *A&A*402:701–712, DOI 10.1051/0004-6361:20030252, arXiv:astro-ph/0302293

Baron F, Young JS (2008) Image reconstruction at Cambridge University. In: Society of Photo-Optical Instrumentation Engineers (SPIE) Conference Series, Presented at the So-

ciety of Photo-Optical Instrumentation Engineers (SPIE) Conference, vol 7013, DOI 10.1117/12.789115

Batygin K, Stevenson DJ (2010) Inflating Hot Jupiters with Ohmic Dissipation. *ApJ*714:L238–L243, DOI 10.1088/2041-8205/714/2/L238, 1002.3650

Baudoz P, Boccaletti A, Riaud P, Cavarroc C, Baudrand J, Reess JM, Rouan D (2006) Feasibility of the Four-Quadrant Phase Mask in the Mid-Infrared on the James Webb Space Telescope. *PASP*118:765–773, DOI 10.1086/503124

Beckwith SVW, Sargent AI (1991) Particle emissivity in circumstellar disks. *ApJ*381:250–258, DOI 10.1086/170646

Beckwith SVW, Sargent AI, Chini RS, Guesten R (1990) A survey for circumstellar disks around young stellar objects. *AJ*99:924–945, DOI 10.1086/115385

Begelman MC, McKee CF, Shields GA (1983) Compton heated winds and coronae above accretion disks. I Dynamics. *ApJ*271:70–88, DOI 10.1086/161178

Beichman CA, Krist J, Trauger JT, Greene T, Oppenheimer B, Sivaramakrishnan A, Doyon R, Boccaletti A, Barman TS, Rieke M (2010) Imaging Young Giant Planets From Ground and Space. *PASP*122:162–200, DOI 10.1086/651057, 1001.0351

Belu AR, Selsis F, Morales JC, Ribas I, Cossou C, Rauer H (2011) Primary and secondary eclipse spectroscopy with JWST: exploring the exoplanet parameter space. *A&A*525:A83+, DOI 10.1051/0004-6361/201014995, 1008.0028

Benisty M, Natta A, Isella A, Berger J, Massi F, Le Bouquin J, Mérand A, Duvert G, Kraus S, Malbet F, Olofsson J, Robbe-Dubois S, Testi L, Vannier M, Weigelt G (2010) Strong near-infrared emission in the sub-AU disk of the Herbig Ae star HD 163296: evidence of refractory dust? *A&A*511:A74+, DOI 10.1051/0004-6361/200912898, 0911.4363

Beuther H, Schilke P, Menten KM, Motte F, Sridharan TK, Wyrowski F (2002) High-Mass Protostellar Candidates. II. Density Structure from Dust Continuum and CS Emission. *ApJ*566:945–965, DOI 10.1086/338334, arXiv:astro-ph/0110370

Birnstiel T, Ricci L, Trotta F, Dullemond CP, Natta A, Testi L, Dominik C, Henning T, Ormel CW, Zsom A (2010) Testing the theory of grain growth and fragmentation by millimeter observations of protoplanetary disks. *A&A*516:L14+, DOI 10.1051/0004-6361/201014893, 1006.0940

Boccaletti A, Augereau JC, Marchis F, Hahn J (2003) Ground-based Near-Infrared Imaging of the HD 141569 Circumstellar Disk. *ApJ*585:494–501, DOI 10.1086/346019, arXiv:astro-ph/0211648

Bodenheimer P, Pollack JB (1986) Calculations of the accretion and evolution of giant planets: The effects of solid cores. *Icarus* 67:391

Bodenheimer P, Hubickyj O, Lissauer JJ (2000) Models of the in situ formation of detected extrasolar giant planets. *Icarus* 143:2

Boley AC (2009) The two modes of gas giant planet formation. *The Astrophysical Journal Letters* 695:L53

Boss AP (2007) Testing Disk Instability Models for Giant Planet Formation. *ApJ*661:L73–L76

Bouvier J, Alencar SHP, Boutelier T, Dougados C, Balog Z, Grankin K, Hodgkin ST, Ibrahimov MA, Kun M, Magakian TY, Pinte C (2007) Magnetospheric accretion-ejection processes in the classical T Tauri star AA Tauri. *A&A*463:1017–1028, DOI 10.1051/0004-6361:20066021, arXiv:astro-ph/0611787

Bouwman J, de Koter A, Dominik C, Waters LBFM (2003) The origin of crystalline silicates in the Herbig Be star HD 100546 and in comet Hale-Bopp. *A&A*401:577–592, DOI 10.1051/0004-6361:20030043, arXiv:astro-ph/0301254

Bowler BP, Liu MC, Dupuy TJ, Cushing MC (2010) Near-infrared Spectroscopy of the Extrasolar Planet HR 8799 b. *ApJ*723:850–868, DOI 10.1088/0004-637X/723/1/850, 1008.4582

Brauer F, Dullemond CP, Henning T (2008a) Coagulation, fragmentation and radial motion of solid particles in protoplanetary disks. *A&A*480:859–877

Brauer F, Henning T, Dullemond CP (2008b) Planetesimal formation near the snow line in MRI-driven turbulent protoplanetary disks. *A&A*487:L1–L4, DOI 10.1051/0004-6361:200809780, 0806.1646

Brown JM, Blake GA, Qi C, Dullemond CP, Wilner DJ, Williams JP (2009) Evidence for Dust Clearing Through Resolved Submillimeter Imaging. *ApJ*704:496–502, DOI 10.1088/0004-637X/704/1/496, 0909.5595

Buenzli E, Thalmann C, Vigan A, Boccaletti A, Chauvin G, Augereau JC, Meyer MR, Ménard F, Desidera S, Messina S, Henning T, Carson J, Montagnier G, Beuzit JL, Bonavita M, Eggenberger A, Lagrange AM, Mesa D, Mouillet D, Quanz SP (2010) Dissecting the Moth: discovery of an off-centered ring in the HD 61005 debris disk with high-resolution imaging. *A&A*524:L1+, DOI 10.1051/0004-6361/201015799, 1011.2496

Burrows CJ, Stapelfeldt KR, Watson AM, Krist JE, Ballester GE, Clarke JT, Crisp D, Gallagher JS III, Griffiths RE, Hester JJ, Hoessel JG, Holtzman JA, Mould JR, Scowen PA, Trauger JT, Westphal JA (1996) Hubble Space Telescope Observations of the Disk and Jet of HH 30. *ApJ*473:437–+, DOI 10.1086/178156

Cai K, Pickett MK, Durisen RH, Milne AM (2010) Giant Planet Formation by Disk Instability: A Comparison Simulation with an Improved Radiative Scheme. *ApJ*716:L176–L180

Carr JS, Najita JR (2008) Organic Molecules and Water in the Planet Formation Region of Young Circumstellar Disks. *Science* 319:1504–, DOI 10.1126/science.1153807

Casse F, Ferreira J (2000) Magnetized accretion-ejection structures. IV. Magnetically-driven jets from resistive, viscous, Keplerian discs. *A&A*353:1115–1128

Cesaroni R (2008) High-mass star forming regions: An ALMA view. *Ap&SS*313:23–28, DOI 10.1007/s10509-007-9596-3

Cesaroni R, Neri R, Olmi L, Testi L, Walmsley CM, Hofner P (2005) A study of the Keplerian accretion disk and precessing outflow in the massive protostar IRAS 20126+4104. *A&A*434:1039–1054, DOI 10.1051/0004-6361:20041639

Chiang E, Murray-Clay R (2007) Inside-out evacuation of transitional protoplanetary discs by the magneto-rotational instability. *Nature Physics* 3:604–608, DOI 10.1038/nphys661, 0706.1241

Chiang EI, Joung MK, Creech-Eakman MJ, Qi C, Kessler JE, Blake GA, van Dishoeck EF (2001) Spectral Energy Distributions of Passive T Tauri and Herbig Ae Disks: Grain Mineralogy, Parameter Dependences, and Comparison with Infrared Space Observatory LWS Observations. *ApJ*547:1077–1089, DOI 10.1086/318427, arXiv:astro-ph/0009428

Chin JCY, Stalcup T, Wizinowich P, Pantaleev S, Neyman C, Tsubota K, Summers D, Stomski P, Medeiros D, Nance C, Grace K, Cooper A, Wetherell E, Doyle S (2010) Keck I laser guide star AO system integration. In: Society of Photo-Optical Instrumentation Engineers (SPIE) Conference Series, Presented at the Society of Photo-Optical Instrumentation Engineers (SPIE) Conference, vol 7736, DOI 10.1117/12.857598

Churchwell E, Babler BL, Meade MR, Whitney BA, Benjamin R, Indebetouw R, Cyganowski C, Robitaille TP, Povich M, Watson C, Bracker S (2009) The Spitzer/GLIMPSE Surveys: A New View of the Milky Way. *PASP*121:213–230, DOI 10.1086/597811

Cieza LA, Swift JJ, Mathews GS, Williams JP (2008) The Masses of Transition Circumstellar Disks: Observational Support for Photoevaporation Models. *ApJ*686:L115–L118, DOI 10.1086/592965, 0809.0030

Clampin M (2009) Comparative Planetology: Transiting Exoplanet Science with JWST. In: astro2010: The Astronomy and Astrophysics Decadal Survey, *Astronomy*, vol 2010, pp 46–+

Clampin M, Krist JE, Ardila DR, Golimowski DA, Hartig GF, Ford HC, Illingworth GD, Bartko F, Benítez N, Blakeslee JP, Bouwens RJ, Broadhurst TJ, Brown RA, Burrows CJ, Cheng ES, Cross NJG, Feldman PD, Franx M, Gronwall C, Infante L, Kimble RA, Lesser MP, Martel AR, Menanteau F, Meurer GR, Miley GK, Postman M, Rosati P, Sirianni M, Sparks WB, Tran HD, Tsvetanov ZI, White RL, Zheng W (2003) Hubble Space Telescope ACS Coronagraphic Imaging of the Circumstellar Disk around HD 141569A. *AJ*126:385–392, DOI 10.1086/375460, arXiv:astro-ph/0303605

Clarke CJ (2009) Pseudo-viscous modelling of self-gravitating discs and the formation of low mass ratio binaries. *MNRAS*396:1066–1074, DOI 10.1111/j.1365-2966.2009.14774.x, 0904.3549

Clarke CJ, Gendrin A, Sotomayor M (2001) The dispersal of circumstellar discs: the role of the ultraviolet switch. *MNRAS*328:485–491, DOI 10.1046/j.1365-8711.2001.04891.x

Colavita MM, Wallace JK, Hines BE, Gursel Y, Malbet F, Palmer DL, Pan XP, Shao M, Yu JW, Boden AF, Dumont PJ, Gubler J, Koresko CD, Kulkarni SR, Lane BF, Mobley DW, van Belle GT (1999) The Palomar Testbed Interferometer. *ApJ*510:505–521, DOI 10.1086/306579, arXiv:astro-ph/9810262

Colavita MM, Serabyn E, Booth AJ, Crawford SL, Garcia-Gathright JI, Ligon ER, Mennesson BL, Paine CG, Wizinowich PL, Ragland S, Appleby EC, Berkey BC, Cooper A, Dahl W, Gathright JT, Hrynevych MA, Medeiros DW, Morrison D, Panteleeva T, Smith B, Summers KR, Tsubota K, Tyau C, Wetherell E, Woillez JM, Akeson RL, Millan-Gabet R, Felizardo C, Koresko CD, Herstein JS (2008) Keck Interferometer noller update. In: Society of Photo-Optical Instrumentation Engineers (SPIE) Conference Series, Presented at the Society of Photo-Optical Instrumentation Engineers (SPIE) Conference, vol 7013, DOI 10.1117/12.789476

Cossins P, Lodato G, Testi L (2010) Resolved images of self-gravitating circumstellar discs with ALMA. *MNRAS*407:181–188, DOI 10.1111/j.1365-2966.2010.16934.x, 1004.5389

Cowan NB, Agol E (2011) The Statistics of Albedo and Heat Recirculation on Hot Exoplanets. *ApJ*729:54–+, DOI 10.1088/0004-637X/729/1/54, 1001.0012

Creech-Eakman M, Young J, Haniff C, Buscher D, Elvis M, Chiavassa A, Schartmann M (2010a) Imaging simulations of selected science with the Magdalena Ridge Observatory Interferometer. In: Society of Photo-Optical Instrumentation Engineers (SPIE) Conference Series, Presented at the Society of Photo-Optical Instrumentation Engineers (SPIE) Conference, vol 7734, DOI 10.1117/12.858359

Creech-Eakman MJ, Romero V, Westpfahl D, Cormier C, Haniff C, Buscher D, Bakker E, Berger L, Block E, Coleman T, Festler P, Jurgenson C, King R, Klinglesmith D, McCord K, Olivares A, Parameswariah C, Payne I, Paz T, Ryan E, Salcido C, Santoro F, Selina R, Shtromberg A, Steenson J, Baron F, Boysen R, Coyne J, Fisher M, Seneta E, Sun X, Thureau N, Wilson D, Young J (2008) Magdalena Ridge Observatory Interferometer: progress toward first light. In: Society of Photo-Optical Instrumentation Engineers (SPIE) Conference Series, Society of Photo-Optical Instrumentation Engineers (SPIE) Conference Series, vol 7013, DOI 10.1117/12.789859

Creech-Eakman MJ, Romero V, Payne I, Haniff C, Buscher D, Aitken C, Anderson C, Bakker E, Coleman T, Dahl C, Farris A, Jiminez S, Jurgenson C, King R, Klinglesmith D III, McCord K, McCracken T, Nyland K, Olivares A, Richmond M, Romero M, Saldado C, Sandoval J, Santoro F, Seamons J, Selina R, Shtromberg A, Steenson J, Torres N, Westpfahl D, Baron F, Fisher M, Seneta E, Sun X, Wilson D, Young J (2010b) Magdalena Ridge Observatory Interferometer: advancing to first light and new science. In: Society of Photo-Optical Instrumentation Engineers (SPIE) Conference Series, Presented at the Society of Photo-Optical Instrumentation Engineers (SPIE) Conference, vol 7734, DOI 10.1117/12.857359

Crida A, Morbidelli A (2007) Cavity opening by a giant planet in a protoplanetary disc and effects on planetary migration. *MNRAS* 377:1324–1336

Cuzzi JN, Hogan RC, Shariff K (2008) Toward Planetesimals: Dense Chondrule Clumps in the Protoplanetary Nebula. *ApJ* 687:1432–1447

Cyganowski CJ, Brogan CL, Hunter TR, Churchwell E, Zhang Q (2011) Bipolar Molecular Outflows and Hot Cores in Glimpse Extended Green Objects (EGOs). *ApJ* 729:124–+, DOI 10.1088/0004-637X/729/2/124, 1012.0851

D'Alessio P, Calvet N, Hartmann L, Muzerolle J, Sitko M (2004) Models of Accretion Disks Around Young Stars. In: M G Burton, R Jayawardhana, & T L Bourke (ed) Star Formation at High Angular Resolution, IAU Symposium, vol 221, pp 403–+, arXiv: astro-ph/0309590

D'Angelo G, Durisen RH, Lissauer JJ (2010) Giant Planet Formation. ArXiv e-prints 1006.5486

Dartois E, Dutrey A, Guilloteau S (2003) Structure of the DM Tau Outer Disk: Probing the vertical kinetic temperature gradient. *A&A* 399:773–787, DOI 10.1051/0004-6361:20021638

Delplancke F (2008) The PRIMA facility phase-referenced imaging and micro-arcsecond astrometry. *New Astronomy Reviews* 52:199–207, DOI 10.1016/j.newar.2008.04.016

Dougados C (2009) Magnetic Jets from Young Stars: high-angular resolution observations. In: M Heydari-Malayeri, C Reyl'E, & R Samadi (ed) SF2A-2009: Proceedings of the Annual meeting of the French Society of Astronomy and Astrophysics, pp 3–+

Dougados C, Bouvier J, Duvert G, Garcia PJV, Folha DFM (2003) Probing the magnetosphere in young stars with AMBER/VLTI. *Ap&SS* 286:151–156, DOI 10.1023/A:1026147204051

Doyon R, Rowlands N, Hutchings J, Evans CE, Greenberg E, Scott AD, Touhari D, Beaulieu M, Abraham R, Ferrarese L, Fullerton AW, Jayawardhana R, Johnston D, Meyer MR, Pipher J, Sawicki M (2008) The JWST tunable filter imager (TFI). In: Society of Photo-Optical Instrumentation Engineers (SPIE) Conference Series, Presented at the Society of Photo-Optical Instrumentation Engineers (SPIE) Conference, vol 7010, DOI 10.1117/12.789504

Duchêne G, Ghez AM, McCabe C (2002) Resolved Near-Infrared Spectroscopy of the Mysterious Pre-Main-Sequence Binary System T Tauri S. *ApJ* 568:771–778, DOI 10.1086/338987, arXiv:astro-ph/0112103

Duchêne G, McCabe C, Ghez AM, Macintosh BA (2004) A Multiwavelength Scattered Light Analysis of the Dust Grain Population in the GG Tauri Circumbinary Ring. *ApJ* 606:969–982, DOI 10.1086/383126, arXiv:astro-ph/0401560

Dullemond CP, Dominik C (2004a) Flaring vs. self-shadowed disks: The SEDs of Herbig Ae/Be stars. *A&A* 417:159–168, DOI 10.1051/0004-6361:20031768, arXiv: astro-ph/0401495

Dullemond CP, Dominik C (2004b) The effect of dust settling on the appearance of protoplanetary disks. *A&A*421:1075–1086, DOI 10.1051/0004-6361:20040284, [astro-ph/0405226](#)

Dullemond CP, Dominik C, Natta A (2001) Passive Irradiated Circumstellar Disks with an Inner Hole. *ApJ*560:957–969, DOI 10.1086/323057, [arXiv:astro-ph/0106470](#)

Dullemond CP, Hollenbach D, Kamp I, D'Alessio P (2007) Models of the Structure and Evolution of Protoplanetary Disks. *Protostars and Planets V* pp 555–572, [arXiv:astro-ph/0602619](#)

Durán-Rojas MC, Watson AM, Stapelfeldt KR, Hiriart D (2009) The Polarimetric and Photometric Variability of HH 30. *AJ*137:4330–4338, DOI 10.1088/0004-6256/137/5/4330

Durisen RH, Mejia AC, Pickett BK, Hartquist TW (2001) Gravitational Instabilities in the Disks of Massive Protostars as an Explanation for Linear Distributions of Methanol Masers. *ApJ*563:L157–L160, DOI 10.1086/338738

Dutrey A, Guilloteau S, Duvert G, Prato L, Simon M, Schuster K, Menard F (1996) Dust and gas distribution around T Tauri stars in Taurus-Auriga. I. Interferometric 2.7mm continuum and 13CO J=1-0 observations. *A&A*309:493–504

Dutrey A, Guilloteau S, Guelin M (1997) Chemistry of protosolar-like nebulae: The molecular content of the DM Tau and GG Tau disks. *A&A*317:L55–L58

Dutrey A, Guilloteau S, Ho P (2007) Interferometric Spectroimaging of Molecular Gas in Protoplanetary Disks. *Protostars and Planets V* pp 495–506

Dzyurkevich N, Flock M, Turner NJ, Klahr H, Henning T (2010) Trapping solids at the inner edge of the dead zone: 3-D global MHD simulations. *A&A*515:A70+

Edgar RG, Quillen AC (2008) The vertical structure of planet-induced gaps in protoplanetary discs. *MNRAS*387:387–396, DOI 10.1111/j.1365-2966.2008.13242.x, 0709.1649

Eisenhauer F, Quirrenbach A, Zinnecker H, Genzel R (1998) Stellar Content of the Galactic Starburst Template NGC 3603 from Adaptive Optics Observations. *ApJ*498:278–+, DOI 10.1086/305552

Eisner JA (2007) Water vapour and hydrogen in the terrestrial-planet-forming region of a protoplanetary disk. *Nature*447:562–564, DOI 10.1038/nature05867, 0706.1239

Eisner JA, Hillenbrand LA, White RJ, Akeson RL, Sargent AI (2005) Observations of T Tauri Disks at Sub-AU Radii: Implications for Magnetospheric Accretion and Planet Formation. *ApJ*623:952–966, DOI 10.1086/428828

Eisner JA, Chiang EI, Hillenbrand LA (2006) Spatially Resolving the Inner Disk of TW Hydrae. *ApJ*637:L133–L136, DOI 10.1086/500689, [arXiv:astro-ph/0601034](#)

Eisner JA, Chiang EI, Lane BF, Akeson RL (2007a) Spectrally Dispersed K-Band Interferometric Observations of Herbig Ae/Be Sources: Inner Disk Temperature Profiles. *ApJ*657:347–358, DOI 10.1086/510833

Eisner JA, Hillenbrand LA, White RJ, Bloom JS, Akeson RL, Blake CH (2007b) Near-Infrared Interferometric, Spectroscopic, and Photometric Monitoring of T Tauri Inner Disks. *ApJ*669:1072–1084, DOI 10.1086/521874

Eisner JA, Graham JR, Akeson RL, Najita J (2009) Spatially Resolved Spectroscopy of Sub-AU-Sized Regions of T Tauri and Herbig Ae/Be Disks. *ApJ*692:309–323, DOI 10.1088/0004-637X/692/1/309

Eisner JA, Monnier JD, Woillez J, Akeson RL, Millan-Gabet R, Graham JR, Hillenbrand LA, Pott J, Ragland S, Wizinowich P (2010) Spatially and Spectrally Resolved Hydrogen Gas within 0.1 AU of T Tauri and Herbig Ae/Be Stars. *ApJ*718:774–794, DOI 10.1088/0004-637X/718/2/774, 1006.1651

Ercolano B, Owen JE (2010) Theoretical spectra of photoevaporating protoplanetary discs: an atlas of atomic and low-ionization emission lines. *MNRAS*406:1553–1569, DOI 10.

1111/j.1365-2966.2010.16798.x, 1004.1203

Ercolano B, Clarke CJ, Drake JJ (2009) X-Ray Irradiated Protoplanetary Disk Atmospheres. II. Predictions from Models in Hydrostatic Equilibrium. *ApJ*699:1639–1649, DOI 10.1088/0004-637X/699/2/1639, 0905.1001

Farris A, Klingsmith D, Seamons J, Torres N, Buscher D, Young J (2010) Software architecture of the Magdalena Ridge Observatory Interferometer. In: Society of Photo-Optical Instrumentation Engineers (SPIE) Conference Series, Presented at the Society of Photo-Optical Instrumentation Engineers (SPIE) Conference, vol 7740, DOI 10.1117/12.856497

Fedele D, van den Ancker ME, Acke B, van der Plas G, van Boekel R, Wittkowski M, Henning T, Bouwman J, Meeus G, Rafanelli P (2008) The structure of the protoplanetary disk surrounding three young intermediate mass stars. II. Spatially resolved dust and gas distribution. *A&A*491:809–820, DOI 10.1051/0004-6361:200810126, 0809.3947

Fedele D, van den Ancker ME, Henning T, Jayawardhana R, Oliveira JM (2010) Timescale of mass accretion in pre-main-sequence stars. *A&A*510:A72+, DOI 10.1051/0004-6361/200912810, 0911.3320

Fischer DA, Valenti J (2005) The Planet-Metallicity Correlation. *ApJ*622:1102–1117, DOI 10.1086/428383

Fisher M, Boysen RC, Buscher DF, Haniff CA, Seneta EB, Sun X, Wilson DMA, Young JS (2010) Design of the MROI delay line optical path compensator. In: Society of Photo-Optical Instrumentation Engineers (SPIE) Conference Series, Presented at the Society of Photo-Optical Instrumentation Engineers (SPIE) Conference, vol 7734, DOI 10.1117/12.857168

Fitzgerald MP, Kalas PG, Duchêne G, Pinte C, Graham JR (2007a) The AU Microscopii Debris Disk: Multiwavelength Imaging and Modeling. *ApJ*670:536–556, DOI 10.1086/521344, 0705.4196

Fitzgerald MP, Kalas PG, Graham JR (2007b) A Ring of Warm Dust in the HD 32297 Debris Disk. *ApJ*670:557–564, DOI 10.1086/521699, 0707.3295

Font AS, McCarthy IG, Johnstone D, Ballantyne DR (2004) Photoevaporation of Circumstellar Disks around Young Stars. *ApJ*607:890–903, DOI 10.1086/383518, arXiv:astro-ph/0402241

Fortney JJ, Marley MS, Hubickyj O, Bodenheimer PH, Lissauer JJ (2005) Young jupiters are faint: new models of the early evolution of giant planets. *Astronomische Nachrichten* 326:925

Fortney JJ, Lodders K, Marley MS, Freedman RS (2008a) A Unified Theory for the Atmospheres of the Hot and Very Hot Jupiters: Two Classes of Irradiated Atmospheres. *ApJ*678:1419–1435, DOI 10.1086/528370, 0710.2558

Fortney JJ, Marley MS, Saumon D, Lodders K (2008b) Synthetic Spectra and Colors of Young Giant Planet Atmospheres: Effects of Initial Conditions and Atmospheric Metallicity. *ApJ*683:1104–1116, DOI 10.1086/589942, 0805.1066

Fromang S (2005) The effect of MHD turbulence on massive protoplanetary disk fragmentation. *A&A*441:1–8, DOI 10.1051/0004-6361:20053080, arXiv:astro-ph/0506216

Fromang S, Balbus SA, Terquem C, De Villiers JP (2004) Evolution of Self-Gravitating Magnetized Disks. II. Interaction between Magnetohydrodynamic Turbulence and Gravitational Instabilities. *ApJ*616:364–375, DOI 10.1086/424829, arXiv:astro-ph/0409404

Fukagawa M, Hayashi M, Tamura M, Itoh Y, Hayashi SS, Oasa Y, Takeuchi T, Morino Ji, Murakawa K, Oya S, Yamashita T, Suto H, Mayama S, Naoi T, Ishii M, Pyo TS, Nishikawa T, Takato N, Usuda T, Ando H, Iye M, Miyama SM, Kaifu N (2004) Spiral

Structure in the Circumstellar Disk around AB Aurigae. *ApJ*605:L53–L56, DOI 10.1086/420699

Gammie CF (1996) Layered Accretion in T Tauri Disks. *ApJ*457:355–+, DOI 10.1086/176735

Gammie CF (2001) Nonlinear Outcome of Gravitational Instability in Cooling, Gaseous Disks. *ApJ*553:174–183

Gardner JP, Mather JC, Clampin M, Doyon R, Greenhouse MA, Hammel HB, Hutchings JB, Jakobsen P, Lilly SJ, Long KS, Lunine JI, McCaughrean MJ, Mountain M, Nella J, Rieke GH, Rieke MJ, Rix HW, Smith EP, Sonneborn G, Stiavelli M, Stockman HS, Windhorst RA, Wright GS (2006) Science with the James Webb space telescope. In: Society of Photo-Optical Instrumentation Engineers (SPIE) Conference Series, Presented at the Society of Photo-Optical Instrumentation Engineers (SPIE) Conference, vol 6265, DOI 10.1117/12.670492

Gillessen S, Eisenhauer F, Perrin G, Brandner W, Straubmeier C, Perraut K, Amorim A, Schöller M, Araujo-Hauck C, Bartko H, Baumeister H, Berger J, Carvas P, Cassaing F, Chapron F, Choquet E, Clenet Y, Collin C, Eckart A, Fedou P, Fischer S, Gendron E, Genzel R, Gitton P, Gonte F, Gräter A, Hagueauer P, Haug M, Haubois X, Henning T, Hippler S, Hofmann R, Jocou L, Kellner S, Kervella P, Klein R, Kudryavtseva N, Lacour S, Lapeyrere V, Laun W, Lena P, Lenzen R, Lima J, Moratschke D, Moch D, Moulin T, Naranjo V, Neumann U, Nolot A, Paumard T, Pfuhl O, Rabien S, Ramos J, Rees JM, Rohloff R, Rouan D, Rousset G, Sevin A, Thiel M, Wagner K, Wiest M, Yazici S, Ziegler D (2010) GRAVITY: a four-telescope beam combiner instrument for the VLTI. In: Society of Photo-Optical Instrumentation Engineers (SPIE) Conference Series, Presented at the Society of Photo-Optical Instrumentation Engineers (SPIE) Conference, vol 7734, DOI 10.1117/12.856689, 1007.1612

Gilmozzi R, Spyromilio J (2008) The 42m European ELT: status. In: Society of Photo-Optical Instrumentation Engineers (SPIE) Conference Series, Presented at the Society of Photo-Optical Instrumentation Engineers (SPIE) Conference, vol 7012, DOI 10.1117/12.790801

Glauser AM, Ménard F, Pinte C, Duchêne G, Güdel M, Monin JL, Padgett DL (2008) Multiwavelength studies of the gas and dust disc of IRAS 04158+2805. *A&A*485:531–540, DOI 10.1051/0004-6361:20065685, 0804.3483

Glindemann A, Algomedo J, Amestica R, Ballester P, Bauvir B, Bugueño E, Correia S, Delgado F, Delplancke F, Derie F, Duhoux P, di Folco E, Gennai A, Gilli B, Giordano P, Gitton P, Guisard S, Housen N, Huxley A, Kervella P, Kiekebusch M, Koehler B, Lévéque S, Longinotti A, Ménardi S, Morel S, Paresce F, Phan Duc T, Richichi A, Schöller M, Tarenghi M, Wallander A, Wittkowski M, Wilhelm R (2003) The VLTI - A Status Report. *Ap&SS*286:35–44, DOI 10.1023/A:1026145709077

Goldreich P, Tremaine S (1980) Disk-satellite interactions. *ApJ*241:425

Goldreich P, Ward WR (1973) The Formation of Planetesimals. *ApJ*183:1051–1062

Goldreich P, Lithwick Y, Sari R (2004) Final stages of planet formation. *ApJ*614:497

Golimowski DA, Ardila DR, Krist JE, Clampin M, Ford HC, Illingworth GD, Bartko F, Benítez N, Blakeslee JP, Bouwens RJ, Bradley LD, Broadhurst TJ, Brown RA, Burrows CJ, Cheng ES, Cross NJG, Demarco R, Feldman PD, Franx M, Goto T, Gronwall C, Hartig GF, Holden BP, Homeier NL, Infante L, Jee MJ, Kimble RA, Lesser MP, Martel AR, Mei S, Menanteau F, Meurer GR, Miley GK, Motta V, Postman M, Rosati P, Sirianni M, Sparks WB, Tran HD, Tsvetanov ZI, White RL, Zheng W, Zirm AW (2006) Hubble Space Telescope ACS Multiband Coronagraphic Imaging of the Debris Disk around β Pictoris. *AJ*131:3109–3130, DOI 10.1086/503801, arXiv:astro-ph/0602292

Goodman AA, Benson PJ, Fuller GA, Myers PC (1993) Dense cores in dark clouds. VIII - Velocity gradients. *ApJ*406:528–547, DOI 10.1086/172465

Gorti U, Hollenbach D (2008) Line Emission from Gas in Optically Thick Dust Disks around Young Stars. *ApJ*683:287–303, DOI 10.1086/589616, 0804.3381

Gorti U, Hollenbach D (2009) Photoevaporation of Circumstellar Disks By Far-Ultraviolet, Extreme-Ultraviolet and X-Ray Radiation from the Central Star. *ApJ*690:1539–1552, DOI 10.1088/0004-637X/690/2/1539, 0809.1494

Gorti U, Dullemond CP, Hollenbach D (2009) Time Evolution of Viscous Circumstellar Disks due to Photoevaporation by Far-Ultraviolet, Extreme-Ultraviolet, and X-ray Radiation from the Central Star. *ApJ*705:1237–1251, DOI 10.1088/0004-637X/705/2/1237, 0909.1836

Gould A, Dorsher S, Gaudi BS, Udalski A (2006) Frequency of Hot Jupiters and Very Hot Jupiters from the OGLE-III Transit Surveys toward the Galactic Bulge and Carina. *Acta Astr* 56:1–50, arXiv:astro-ph/0601001

Gräfe C, Wolf S, Roccatagliata V, Sauter J, Ertel S (2011) Mid-infrared observations of the transitional disks around DH Tau, DM Tau, and GM Aur. *ArXiv e-prints* 1108.2373

Graham JR, Kalas PG, Matthews BC (2007) The Signature of Primordial Grain Growth in the Polarized Light of the AU Microscopii Debris Disk. *ApJ*654:595–605, DOI 10.1086/509318, arXiv:astro-ph/0609332

Green JJ, Beichman C, Basinger SA, Horner S, Meyer M, Redding DC, Rieke M, Trauger JT (2005) High contrast imaging with the JWST NIRCAM coronagraph. In: D R Coulter (ed) Society of Photo-Optical Instrumentation Engineers (SPIE) Conference Series, Presented at the Society of Photo-Optical Instrumentation Engineers (SPIE) Conference, vol 5905, pp 185–195, DOI 10.1117/12.619343

Guilloteau S, Dutrey A, Piétu V, Boehler Y (2011) A dual-frequency sub-arcsecond study of proto-planetary disks at mm wavelengths: first evidence for radial variations of the dust properties. *A&A*529:A105+, DOI 10.1051/0004-6361/201015209, 1103.1296

Gullbring E, Hartmann L, Briceno C, Calvet N (1998) Disk Accretion Rates for T Tauri Stars. *ApJ*492:323–+, DOI 10.1086/305032

Haisch KE Jr, Lada EA, Lada CJ (2001) Disk Frequencies and Lifetimes in Young Clusters. *ApJ*553:L153–L156, DOI 10.1086/320685, arXiv:astro-ph/0104347

Hartigan P, Edwards S, Ghandour L (1995) Disk Accretion and Mass Loss from Young Stars. *ApJ*452:736–+, DOI 10.1086/176344

Hartmann L, Hewett R, Calvet N (1994) Magnetospheric accretion models for T Tauri stars. 1: Balmer line profiles without rotation. *ApJ*426:669–687, DOI 10.1086/174104

Hartmann L, Calvet N, Gullbring E, D'Alessio P (1998) Accretion and the Evolution of T Tauri Disks. *ApJ*495:385–+, DOI 10.1086/305277

Haupt C, Rykaczewski H (2007) Progress of the ALMA Project. *The Messenger* 128:25–+

Hayashi C (1981) Structure of the solar nebula, growth and decay of magnetic fields and effects of magnetic and turbulent viscosities on the nebula. *Progress of Theoretical Physics Supplement* 70:35

Herczeg GJ (2007) Observational constraints on disk photoevaporation by the central star. In: J Bouvier & I Appenzeller (ed) IAU Symposium, IAU Symposium, vol 243, pp 147–154, DOI 10.1017/S1743921307009507

Hofner P, Jordan E, Araya E, Kurtz S (2007) The 44 GHz methanol maser line in massive star forming regions. In: J M Chapman & W A Baan (ed) IAU Symposium, IAU Symposium, vol 242, pp 160–161, DOI 10.1017/S174392130701280X

Hogerheijde M (2006) The ALMA Design Reference Science Plan. *The Messenger* 123:20–+

Hollenbach D, Johnstone D, Lizano S, Shu F (1994) Photoevaporation of disks around massive stars and application to ultracompact H II regions. *ApJ*428:654–669, DOI 10.1086/174276

Honda M, Inoue AK, Fukagawa M, Oka A, Nakamoto T, Ishii M, Terada H, Takato N, Kawakita H, Okamoto YK, Shibai H, Tamura M, Kudo T, Itoh Y (2009) Detection of Water Ice Grains on the Surface of the Circumstellar Disk Around HD 142527. *ApJ*690:L110–L113, DOI 10.1088/0004-637X/690/2/L110

Howard AW, Marcy GW, Johnson JA, Fischer DA, Wright JT, Isaacson H, Valenti JA, Anderson J, Lin DNC, Ida S (2010) The Occurrence and Mass Distribution of Close-in Super-Earths, Neptunes, and Jupiters. *Science* 330:653–, DOI 10.1126/science.1194854, 1011.0143

Hughes AM, Wilner DJ, Calvet N, D'Alessio P, Claussen MJ, Hogerheijde MR (2007) An Inner Hole in the Disk around TW Hydrae Resolved in 7 mm Dust Emission. *ApJ*664:536–542, DOI 10.1086/518885, 0704.2422

Hughes AM, Wilner DJ, Qi C, Hogerheijde MR (2008) Gas and Dust Emission at the Outer Edge of Protoplanetary Disks. *ApJ*678:1119–1126, DOI 10.1086/586730, 0801.4763

Hughes AM, Andrews SM, Espaillat C, Wilner DJ, Calvet N, D'Alessio P, Qi C, Williams JP, Hogerheijde MR (2009) A Spatially Resolved Inner Hole in the Disk Around GM Aurigae. *ApJ*698:131–142, DOI 10.1088/0004-637X/698/1/131, 0903.4455

Hughes AM, Wilner DJ, Andrews SM, Qi C, Hogerheijde MR (2011) Empirical Constraints on Turbulence in Protoplanetary Accretion Disks. *ApJ*727:85–, DOI 10.1088/0004-637X/727/2/85, 1011.3826

Ida S, Lin DNC (2004a) Toward a deterministic model of planetary formation. i. a desert in the mass and semimajor axis distributions of extrasolar planets. *ApJ*604:388

Ida S, Lin DNC (2004b) Toward a deterministic model of planetary formation. ii. the formation and retention of gas giant planets around stars with a range of metallicities. *ApJ*616:567

Ida S, Makino J (1993) Scattering of planetesimals by a protoplanet - Slowing down of runaway growth. *Icarus* 106:210

Inaba S, Tanaka H, Nakazawa K, Wetherill GW, Kokubo E (2001) High-Accuracy Statistical Simulation of Planetary Accretion: II. Comparison with N-Body Simulation. *Icarus* 149:235–250

Ingleby L, Calvet N, Bergin E, Yerasi A, Espaillat C, Herczeg G, Roueff E, Abgrall H, Hernández J, Briceño C, Pascucci I, Miller J, Fogel J, Hartmann L, Meyer M, Carpenter J, Crockett N, McClure M (2009) Far-Ultraviolet H₂ Emission from Circumstellar Disks. *ApJ*703:L137–L141, DOI 10.1088/0004-637X/703/2/L137, 0909.0688

Ireland MJ, Kraus AL (2008) The Disk Around CoKu Tauri/4: Circumbinary, Not Transi-tional. *ApJ*678:L59–L62, DOI 10.1086/588216, 0803.2044

Isella A, Natta A (2005) The shape of the inner rim in proto-planetary disks. *A&A*438:899–907, DOI 10.1051/0004-6361:20052773, arXiv:astro-ph/0503635

Isella A, Tatulli E, Natta A, Testi L (2008) Gas and dust in the inner disk of the Herbig Ae star MWC 758. *A&A*483:L13–L16, DOI 10.1051/0004-6361:200809641

Isella A, Carpenter JM, Sargent AI (2009) Structure and Evolution of Pre-main-sequence Circumstellar Disks. *ApJ*701:260–282, DOI 10.1088/0004-637X/701/1/260, 0906.2227

Isella A, Carpenter JM, Sargent AI (2010a) Investigating Planet Formation in Circumstellar Disks: CARMA Observations of Ry Tau and Dg Tau. *ApJ*714:1746–1761, DOI 10.1088/0004-637X/714/2/1746, 1003.4318

Isella A, Carpenter JM, Sargent AI (2010b) Investigating Planet Formation in Circumstellar Disks: CARMA Observations of Ry Tau and Dg Tau. *ApJ*714:1746–1761, DOI 10.1088/0004-637X/714/2/1746, 1003.4318

Joergens V, Quirrenbach A (2005) Towards characterization of exoplanetary atmospheres with the VLT interferometer. In: F Favata, G A J Hussain, & B Battrick (ed) 13th Cambridge Workshop on Cool Stars, Stellar Systems and the Sun, ESA Special Publication, vol 560, pp 677–+

Johansen A, Klahr H, Henning T (2006) Gravitoturbulent Formation of Planetesimals. *ApJ*636:1121–1134

Johansen A, Oishi JS, Low MMM, Klahr H, Henning T, Youdin A (2007) Rapid planetesimal formation in turbulent circumstellar disks. *Nature* 448:1022

Johnson BM, Gammie CF (2003) Nonlinear Outcome of Gravitational Instability in Disks with Realistic Cooling. *ApJ*597:131–141, DOI 10.1086/378392, arXiv:astro-ph/0312507

Johnstone D, Hollenbach D, Bally J (1998) Photoevaporation of Disks and Clumps by Nearby Massive Stars: Application to Disk Destruction in the Orion Nebula. *ApJ*499:758–+, DOI 10.1086/305658

Jorgensen AM, Mozurkewich D (2010) Coherent integration: to real time or not to real time? That is the question. In: Society of Photo-Optical Instrumentation Engineers (SPIE) Conference Series, Presented at the Society of Photo-Optical Instrumentation Engineers (SPIE) Conference, vol 7734, DOI 10.1117/12.858277

Kalas P, Graham JR, Clampin M (2005) A planetary system as the origin of structure in Fomalhaut's dust belt. *Nature*435:1067–1070, DOI 10.1038/nature03601, arXiv:astro-ph/0506574

Kalas P, Duchene G, Fitzgerald MP, Graham JR (2007a) Discovery of an Extended Debris Disk around the F2 V Star HD 15745. *ApJ*671:L161–L164, DOI 10.1086/525252, 0712.0378

Kalas P, Fitzgerald MP, Graham JR (2007b) Discovery of Extreme Asymmetry in the Debris Disk Surrounding HD 15115. *ApJ*661:L85–L88, DOI 10.1086/518652, 0704.0645

Kalas P, Graham JR, Chiang E, Fitzgerald MP, Clampin M, Kite ES, Stapelfeldt K, Marois C, Krist J (2008a) Optical Images of an Exosolar Planet 25 Light-Years from Earth. *Science* 322:1345–, DOI 10.1126/science.1166609, 0811.1994

Kalas P, Graham JR, Chiang E, Fitzgerald MP, Clampin M, Kite ES, Stapelfeldt K, Marois C, Krist J (2008b) Optical Images of an Exosolar Planet 25 Light-Years from Earth. *Science* 322:1345–, DOI 10.1126/science.1166609, 0811.1994

Kama M, Min M, Dominik C (2009) The inner rim structures of protoplanetary discs. *A&A*506:1199–1213, DOI 10.1051/0004-6361/200912068, 0908.1692

Kastner JH, Zuckerman B, Weintraub DA, Forveille T (1997) X-ray and molecular emission from the nearest region of recent star formation. *Science* 277:67–71, DOI 10.1126/science.277.5322.67

Kenyon SJ, Hartmann L (1995) Pre-Main-Sequence Evolution in the Taurus-Auriga Molecular Cloud. *ApJS*101:117–+, DOI 10.1086/192235

Kitamura Y, Momose M, Yokogawa S, Kawabe R, Tamura M, Ida S (2002) Investigation of the Physical Properties of Protoplanetary Disks around T Tauri Stars by a 1 Arc-second Imaging Survey: Evolution and Diversity of the Disks in Their Accretion Stage. *ApJ*581:357–380, DOI 10.1086/344223

Klahr H, Bodenheimer P (2006) Formation of giant planets by concurrent accretion of solids and gas inside an anticyclonic vortex. *ApJ*639:432

Klahr H, Brandner W (2006) *Planet Formation*. Cambridge ; New York : Cambridge University Press

Klahr H, Kley W (2006) 3d-radiation hydro simulations of disk-planet interactions. i. numerical algorithm and test cases. *Astronomy and Astrophysics* 445:747

Kley W, Bitsch B, Klahr H (2009) Planet migration in three-dimensional radiative discs. *A&A*506:971–987

Knutson HA, Charbonneau D, Cowan NB, Fortney JJ, Showman AP, Agol E, Henry GW, Everett ME, Allen LE (2009) Multiwavelength Constraints on the Day-Night Circulation Patterns of HD 189733b. *ApJ*690:822–836, DOI 10.1088/0004-637X/690/1/822, 0802.1705

Koerner DW, Sargent AI, Beckwith SVW (1993) A rotating gaseous disk around the T Tauri star GM Aurigae. *Icarus*106:2–+, DOI 10.1006/icar.1993.1154

Koerner DW, Ressler ME, Werner MW, Backman DE (1998) Mid-Infrared Imaging of a Circumstellar Disk around HR 4796: Mapping the Debris of Planetary Formation. *ApJ*503:L83+, DOI 10.1086/311525, arXiv:astro-ph/9806268

Kraus S, Hofmann KH, Benisty M, Berger JP, Chesneau O, Isella A, Malbet F, Meilland A, Nardetto N, Natta A, Preibisch T, Schertl D, Smith M, Stee P, Tatulli E, Testi L, Weigelt G (2008) The origin of hydrogen line emission for five Herbig Ae/Be stars spatially resolved by VLTI/AMBER spectro-interferometry. *A&A*489:1157–1173, DOI 10.1051/0004-6361:200809946

Kraus S, Hofmann KH, Menten KM, Schertl D, Weigelt G, Wyrowski F, Meilland A, Perraut K, Petrov R, Robbe-Dubois S, Schilke P, Testi L (2010) A hot compact dust disk around a massive young stellar object. *Nature*466:339–342, DOI 10.1038/nature09174, 1007.5062

Krist JE, Beichman CA, Trauger JT, Rieke MJ, Somerstein S, Green JJ, Horner SD, Stansberry JA, Shi F, Meyer MR, Stapelfeldt KR, Roellig TL (2007) Hunting planets and observing disks with the JWST NIRCam coronagraph. In: Society of Photo-Optical Instrumentation Engineers (SPIE) Conference Series, Presented at the Society of Photo-Optical Instrumentation Engineers (SPIE) Conference, vol 6693, DOI 10.1117/12.734873

Krumholz MR, Klein RI, McKee CF (2007) Molecular Line Emission from Massive Protostellar Disks: Predictions for ALMA and EVLA. *ApJ*665:478–491, DOI 10.1086/519305, 0705.0536

Kurz R, Guilloteau S, Shaver P (2002) The Atacama Large Millimetre Array. *The Messenger* 107:7–12

Lagage PO, Doucet C, Pantin E, Habart E, Duchêne G, Ménard F, Pinte C, Charnoz S, Pel JW (2006) Anatomy of a Flaring Proto-Planetary Disk Around a Young Intermediate-Mass Star. *Science* 314:621–623, DOI 10.1126/science.1131436

Lagrange AM, Gratadour D, Chauvin G, Fusco T, Ehrenreich D, Mouillet D, Rousset G, Rouan D, Allard F, Gendron É, Charton J, Mugnier L, Rabou P, Montri J, Lacombe F (2009) A probable giant planet imaged in the β Pictoris disk. VLT/NaCo deep L'-band imaging. *A&A*493:L21–L25, DOI 10.1051/0004-6361:200811325, 0811.3583

Lahuis F, van Dishoeck EF, Boogert ACA, Pontoppidan KM, Blake GA, Dullemond CP, Evans NJ II, Hogerheijde MR, Jørgensen JK, Kessler-Silacci JE, Knez C (2006) Hot Organic Molecules toward a Young Low-Mass Star: A Look at Inner Disk Chemistry. *ApJ*636:L145–L148, DOI 10.1086/500084, arXiv:astro-ph/0511786

Lai D, Foucart F, Lin DNC (2011) Evolution of spin direction of accreting magnetic protostars and spin-orbit misalignment in exoplanetary systems. *MNRAS*412:2790–2798, DOI 10.1111/j.1365-2966.2010.18127.x, 1008.3148

Lammer H, Bredehoff JH, Coustenis A, Khodachenko ML, Kaltenegger L, Grasset O, Prieur D, Raulin F, Ehrenfreund P, Yamauchi M, Wahlund JE, Grießmeier JM, Stangl G, Cockell CS, Kulikov YN, Grenfell JL, Rauer H (2009) What makes a planet habitable? *A&A Rev.* 17:181–249, DOI 10.1007/s00159-009-0019-z

Launhardt R (2009) Exoplanet search with astrometry. *New A Rev.* 53:294–300, DOI 10.1016/j.newar.2010.07.006, 0904 .1100

Launhardt R, Queloz D, Henning T, Quirrenbach A, Delplancke F, Andolfato L, Baumeister H, Bizenberger P, Bleuler H, Chazelas B, Dérie F, Di Lieto L, Duc TP, Duvanel O, Elias NM II, Fluery M, Geisler R, Gillet D, Graser U, Koch F, Köhler R, Maire C, Mégevand D, Michellod Y, Moresmau JM, Müller A, Müllhaupt P, Naranjo V, Pepe F, Reffert S, Sache L, Ségransan D, Salvadé Y, Schulze-Hartung T, Setiawan J, Simond G, Sosnowska D, Stilz I, Tubbs B, Wagner K, Weber L, Weise P, Zago L (2008) The ESPRI project: astrometric exoplanet search with PRIMA. In: Society of Photo-Optical Instrumentation Engineers (SPIE) Conference Series, Presented at the Society of Photo-Optical Instrumentation Engineers (SPIE) Conference, vol 7013, DOI 10.1117/12.789318

Leinert C, Graser U, Przygodda F, Waters LBFM, Perrin G, Jaffe W, Lopez B, Bakker EJ, Böhm A, Chesneau O, Cotton WD, Damstra S, de Jong J, Glazeborg-Kluttig AW, Grimm B, Hanenburg H, Laun W, Lenzen R, Ligori S, Mathar RJ, Meisner J, Morel S, Morr W, Neumann U, Pel JW, Schuller P, Rohloff RR, Stecklum B, Storz C, von der Lühe O, Wagner K (2003) MIDI - the 10 μ m instrument on the VLTI. *Ap&SS* 286:73–83, DOI 10.1023/A:1026158127732

Leinert C, van Boekel R, Waters LBFM, Chesneau O, Malbet F, Köhler R, Jaffe W, Ratzka T, Dutrey A, Preibisch T, Graser U, Bakker E, Chagnon G, Cotton WD, Dominik C, Dullemond CP, Glazeborg-Kluttig AW, Glindemann A, Henning T, Hofmann K, de Jong J, Lenzen R, Ligori S, Lopez B, Meisner J, Morel S, Paresce F, Pel J, Percheron I, Perrin G, Przygodda F, Richichi A, Schöller M, Schuller P, Stecklum B, van den Ancker ME, von der Lühe O, Weigelt G (2004) Mid-infrared sizes of circumstellar disks around Herbig Ae/Be stars measured with MIDI on the VLTI. *A&A* 423:537–548, DOI 10.1051/0004-6361:20047178

Lestrade JF, Wyatt MC, Bertoldi F, Menten KM, Labaigt G (2009) Search for cold debris disks around M-dwarfs. II. *A&A* 506:1455–1467, DOI 10.1051/0004-6361/200912306, 0907 .4782

Liffman K (2003) The Gravitational Radius of an Irradiated Disk. *PASA* 20:337–339, DOI 10.1071/AS03019

Lin DNC, Papaloizou JCB (1986) On the tidal interaction between protoplanets and the protoplanetary disk. iii - orbital migration of protoplanets. *ApJ* 309:846

Lissauer JJ (1993) Planet formation. *ARA&A* 31:129

Lissauer JJ, Hubickyj O, D'Angelo G, Bodenheimer P (2009) Models of Jupiter's growth incorporating thermal and hydrodynamic constraints. *Icarus* 199:338–350

Lissauer JJ, Ragozzine D, Fabrycky DC, Steffen JH, Ford EB, Jenkins JM, Shporer A, Holman MJ, Rowe JF, Quintana EV, Batalha NM, Borucki WJ, Bryson ST, Caldwell DA, Carter JA, Ciardi D, Dunham EW, Fortney JJ, Gautier TN III, Howell SB, Koch DG, Latham DW, Marcy GW, Morehead RC, Sasselov D (2011) Architecture and Dynamics of Kepler's Candidate Multiple Transiting Planet Systems. *ApJS* 197:8–+, DOI 10.1088/0067-0049/197/1/8, 1102 .0543

Lodato G (2008) Classical disc physics. *New A Rev.* 52:21–41, DOI 10.1016/j.newar.2008.04.002

Lodato G, Rice WKM (2004) Testing the locality of transport in self-gravitating accretion discs. *MNRAS* 351:630–642, DOI 10.1111/j.1365-2966.2004.07811.x, arXiv:

astro-ph/0403185

Lodato G, Rice WKM (2005) Testing the locality of transport in self-gravitating accretion discs - II. The massive disc case. *MNRAS*358:1489–1500, DOI 10.1111/j.1365-2966.2005.08875.x, arXiv:astro-ph/0501638

Lommen D, Maddison ST, Wright CM, van Dishoeck EF, Wilner DJ, Bourke TL (2009) Large grains in discs around young stars: ATCA observations of WW Chamaeleontis, RU Lupi, and CS Chamaeleontis. *A&A*495:869–879, DOI 10.1051/0004-6361:200810999, 0812.3849

Lopez B, Lagarde S, Wolf S, Jaffe W, Weigelt G, Antonelli P, Abraham P, Augereau JC, Beckman U, Behrend J, Berruyer N, Bresson Y, Chesneau O, Clausse JM, Connot C, Danchi WC, Delbo M, Demyk K, Domiciano A, Dugué M, Glazeborg A, Graser U, Hanenburg H, Henning T, Heininger M, Hofmann KH, Hugues Y, Jankov S, Kraus S, Laun W, Leinert C, Linz H, Matter A, Mathias P, Meisenheimer K, Menut JL, Millour F, Mosoni L, Neumann U, Niedzielski A, Nussbaum E, Petrov R, Ratzka T, Robbe-Dubois S, Roussel A, Schertl D, Schmider FX, Stecklum B, Thiebaut E, Vakili F, Wagner K, Waters LBFM, Absil O, Hron J, Nardetto N, Olofsson J, Valat B, Vannier M, Goldman B, Höning S, Cotton WD (2009) Matisse. In: A Moorwood (ed) *Science with the VLT in the ELT Era*, pp 353–+, DOI 10.1007/978-1-4020-9190-259

Lovis C, Segransan D, Mayor M, Udry S, Benz W, Bertaux JL, Bouchy F, Correia ACM, Laskar J, Curto GL, Mordasini C, Pepe F, Queloz D, Santos NC (2011) The harps search for southern extra-solar planets xxvii. up to seven planets orbiting hd 10180: probing the architecture of low-mass planetary systems. *A&A*528:A112+

Lubow SH, Seibert M, Artymowicz P (1999) Disk accretion onto high-mass planets. *The Astrophysical Journal* 526:1001

Lynden-Bell D, Pringle JE (1974) The evolution of viscous discs and the origin of the nebular variables. *MNRAS*168:603–637

Malbet F, Benisty M, de Wit WJ, Kraus S, Meilland A, Millour F, Tatulli E, Berger JP, Chesneau O, Hofmann KHea (2007) Disk and wind interaction in the young stellar object <ASTROBJ>MWC 297</ASTROBJ> spatially resolved with AMBER/VLTI. *A&A*464:43–53, DOI 10.1051/0004-6361:20053924

Malbet F, Buscher D, Weigelt G, Garcia P, Gai M, Lorenzetti D, Surdej J, Hron J, Neuhauser R, Kern P, Jocou L, Berger JP, Absil O, Beckmann U, Corcione L, Duvert G, Filho M, Labeye P, Le Coarer E, Li Causi G, Lima J, Perraut K, Tatulli E, Thiébaut E, Young J, Zins G, Amorim A, Aringer B, Beckert T, Benisty M, Bonfils X, Cabral A, Chelli A, Chesneau O, Chiavassa A, Corradi R, De Becker M, Delboulbé A, Duch”ne G, Forveille T, Haniff C, Herwats E, Hofmann KH, Le Bouquin JB, Ligori S, Loreggia D, Marconi A, Moitinho A, Nisini B, Petrucci PO, Rebordao J, Speziali R, Testi L, Vitali F (2008) VSI: the VLTI spectro-imager. In: *Society of Photo-Optical Instrumentation Engineers (SPIE) Conference Series*, *Society of Photo-Optical Instrumentation Engineers (SPIE) Conference Series*, vol 7013, DOI 10.1117/12.789710, 0807.1062

Maness HL, Fitzgerald MP, Paladini R, Kalas P, Duchene G, Graham JR (2008) CARMA Millimeter-Wave Aperture Synthesis Imaging of the HD 32297 Debris Disk. *ApJ*686:L25–L28, DOI 10.1086/592783, 0808.3582

Marcy G, Butler RP, Fischer D, Vogt S, Wright JT, Tinney CG, Jones HRA (2005) Observed Properties of Exoplanets: Masses, Orbits, and Metallicities. *Progress of Theoretical Physics Supplement* 158:24–42, DOI 10.1143/PTPS.158.24, arXiv:astro-ph/0505003

Marois C, Macintosh B, Barman T, Zuckerman B, Song I, Patience J, Lafrenière D, Doyon R (2008) Direct Imaging of Multiple Planets Orbiting the Star HR 8799. *Science* 322:1348–,

DOI 10.1126/science.1166585, 0811.2606

Mather JC (2010) The James Webb Space Telescope Mission. In: D J Whalen, V Bromm, & N Yoshida (ed) American Institute of Physics Conference Series, American Institute of Physics Conference Series, vol 1294, pp 1–8, DOI 10.1063/1.3518853

Mayer L, Quinn T, Wadsley J, Stadel J (2004) The evolution of gravitationally unstable protoplanetary disks: Fragmentation and possible giant planet formation. *ApJ*609:1045

Mazeh T, Zucker S, Pont F (2005) An intriguing correlation between the masses and periods of the transiting planets. *MNRAS*356:955–957, DOI 10.1111/j.1365-2966.2004.08511.x, arXiv:astro-ph/0411701

McCabe C, Duchêne G, Ghez AM (2003) The First Detection of Spatially Resolved Mid-Infrared Scattered Light from a Protoplanetary Disk. *ApJ*588:L113–L116, DOI 10.1086/375632, arXiv:astro-ph/0304083

McCabe C, Duchêne G, Pinte C, Stapelfeldt KR, Ghez AM, Ménard F (2011) Spatially Resolving the HK Tau B Edge-on Disk from 1.2 to 4.7 μ m: A Unique Scattered Light Disk. *ApJ*727:90–+, DOI 10.1088/0004-637X/727/2/90

McCaughrean MJ, Stauffer JR (1994) High resolution near-infrared imaging of the trapezium: A stellar census. *AJ*108:1382–1397, DOI 10.1086/117160

Meeus G, Waters LBFM, Bouwman J, van den Ancker ME, Waelkens C, Malfait K (2001) ISO spectroscopy of circumstellar dust in 14 Herbig Ae/Be systems: Towards an understanding of dust processing. *A&A*365:476–490, DOI 10.1051/0004-6361:20000144, arXiv:astro-ph/0012295

Meyer MR, Carpenter JM, Mamajek EE, Hillenbrand LA, Hollenbach D, Moro-Martin A, Kim JS, Silverstone MD, Najita J, Hines DC, Pascucci I, Stauffer JR, Bouwman J, Backman DE (2008) Evolution of Mid-Infrared Excess around Sun-like Stars: Constraints on Models of Terrestrial Planet Formation. *ApJ*673:L181–L184, DOI 10.1086/527470, 0712.1057

Millan-Gabet R, Malbet F, Akeson R, Leinert C, Monnier J, Waters R (2007) The Circumstellar Environments of Young Stars at AU Scales. *Protostars and Planets V* pp 539–554, arXiv:astro-ph/0603554

Millan-Gabet R, Serabyn E, Mennesson B, Traub WA, Barry RK, Danchi WC, Kuchner M, Stark CC, Ragland S, Hrynevych M, Woillez J, Stapelfeldt K, Bryden G, Colavita MM, Booth AJ (2011) Exozodiacal Dust Levels for Nearby Main-sequence Stars: A Survey with the Keck Interferometer Nuller. *ApJ*734:67–+, DOI 10.1088/0004-637X/734/1/67

Miller-Ricci E, Meyer MR, Seager S, Elkins-Tanton L (2009) On the Emergent Spectra of Hot Protoplanet Collision Afterglows. *ApJ*704:770–780, DOI 10.1088/0004-637X/704/1/770, 0907.2931

Mizuno H, Nakazawa K, Hayashi C (1978) Instability of a gaseous envelope surrounding a planetary core and formation of giant planets. *Progress of Theoretical Physics* 60:699

Monnier JD (2000) An Introduction to Closure Phases. In: P R Lawson (ed) *Principles of Long Baseline Stellar Interferometry*, pp 203–+

Monnier JD, Berger JP, Millan-Gabet R, ten Brummelaar TA (2004) The Michigan Infrared Combiner (MIRC): IR imaging with the CHARA Array. In: W A Traub (ed) *Society of Photo-Optical Instrumentation Engineers (SPIE) Conference Series*, *Society of Photo-Optical Instrumentation Engineers (SPIE) Conference Series*, vol 5491, pp 1370–+

Monnier JD, Millan-Gabet R, Billmeier R, Akeson RL, Wallace D, Berger JP, Calvet N, D'Alessio P, Danchi WC, Hartmann Lea (2005) The Near-Infrared Size-Luminosity Relations for Herbig Ae/Be Disks. *ApJ*624:832–840, DOI 10.1086/429266

Monnier JD, Berger J, Millan-Gabet R, Traub WA, Schloerb FP, Pedretti E, Benisty M, Carleton NP, Haguenauer P, Kern P, Labeye P, Lacasse MG, Malbet F, Perraut K, Pearlman

M, Zhao M (2006) Few Skewed Disks Found in First Closure-Phase Survey of Herbig Ae/Be Stars. *ApJ*647:444–463, DOI 10.1086/505340, arXiv: astro-ph/0606052

Morbidelli A, Bottke WF, Nesvorný D, Levison HF (2009) Asteroids were born big. *Icarus* 204:558–573

Mordasini C, Alibert Y, Benz W (2009a) Extrasolar planet population synthesis i: Method, formation tracks and mass-distance distribution. *A&A*501:1139–1160

Mordasini C, Alibert Y, Benz W, Naef D (2009b) Extrasolar planet population synthesis ii: Statistical comparison with observation. *A&A*501:1161–1184

Mordasini C, Alibert Y, Benz W, Klahr H, Henning T (in prep.) Extrasolar planet population synthesis iv. Correlations with disk metallicity, mass and lifetime.

Mouillet D, Larwood JD, Papaloizou JCB, Lagrange AM (1997) A planet on an inclined orbit as an explanation of the warp in the Beta Pictoris disc. *MNRAS*292:896–+, arXiv: astro-ph/9705100

Mouillet D, Lagrange AM, Augereau JC, Ménard F (2001) Asymmetries in the HD 141569 circumstellar disk. *A&A*372:L61–L64, DOI 10.1051/0004-6361:20010660

Mourard D, Tallon M, Bério P, Bonneau D, Chesneau O, Clausse JM, Delaa O, Nardetto N, Perraut K, Spang A, Stee P, Tallon-Bosc I, McAlister H, Ten Brummelaar T, Sturmann J, Sturmann L, Turner N, Farrington C, Goldfinger PJ (2010) Performances and first science results with the VEGA/CHARA visible instrument. In: Society of Photo-Optical Instrumentation Engineers (SPIE) Conference Series, Society of Photo-Optical Instrumentation Engineers (SPIE) Conference Series, vol 7734, DOI 10.1117/12.856100

Muterspaugh MW, Lane BF, Konacki M, Wiktorowicz S, Burke BF, Colavita MM, Kulkarni SR, Shao M (2006) PHASES Differential Astrometry and Iodine Cell Radial Velocities of the κ Pegasi Triple Star System. *ApJ*636:1020–1032, DOI 10.1086/498209, arXiv: astro-ph/0509406

Muzerolle J, Briceño C, Calvet N, Hartmann L, Hillenbrand L, Gullbring E (2000) Detection of Disk Accretion at the Substellar Limit. *ApJ*545:L141–L144, DOI 10.1086/317877

Muzerolle J, D’Alessio P, Calvet N, Hartmann L (2004) Magnetospheres and Disk Accretion in Herbig Ae/Be Stars. *ApJ*617:406–417, DOI 10.1086/425260, arXiv: astro-ph/0409008

Muzerolle J, Allen LE, Megeath ST, Hernández J, Gutermuth RA (2010) A Spitzer Census of Transitional Protoplanetary Disks with AU-scale Inner Holes. *ApJ*708:1107–1118, DOI 10.1088/0004-637X/708/2/1107, 0911.2704

Najita JR, Strom SE, Muzerolle J (2007) Demographics of transition objects. *MNRAS*378:369–378, DOI 10.1111/j.1365-2966.2007.11793.x, 0704.1681

Najita JR, Doppmann GW, Carr JS, Graham JR, Eisner JA (2009) High-Resolution K-Band Spectroscopy of MWC 480 and V1331 Cyg. *ApJ*691:738–748, DOI 10.1088/0004-637X/691/1/738, 0809.4267

Nakagawa T (2011) SPICA: The Space Infrared Telescope for Cosmology and Astrophysics. In: American Astronomical Society Meeting Abstracts #218, pp 314.01–+

Naoz S, Farr WM, Lithwick Y, Rasio FA, Teyssandier J (2011) Hot Jupiters from secular planet-planet interactions. *Nature*473:187–189, DOI 10.1038/nature10076, 1011.2501

Natta A, Testi L (2008) The study of young substellar objects with ALMA. *Ap&SS*313:113–117, DOI 10.1007/s10509-007-9635-0

Natta A, Prusti T, Neri R, Wooden D, Grinin VP, Mannings V (2001) A reconsideration of disk properties in Herbig Ae stars. *A&A*371:186–197, DOI 10.1051/0004-6361:20010334

Natta A, Testi L, Calvet N, Henning T, Waters R, Wilner D (2007) Dust in Protoplanetary Disks: Properties and Evolution. *Protostars and Planets V* pp 767–781, arXiv:

astro-ph/0602041

Nelson RP, Papaloizou JCB, Masset F, Kley W (2000) The migration and growth of protoplanets in protostellar discs. *MNRAS*318:18–36, DOI 10.1046/j.1365-8711.2000.03605.x, arXiv:astro-ph/9909486

Okamoto YK, Kataza H, Honda M, Fujiwara H, Momose M, Ohashi N, Fujiyoshi T, Sakon I, Sako S, Yamashita T, Miyata T, Onaka T (2009) Direct Detection of a Flared Disk Around a Young Massive Star HD200775 and its 10 to 1000 AU Scale Properties. *ApJ*706:665–675, DOI 10.1088/0004-637X/706/1/665, 0910.4328

Olofsson J, Benisty M, Augereau JC, Pinte C, Ménard F, Tatulli E, Berger JP, Malbet F, Merín B, van Dishoeck EF, Lacour S, Pontoppidan KM, Monin JL, Brown JM, Blake GA (2011) Warm dust resolved in the cold disk around T Chamaeleontis with VLTI/AMBER. *A&A*528:L6+, DOI 10.1051/0004-6361/201016074, 1102.4976

Ormel CW, Dullemond CP, Spaans M (2010) Accretion among preplanetary bodies: the many faces of runaway growth. *ArXiv e-prints* 1006.3186

Owen JE, Ercolano B, Clarke CJ, Alexander RD (2010) Radiation-hydrodynamic models of X-ray and EUV photoevaporating protoplanetary discs. *MNRAS*401:1415–1428, DOI 10.1111/j.1365-2966.2009.15771.x, 0909.4309

Owen JE, Ercolano B, Clarke CJ (2011) Protoplanetary disc evolution and dispersal: the implications of X-ray photoevaporation. *MNRAS*412:13–25, DOI 10.1111/j.1365-2966.2010.17818.x, 1010.0826

Paardekooper S, Baruteau C, Crida A, Kley W (2010) A torque formula for non-isothermal type I planetary migration - I. Unsaturated horseshoe drag. *MNRAS*401:1950–1964

Papaloizou JCB, Nelson RP (2005) Models of accreting gas giant protoplanets in protostellar disks. *A&A*433:247–265

Papaloizou JCB, Terquem C (1999) Critical protoplanetary core masses in protoplanetary disks and the formation of short-period giant planets. *ApJ*521:823

Papaloizou JCB, Terquem C (2006) Planet formation and migration. *Rep Prog Phys* 69:119

Pascucci I, Sterzik M (2009) Evidence for Disk Photoevaporation Driven by the Central Star. *ApJ*702:724–732, DOI 10.1088/0004-637X/702/1/724, 0908.2367

Pascucci I, Sterzik M, Alexander RD, Alencar SHP, Gorti U, Hollenbach D, Owen J, Ercolano B, Edwards S (2011) The Photoevaporative Wind from the Disk of TW Hya. *ApJ*736:13–+, DOI 10.1088/0004-637X/736/1/13, 1105.0045

Pedretti E, Traub WA, Monnier JD, Schuller PA, Ragland S, Berger J, Millan-Gabet R, Wallace G, Burke M, Lacasse MG, Thureau ND, Carleton N (2008) Last technology and results from the IOTA interferometer. In: Society of Photo-Optical Instrumentation Engineers (SPIE) Conference Series, Society of Photo-Optical Instrumentation Engineers (SPIE) Conference Series, vol 7013, DOI 10.1117/12.789751

Perri F, Cameron AGW (1974) Hydrodynamic instability of the solar nebula in the presence of a planetary core. *Icarus* 22:416

Perrin G, Woillez J, Lai O, Guérin J, Kotani T, Wizinowich PL, Le Mignant D, Hrynevych M, Gathright J, Léna P, Chaffee F, Vergnole S, Delage L, Reynaud F, Adamson AJ, Berthod C, Brient B, Collin C, Crétenet J, Dauny F, Deléglise C, Fédou P, Goeltzenlichter T, Guyon O, Hulin R, Marlot C, Marteaud M, Melse BT, Nishikawa J, Reess JM, Ridgway ST, Rigaut F, Roth K, Tokunaga AT, Ziegler D (2006a) Interferometric coupling of the Keck telescopes with single-mode fibers. *Science* 311:194–+, DOI 10.1126/science.1120249

Perrin MD, Duchêne G, Kalas P, Graham JR (2006b) Discovery of an Optically Thick, Edge-on Disk around the Herbig Ae Star PDS 144N. *ApJ*645:1272–1282, DOI 10.1086/504510, arXiv:astro-ph/0603667

Perrin MD, Schneider G, Duchene G, Pinte C, Grady CA, Wisniewski JP, Hines DC (2009) The Case of AB Aurigae's Disk in Polarized Light: Is there Truly a Gap? *ApJ*707:L132–L136, DOI 10.1088/0004-637X/707/2/L132, 0911.1130

Pesenti N, Dougados C, Cabrit S, O'Brien D, Garcia P, Ferreira J (2003) Near-IR [Fe II] emission diagnostics applied to cold disk winds in young stars. *A&A*410:155–164, DOI 10.1051/0004-6361:20031131

Petrov RG, The AMBER Consortium (2003) Introducing the near infrared VLTI instrument AMBER to its users. *Ap&SS*286:57–67, DOI 10.1023/A:1026102009986

Petrov RG, Malbet F, Weigelt G, Antonelli P, Beckmann U, Bresson Y, Chelli A, Dugué M, Duvert G, Gennari S, Glück L, Kern P, Lagarde S, Le Coarer E, Lisi F, Millour F, Perraut K, Puget P, Rantakyrö F, Robbe-Dubois S, Roussel A, Salinari P, Tatulli E, Zins G, Accardo M, Acke B, Agabi K, Altariba E, Arezki B, Aristidi E, Baffa C, Behrend J, Blöcker T, Bonhomme S, Busoni S, Cassaing F, Clausse J, Colin J, Connot C, Delboulbé A, Domiciano de Souza A, Driebe T, Feautrier P, Ferruzzi D, Forveille T, Fossat E, Foy R, Fraix-Burnet D, Gallardo A, Giani E, Gil C, Glentzlin A, Heiden M, Heininger M, Hernandez Utrera O, Hofmann K, Kamm D, Kiekebusch M, Kraus S, Le Contel D, Le Contel J, Lesourd T, Lopez B, Lopez M, Magnard Y, Marconi A, Mars G, Martinot-Lagarde G, Mathias P, Mège P, Monin J, Mouillet D, Mourard D, Nussbaum E, Ohnaka K, Pacheco J, Perrier C, Rabbia Y, Rebattu S, Reynaud F, Richichi A, Robini A, Sacchettini M, Schertl D, Schöller M, Solscheid W, Spang A, Stee P, Stefanini P, Tallon M, Tallon-Bosc I, Tasso D, Testi L, Vakili F, von der Lühe O, Valtier J, Vannier M, Ventura N (2007) AMBER, the near-infrared spectro-interferometric three-telescope VLTI instrument. *A&A*464:1–12, DOI 10.1051/0004-6361:20066496

Piétu V, Guilloteau S, Dutrey A (2005) Sub-arcsec imaging of the AB Aur molecular disk and envelope at millimeter wavelengths: a non Keplerian disk. *A&A*443:945–954, DOI 10.1051/0004-6361:20042050, arXiv:astro-ph/0504023

Piétu V, Dutrey A, Guilloteau S, Chapillon E, Pety J (2006) Resolving the inner dust disks surrounding LkCa 15 and MWC 480 at mm wavelengths. *A&A*460:L43–L47, DOI 10.1051/0004-6361:20065968, arXiv:astro-ph/0610200

Piétu V, Dutrey A, Guilloteau S (2007) Probing the structure of protoplanetary disks: a comparative study of DM Tau, LkCa 15, and MWC 480. *A&A*467:163–178, DOI 10.1051/0004-6361:20066537, arXiv:astro-ph/0701425

Pinte C, Ménard F, Berger JP, Benisty M, Malbet F (2008a) The Inner Radius of T Tauri Disks Estimated from Near-Infrared Interferometry: The Importance of Scattered Light. *ApJ*673:L63–L66, DOI 10.1086/527378, 0712.0012

Pinte C, Ménard F, Berger JP, Benisty M, Malbet F (2008b) The Inner Radius of T Tauri Disks Estimated from Near-Infrared Interferometry: The Importance of Scattered Light. *ApJ*673:L63–L66, DOI 10.1086/527378

Pinte C, Padgett DL, Ménard F, Stapelfeldt KR, Schneider G, Olofsson J, Panić O, Augereau JC, Duchêne G, Krist J, Pontoppidan K, Perrin MD, Grady CA, Kessler-Silacci J, van Dishoeck EF, Lommen D, Silverstone M, Hines DC, Wolf S, Blake GA, Henning T, Stecklum B (2008c) Probing dust grain evolution in IM Lupi's circumstellar disc. Multi-wavelength observations and modelling of the dust disc. *A&A*489:633–650, DOI 10.1051/0004-6361:200810121, 0808.0619

Pollack JB, Hubickyj O, Bodenheimer P, Lissauer JJ, Podolak M, Greenzweig NC (1996) Formation of the giant planets by concurrent accretion of solids and gas. *Icarus* 124:62

Pont F (2009) Empirical evidence for tidal evolution in transiting planetary systems. *MNRAS*396:1789–1796, DOI 10.1111/j.1365-2966.2009.14868.x, 0812.1463

Pontoppidan KM, Blake GA, van Dishoeck EF, Smette A, Ireland MJ, Brown J (2008) Spectroastrometric Imaging of Molecular Gas within Protoplanetary Disk Gaps. *ApJ*684:1323–1329, DOI 10.1086/590400, 0805.3314

Pontoppidan KM, Salyk C, Blake GA, Käufl HU (2010) Spectrally Resolved Pure Rotational Lines of Water in Protoplanetary Disks. *ApJ*722:L173–L177, DOI 10.1088/2041-8205/722/2/L173, 1009.3259

Pott JU, Woillez J, Akeson RL, Berkey B, Colavita MM, Cooper A, Eisner JA, Ghez AM, Graham JR, Hillenbrand L, Hrynewich M, Medeiros D, Millan-Gabet R, Monnier J, Morrison D, Panteleeva T, Quataert E, Randolph B, Smith B, Summers K, Tsubota K, Tyau C, Weinberg N, Wetherell E, Wizinowich PL (2009) Astrometry with the Keck Interferometer: The ASTRA project and its science. *New A Rev.*53:363–372, DOI 10.1016/j.newar.2010.07.009, 0811.2264

Pott JU, Woillez J, Ragland S, Wizinowich PL, Eisner JA, Monnier JD, Akeson RL, Ghez AM, Graham JR, Hillenbrand LA, Millan-Gabet R, Appleby E, Berkey B, Colavita MM, Cooper A, Felizardo C, Herstein J, Hrynevich M, Medeiros D, Morrison D, Panteleeva T, Smith B, Summers K, Tsubota K, Tyau C, Wetherell E (2010) Probing Local Density Inhomogeneities in the Circumstellar Disk of a Be Star Using the New Spectro-astrometry Mode at the Keck Interferometer. *ApJ*721:802–808, DOI 10.1088/0004-637X/721/1/802, 1008.1727

Pringle JE (1981) Accretion discs in astrophysics. *ARA&A*19:137–162, DOI 10.1146/annurev.aa.19.090181.001033

Qi C, Ho PTP, Wilner DJ, Takakuwa S, Hirano N, Ohashi N, Bourke TL, Zhang Q, Blake GA, Hogerheijde M, Saito M, Choi M, Yang J (2004) Imaging the Disk around TW Hydrea with the Submillimeter Array. *ApJ*616:L11–L14, DOI 10.1086/421063, arXiv: astro-ph/0403412

Qi C, Wilner DJ, Calvet N, Bourke TL, Blake GA, Hogerheijde MR, Ho PTP, Bergin E (2006) CO J = 6-5 Observations of TW Hydrea with the Submillimeter Array. *ApJ*636:L157–L160, DOI 10.1086/500241, arXiv:astro-ph/0512122

Rafikov RR (2003) The growth of planetary embryos: Orderly, runaway, or oligarchic? *AJ*125:942

Rafikov RR (2005) Can Giant Planets Form by Direct Gravitational Instability? *ApJ*621:L69–L72

Rafikov RR (2009) Properties of Gravitoturbulent Accretion Disks. *ApJ*704:281–291, DOI 10.1088/0004-637X/704/1/281, 0901.4739

Ragland S, Wizinowich P, Akeson R, Colavita M, Appleby E, Berkey B, Booth A, Cooper A, Crawford S, Dahl W, Felizardo C, Garcia-Gathright J, Gathright J, Herstein J, Hrynevich M, Koresko C, Ligon R, Medeiros D, Mennesson B, Millan-Gabet R, Morrison D, Paine C, Parvin B, Panteleeva T, Serabyn E, Smith B, Summers K, Tsubota K, Tyau C, Wetherell E, Woillez J (2008) Recent progress at the Keck Interferometer: operations and V^2 science. In: Society of Photo-Optical Instrumentation Engineers (SPIE) Conference Series, Presented at the Society of Photo-Optical Instrumentation Engineers (SPIE) Conference, vol 7013, DOI 10.1117/12.788070

Ramsay S, D'Odorico S, Casali M, González JC, Hubin N, Kasper M, Käufl HU, Kissler-Patig M, Marchetti E, Paufique J, Pasquini L, Siebenmorgen R, Richichi A, Vernet J, Zerbi FM (2010) An overview of the E-ELT instrumentation programme. In: Society of Photo-Optical Instrumentation Engineers (SPIE) Conference Series, Society of Photo-Optical Instrumentation Engineers (SPIE) Conference Series, vol 7735, DOI 10.1117/12.857037

Ratzka T, Leinert C, Henning T, Bouwman J, Dullemond CP, Jaffe W (2007) High spatial resolution mid-infrared observations of the low-mass young star TW Hydrea.

A&A471:173–185, DOI 10.1051/0004-6361:20077357, 0707.0193

Raymond SN, Scalo J, Meadows VS (2007) A Decreased Probability of Habitable Planet Formation around Low-Mass Stars. *ApJ*669:606–614, DOI 10.1086/521587, 0707.1711

Raymond SN, Barnes R, Mandell AM (2008) Observable consequences of planet formation models in systems with close-in terrestrial planets. *MNRAS*384:663–674

Raymond SN, O’Brien DP, Morbidelli A, Kaib NA (2009) Building the terrestrial planets: Constrained accretion in the inner Solar System. *Icarus*203:644–662

Reche R, Beust H, Augereau JC (2009) Investigating the flyby scenario for the HD 141569 system. *A&A*493:661–669, DOI 10.1051/0004-6361:200810419, 0809.4421

Renard S, Absil O, Berger J, Bonfils X, Forveille T, Malbet F (2008) Prospects for near-infrared characterisation of hot Jupiters with the VLTI Spectro-Imager (VSI). In: Society of Photo-Optical Instrumentation Engineers (SPIE) Conference Series, Presented at the Society of Photo-Optical Instrumentation Engineers (SPIE) Conference, vol 7013, DOI 10.1117/12.790494, 0807.3014

Renard S, Malbet F, Benisty M, Thiébaut E, Berger J (2010) Milli-arcsecond images of the Herbig Ae star HD 163296. *A&A*519:A26+, DOI 10.1051/0004-6361/201014910, 1007.2930

Ricci L, Testi L, Natta A, Brooks KJ (2010a) Dust grain growth in ρ -Ophiuchi protoplanetary disks. *A&A*521:A66+, DOI 10.1051/0004-6361/201015039, 1008.1144

Ricci L, Testi L, Natta A, Neri R, Cabrit S, Herczeg GJ (2010b) Dust properties of protoplanetary disks in the Taurus-Auriga star forming region from millimeter wavelengths. *A&A*512:A15+, DOI 10.1051/0004-6361/200913403, 0912.3356

Safronov VS (1969) Evolution of the Protoplanetary Cloud and Formation of the Earth and the Planets. Nauka, Moscow

Sahlmann J, Ménardi S, Abuter R, Accardo M, Mottini S, Delplancke F (2009) The PRIMA fringe sensor unit. *A&A*507:1739–1757, DOI 10.1051/0004-6361/200912271, 0909.1470

Salyk C, Pontoppidan KM, Blake GA, Lahuis F, van Dishoeck EF, Evans NJ II (2008) H₂O and OH Gas in the Terrestrial Planet-forming Zones of Protoplanetary Disks. *ApJ*676:L49–L52, DOI 10.1086/586894, 0802.0037

Salyk C, Blake GA, Boogert ACA, Brown JM (2009) High-resolution 5 μ m Spectroscopy of Transitional Disks. *ApJ*699:330–347, DOI 10.1088/0004-637X/699/1/330

Santoro FG, Olivares AM, Salcido CD, Jimenez SR, Sun X, Haniff CA, Buscher DF, Creech-Eakman MJ, Jurgenson CA, Shtromberg AV, Bakker EJ, Selina RJ, Fisher M, Young JS, Wilson DMA (2010) Mechanical design of the Magdalena Ridge Observatory Interferometer. In: Society of Photo-Optical Instrumentation Engineers (SPIE) Conference Series, Presented at the Society of Photo-Optical Instrumentation Engineers (SPIE) Conference, vol 7734, DOI 10.1117/12.856591

Santos NC, Israelian G, Mayor M (2004) Spectroscopic [Fe/H] for 98 extra-solar planet-host stars. Exploring the probability formation. *A&A*415:1153–1166, DOI 10.1051/0004-6361:20034469, arXiv:astro-ph/0311541

Sauter J, Wolf S (2011) Observing dust settling and coagulation in circumstellar discs. Selected constraints from high resolution imaging. *A&A*527:A27+, DOI 10.1051/0004-6361/201014546, 1011.4834

Sauter J, Wolf S, Launhardt R, Padgett DL, Stapelfeldt KR, Pinte C, Duchêne G, Ménard F, McCabe CE, Pontoppidan K, Dunham M, Bourke TL, Chen JH (2009) The circumstellar disc in the Bok globule CB 26. Multi-wavelength observations and modelling of the dust disc and envelope. *A&A*505:1167–1182, DOI 10.1051/0004-6361/200912397, 0907.

1074

Sauty C, Trussoni E, Tsinganos K (2004) Nonradial and nonpolytropic astrophysical outflows. VI. Overpressured winds and jets. *A&A*421:797–809, DOI 10.1051/0004-6361:20035790

Schegerer AA, Wolf S (2010) Spatially resolved detection of crystallized water ice in a T Tauri object. *A&A*517:A87+, DOI 10.1051/0004-6361/200911849

Schegerer AA, Wolf S, Ratzka T, Leinert C (2008) The T Tauri star RY Tauri as a case study of the inner regions of circumstellar dust disks. *A&A*478:779–793, DOI 10.1051/0004-6361:20077049, 0712.0696

Schegerer AA, Wolf S, Hummel CA, Quanz SP, Richichi A (2009) Tracing the potential planet-forming regions around seven pre-main-sequence stars. *A&A*502:367–383, DOI 10.1051/0004-6361/200810782, 0905.0565

Schlaufman KC, Lin DNC, Ida S (2009) The Signature of the Ice Line and Modest Type I Migration in the Observed Exoplanet Mass-Semimajor Axis Distribution. *ApJ*691:1322–1327

Schneider G, Smith BA, Becklin EE, Koerner DW, Meier R, Hines DC, Lowrance PJ, Terrile RJ, Thompson RI, Rieke M (1999) NICMOS Imaging of the HR 4796A Circumstellar Disk. *ApJ*513:L127–L130, DOI 10.1086/311921, arXiv:astro-ph/9901218

Schneider G, Silverstone MD, Hines DC, Augereau JC, Pinte C, Ménard F, Krist J, Clampin M, Grady C, Golimowski D, Ardila D, Henning T, Wolf S, Rodmann J (2006) Discovery of an 86 AU Radius Debris Ring around HD 181327. *ApJ*650:414–431, DOI 10.1086/506507, arXiv:astro-ph/0606213

Schneider G, Weinberger AJ, Becklin EE, Debes JH, Smith BA (2009) STIS Imaging of the HR 4796A Circumstellar Debris Ring. *AJ*137:53–61, DOI 10.1088/0004-6256/137/1/53, 0810.0286

Schreyer K, Semenov D, Henning T, Forbrich J (2006) A Rotating Disk around the Very Young Massive Star AFGL 490. *ApJ*637:L129–L132, DOI 10.1086/500732, arXiv:astro-ph/0601270

Selsis F, Kasting JF, Levrard B, Paillet J, Ribas I, Delfosse X (2007) Habitable planets around the star Gliese 581? *A&A*476:1373–1387, DOI 10.1051/0004-6361:20078091, 0710.5294

Semenov D, Pavlyuchenkov Y, Henning T, Wolf S, Launhardt R (2008) Chemical and Thermal Structure of Protoplanetary Disks as Observed with ALMA. *ApJ*673:L195–L198, DOI 10.1086/528795, 0801.1463

Shakura NI, Sunyaev RA (1973) Black holes in binary systems. Observational appearance. *A&A*24:337–355

Shao M, Colavita MM (1992) Potential of long-baseline infrared interferometry for narrow-angle astrometry. *A&A*262:353–358

Shepherd DS, Claussen MJ, Kurtz SE (2001) Evidence for a Solar System-Size Accretion Disk Around the Massive Protostar G192.16-3.82. *Science* 292:1513–1518, DOI 10.1126/science.1059475

Showman AP, Guillot T (2002) Atmospheric circulation and tides of “51 Pegasus b-like” planets. *A&A*385:166–180, DOI 10.1051/0004-6361:20020101, arXiv:astro-ph/0202236

Shu F, Najita J, Ostriker E, Wilkin F, Ruden S, Lizano S (1994) Magnetocentrifugally driven flows from young stars and disks. 1: A generalized model. *ApJ*429:781–796, DOI 10.1086/174363

Sibthorpe B, Vandenbussche B, Greaves JS, Pantin E, Olofsson G, Acke B, Barlow MJ, Blommaert JADL, Bouwman J, Brandeker A, Cohen M, De Meester W, Dent WRF, di

Francesco J, Dominik C, Fridlund M, Gear WK, Glauser AM, Gomez HL, Hargrave PC, Harvey PM, Henning T, Heras AM, Hogerheijde MR, Holland WS, Ivison RJ, Leeks SJ, Lim TL, Liseau R, Matthews BC, Naylor DA, Pilbratt GL, Polehampton ET, Regibo S, Royer P, Sicilia-Aguilar A, Swinyard BM, Waelkens C, Walker HJ, Wesson R (2010) The Vega debris disc: A view from Herschel. *A&A*518:L130+, DOI 10.1051/0004-6361/201014574, 1005.3543

Sicilia-Aguilar A, Bouwman J, Juhász A, Henning T, Roccatagliata V, Lawson WA, Acke B, Feigelson ED, Tielens AGGM, Decin L, Meeus G (2009) The Long-Lived Disks in the η Chamaeleontis Cluster. *ApJ*701:1188–1203, DOI 10.1088/0004-637X/701/2/1188, 0906.3365

Sicilia-Aguilar A, Henning T, Hartmann LW (2010) Accretion in Evolved and Transitional Disks in CEP OB2: Looking for the Origin of the Inner Holes. *ApJ*710:597–612, DOI 10.1088/0004-637X/710/1/597, 1001.3026

Silber J, Gledhill T, Duchêne G, Ménard F (2000) Near-Infrared Imaging Polarimetry of the GG Tauri Circumbinary Ring. *ApJ*536:L89–L92, DOI 10.1086/312731, arXiv: astro-ph/0005303

Simon M, Prato L (1995) Disk Dissipation in Single and Binary Young Star Systems in Taurus. *ApJ*450:824–+, DOI 10.1086/176187

Sing DK, Vidal-Madjar A, Désert JM, Lecavelier des Etangs A, Ballester G (2008) Hubble Space Telescope STIS Optical Transit Transmission Spectra of the Hot Jupiter HD 209458b. *ApJ*686:658–666, DOI 10.1086/590075, 0802.3864

Sivaramakrishnan A, Tuthill PG, Ireland MJ, Lloyd JP, Martinache F, Soummer R, Makidon RB, Doyon R, Beaulieu M, Beichman CA (2009) Planetary system and star formation science with non-redundant masking on JWST. In: Society of Photo-Optical Instrumentation Engineers (SPIE) Conference Series, Presented at the Society of Photo-Optical Instrumentation Engineers (SPIE) Conference, vol 7440, DOI 10.1117/12.826633

Skrutskie MF, Dutkewitch D, Strom SE, Edwards S, Strom KM, Shure MA (1990) A sensitive 10-micron search for emission arising from circumstellar dust associated with solar-type pre-main-sequence stars. *AJ*99:1187–1195, DOI 10.1086/115407

Stapelfeldt KR, Krist JE, Menard F, Bouvier J, Padgett DL, Burrows CJ (1998) An Edge-On Circumstellar Disk in the Young Binary System HK Tauri. *ApJ*502:L65+, DOI 10.1086/311479

Stevenson DJ (1982) Formation of the giant planets. *Planetary and Space Science* 30:755–764

Stolte A, Grebel EK, Brandner W, Figer DF (2002) The mass function of the Arches cluster from Gemini adaptive optics data. *A&A*394:459–478, DOI 10.1051/0004-6361:20021118, arXiv:astro-ph/0208321

Stone JM, Hawley JF, Gammie CF, Balbus SA (1996) Three-dimensional Magnetohydrodynamical Simulations of Vertically Stratified Accretion Disks. *ApJ*463:656–+, DOI 10.1086/177280

Strom KM, Strom SE, Edwards S, Cabrit S, Skrutskie MF (1989) Circumstellar material associated with solar-type pre-main-sequence stars - A possible constraint on the timescale for planet building. *AJ*97:1451–1470, DOI 10.1086/115085

Su KYL, Rieke GH, Misselt KA, Stansberry JA, Moro-Martin A, Stapelfeldt KR, Werner MW, Trilling DE, Bendo GJ, Gordon KD, Hines DC, Wyatt MC, Holland WS, Marengo M, Megeath ST, Fazio GG (2005) The Vega Debris Disk: A Surprise from Spitzer. *ApJ*628:487–500, DOI 10.1086/430819, arXiv:astro-ph/0504086

Tanaka H, Takeuchi T, Ward WR (2002) Three-dimensional interaction between a planet and an isothermal gaseous disk. i. corotation and lindblad torques and planet migration.

ApJ565:1257

Tannirkulam A, Harries TJ, Monnier JD (2007) The Inner Rim of YSO Disks: Effects of Dust Grain Evolution. *ApJ*661:374–384, DOI 10.1086/513265, arXiv:astro-ph/0702044

Tannirkulam A, Monnier JD, Harries TJ, Millan-Gabet R, Zhu Z, Pedretti E, Ireland M, Tuthill P, ten Brummelaar T, McAlister H, Farrington C, Goldfinger PJ, Sturmann J, Sturmann L, Turner N (2008) A Tale of Two Herbig Ae Stars, MWC 275 and AB Aurigae: Comprehensive Models for Spectral Energy Distribution and Interferometry. *ApJ*689:513–531, DOI 10.1086/592346, 0808.1728

Tatulli E, Isella A, Natta A, Testi L, Marconi A, Malbet F, Stee P, Petrov RG, Mil'our F, Chelli Aea (2007) Constraining the wind launching region in Herbig Ae stars: AMBER/VLTI spectroscopy of HD 104237. *A&A*464:55–58, DOI 10.1051/0004-6361:20065719

Tatulli E, Malbet F, Ménard F, Gil C, Testi L, Natta A, Kraus S, Stee P, Robbe-Dubois S (2008) Spatially resolving the hot CO around the young Be star 51 Ophiuchi. *A&A*489:1151–1155, DOI 10.1051/0004-6361:200809627

Tatulli E, Benisty M, Ménard F, Varnière P, Martin-Zaïdi C, Thi WF, Pinte C, Massi F, Weigelt G, Hofmann KH, Petrov RG (2011) Constraining the structure of the planet-forming region in the disk of the Herbig Be star HD 100546. *A&A*531:A1+, DOI 10.1051/0004-6361/201016165, 1104.0905

ten Brummelaar TA, McAlister HA, Ridgway ST, Bagnuolo WG Jr, Turner NH, Sturmann L, Sturmann J, Berger DH, Ogden CE, Cadman R, Hartkopf WI, Hopper CH, Shure MA (2005) First Results from the CHARA Array. II. A Description of the Instrument. *ApJ*628:453–465, DOI 10.1086/430729, arXiv:astro-ph/0504082

Terada H, Tokunaga AT, Kobayashi N, Takato N, Hayano Y, Takami H (2007) Detection of Water Ice in Edge-on Protoplanetary Disks: HK Tauri B and HV Tauri C. *ApJ*667:303–307, DOI 10.1086/520951

Testi L (2008) ALMA Science: the ESO-Garching Astronomers View. *The Messenger* 131:46–47

Testi L, Leurini S (2008) High angular resolution millimeter observations of circumstellar disks. *New A Rev.*52:105–116, DOI 10.1016/j.newar.2008.04.010

Testi L, Natta A, Shepherd DS, Wilner DJ (2001) Constraints on Properties of the Protoplanetary Disks around UX Orionis and CQ Tauri. *ApJ*554:1087–1094, DOI 10.1086/321406, arXiv:astro-ph/0102473

Testi L, Natta A, Shepherd DS, Wilner DJ (2003) Large grains in the disk of CQ Tau. *A&A*403:323–328, DOI 10.1051/0004-6361:20030362, arXiv:astro-ph/0303420

Thalmann C, Grady CA, Goto M, Wisniewski JP, Janson M, Henning T, Fukagawa M, Honda M, Mulders GD, Min M, Moro-Martín A, McElwain MW, Hodapp KW, Carson J, Abe L, Brandner W, Egner S, Feldt M, Fukue T, Golota T, Guyon O, Hashimoto J, Hayano Y, Hayashi M, Hayashi S, Ishii M, Kandori R, Knapp GR, Kudo T, Kusakabe N, Kuzuhara M, Matsuo T, Miyama S, Morino JI, Nishimura T, Pyo TS, Serabyn E, Shibai H, Suto H, Suzuki R, Takami M, Takato N, Terada H, Tomono D, Turner EL, Watanabe M, Yamada T, Takami H, Usuda T, Tamura M (2010) Imaging of a Transitional Disk Gap in Reflected Light: Indications of Planet Formation Around the Young Solar Analog LkCa 15. *ApJ*718:L87–L91, DOI 10.1088/2041-8205/718/2/L87, 1005.5162

Thatte N, Abuter R, Tecza M, Nielsen EL, Clarke FJ, Close LM (2007) Very high contrast integral field spectroscopy of AB Doradus C: 9-mag contrast at 0.2arcsec without a coronagraph using spectral deconvolution. *MNRAS*378:1229–1236, DOI 10.1111/j.1365-2966.

2007.11717.x, arXiv:astro-ph/0703565

Thébault P, Augereau JC (2007) Collisional processes and size distribution in spatially extended debris discs. *A&A*472:169–185, DOI 10.1051/0004-6361:20077709, 0706.0344

Thommes EW, Duncan M, Levison HF (2003) Oligarchic growth of giant planets. *Icarus* 162:431

Toomre A (1964) On the gravitational stability of a disk of stars. *ApJ*139:1217–1238, DOI 10.1086/147861

Toomre A (1981) What amplifies the spirals. In: S M Fall & D Lynden-Bell (ed) *Structure and Evolution of Normal Galaxies*, pp 111–136

Trilling DE, Bryden G, Beichman CA, Rieke GH, Su KYL, Stansberry JA, Blaylock M, Stapelfeldt KR, Beeman JW, Haller EE (2008) Debris Disks around Sun-like Stars. *ApJ*674:1086–1105, DOI 10.1086/525514, 0710.5498

Udry S, Santos NC (2007) Statistical Properties of Exoplanets. *ARA&A*45:397–439, DOI 10.1146/annurev.astro.45.051806.110529

van Boekel R, Min M, Leinert C, Waters LBFM, Richichi A, Chesneau O, Dominik C, Jaffe W, Dutrey A, Graser U, Henning T, de Jong J, Köhler R, de Koter A, Lopez B, Malbet F, Morel S, Paresce F, Perrin G, Preibisch T, Przygoda F, Schöller M, Wittkowski M (2004) The building blocks of planets within the ‘terrestrial’ region of protoplanetary disks. *Nature*432:479–482, DOI 10.1038/nature03088

van Zadelhoff GJ, van Dishoeck EF, Thi WF, Blake GA (2001) Submillimeter lines from circumstellar disks around pre-main sequence stars. *A&A*377:566–580, DOI 10.1051/0004-6361:20011137, arXiv:astro-ph/0108375

Vehoff S, Hummel CA, Monnier JD, Tuthill P, Nürnberger DEA, Siebenmorgen R, Chesneau O, Duschl WJ (2010) Mid-infrared interferometry of the massive young stellar object NGC 3603 - IRS 9A. *A&A*520:A78+, DOI 10.1051/0004-6361/200913546, 1009.1598

Verhoeff AP, Min M, Pantin E, Waters LBFM, Tielens AGGM, Honda M, Fujiwara H, Bouwman J, van Boekel R, Dougherty SM, de Koter A, Dominik C, Mulders GD (2011) The complex circumstellar environment of HD 142527. *A&A*528:A91+, DOI 10.1051/0004-6361/201014952, 1101.5719

Vinković D, Jurkić T (2007) Relation between the Luminosity of Young Stellar Objects and Their Circumstellar Environment. *ApJ*658:462–479, DOI 10.1086/511327

Watson AM, Stapelfeldt KR (2007) Asymmetry and Variability in the HH 30 Circumstellar Disk. *AJ*133:845–861, DOI 10.1086/510455

Watson AM, Stapelfeldt KR, Wood K, Ménard F (2007) Multiwavelength Imaging of Young Stellar Object Disks: Toward an Understanding of Disk Structure and Dust Evolution. *Protostars and Planets V* pp 523–538, 0707.2608

Weidenschilling SJ (1977) Aerodynamics of solid bodies in the solar nebula. *MNRAS*180:57

Weidenschilling SJ, Spaute D, Davis DR, Marzari F, Ohtsuki K (1997) Accretional evolution of a planetesimal swarm. *Icarus* 128:429

Wilner DJ, Ho PTP, Kastner JH, Rodríguez LF (2000) VLA Imaging of the Disk Surrounding the Nearby Young Star TW Hydrae. *ApJ*534:L101–L104, DOI 10.1086/312642, arXiv:astro-ph/0005019

Winn JN, Fabrycky D, Albrecht S, Johnson JA (2010) Hot Stars with Hot Jupiters Have High Obliquities. *ApJ*718:L145–L149, DOI 10.1088/2041-8205/718/2/L145, 1006.4161

Wizinowich PL, Akeson RL, Colavita MM, Gathright J, Appleby E, Bell J, Booth AJ, Dahl W, Goude P, Hrynevych MA, Lynn I, Millan-Gabet R, Neyman CR, Rudeen AC, Saloga

T, Summers K, Tsubota K (2004) Visibility science operations with the Keck Interferometer. In: W A Traub (ed) Society of Photo-Optical Instrumentation Engineers (SPIE) Conference Series, Presented at the Society of Photo-Optical Instrumentation Engineers (SPIE) Conference, vol 5491, pp 1678–+

Woitzel J, Akeson R, Colavita M, Eisner J, Ghez A, Graham J, Hillenbrand L, Millan-Gabet R, Monnier J, Pott JU, Ragland S, Wizinowich P, Appleby E, Berkey B, Cooper A, Felizardo C, Herstein J, Hrynevych M, Martin O, Medeiros D, Morrison D, Panteleeva T, Smith B, Summers K, Tsubota K, Tyau C, Wetherell E (2010) ASTRA: astrometry and phase-referencing astronomy on the Keck interferometer. In: Society of Photo-Optical Instrumentation Engineers (SPIE) Conference Series, Presented at the Society of Photo-Optical Instrumentation Engineers (SPIE) Conference, vol 7734, DOI 10.1117/12.857740

Wolf S (2008a) Signatures of planets in young and evolved circumstellar disks. *Physica Scripta* Volume T 130(1):014,025

Wolf S (2008b) Signatures of planets in young and evolved circumstellar disks. *Physica Scripta* Volume T 130(1):014,025, DOI 10.1088/0031-8949/2008/T130/014025

Wolf S, D'Angelo G (2005) On the Observability of Giant Protoplanets in Circumstellar Disks. *ApJ*619:1114–1122, DOI 10.1086/426662, arXiv:astro-ph/0410064

Wolf S, Gueth F, Henning T, Kley W (2002) Detecting Planets in Protoplanetary Disks: A Prospective Study. *ApJ*566:L97–L99, DOI 10.1086/339544, arXiv:astro-ph/0201197

Wolf S, Padgett DL, Stapelfeldt KR (2003) The Circumstellar Disk of the Butterfly Star in Taurus. *ApJ*588:373–386, DOI 10.1086/374041, astro-ph/0301335

Wolf S, Schegerer A, Beuther H, Padgett DL, Stapelfeldt KR (2008) Submillimeter Structure of the Disk of the Butterfly Star. *ApJ*674:L101–L104, DOI 10.1086/529188, 0801.1422

Wolf S, Lopez B, Jaffe W, Weigelt G, Augereau JC, Berruyer N, Chesneau O, Danchi WC, Delbo M, Demyk K, Domiciano A, Henning T, Hofmann KH, Kraus S, Leinert C, Linz H, Mathias P, Meisenheimer K, Menut JL, Millour F, Mosoni L, Niedzielski A, Petrov R, Ratzka T, Stecklum B, Thiebaut E, Vakili F, Waters LBFM, Absil O, Hron J, Lagarde S, Matter A, Nardetto N, Olofsson J, Valat B, Vannier M (2009) MATISSE Science Cases. In: A Moorwood (ed) Science with the VLT in the ELT Era, pp 359–+, DOI 10.1007/978-1-4020-9190-260

Wolk SJ, Walter FM (1996) A Search for Protoplanetary Disks Around Naked T Tauri Stars. *AJ*111:2066–+, DOI 10.1086/117942

Wuchterl G (1993) The critical mass for protoplanets revisited - Massive envelopes through convection. *Icarus*106:323–334

Yorke HW (2004) Theory of Formation of Massive Stars via Accretion. In: Burton M, Jayawardhana R, Bourke T (eds) Star Formation at High Angular Resolution, IAU Symposium, vol 221, pp 141–+

Yorke HW, Bodenheimer P (1999) The Formation of Protostellar Disks. III. The Influence of Gravitationally Induced Angular Momentum Transport on Disk Structure and Appearance. *ApJ*525:330–342, DOI 10.1086/307867

Youdin AN, Goodman J (2005) Streaming Instabilities in Protoplanetary Disks. *ApJ*620:459–469

Youdin AN, Mitchell JL (2010) The Mechanical Greenhouse: Burial of Heat by Turbulence in Hot Jupiter Atmospheres. *ApJ*721:1113–1126, DOI 10.1088/0004-637X/721/2/1113, 1008.0645

Zhao M, Monnier JD, Che X, Ten Brummelaar T, Pedretti E, Thureau ND (2010) MIRC closure phase studies for high precision measurements. In: Society of Photo-Optical Instru-

mentation Engineers (SPIE) Conference Series, Presented at the Society of Photo-Optical Instrumentation Engineers (SPIE) Conference, vol 7734, DOI 10.1117/12.857538

Zhu Z, Hartmann L, Gammie C (2009) Nonsteady Accretion in Protostars. *ApJ*694:1045–1055, DOI 10.1088/0004-637X/694/2/1045, 0811.1762

Zinnecker H, Yorke HW (2007) Toward Understanding Massive Star Formation. *ARA&A*45:481–563, DOI 10.1146/annurev.astro.44.051905.092549, 0707.1279